

CAPITAL UNIVERSITY OF SCIENCE AND
TECHNOLOGY, ISLAMABAD



Exploring the Inhibitory Compounds of
Peganum harmala against p. Phe508del
Mutated CFTR Protein to Treat Cystic Fibrosis

by

Hafsa Ayub

A dissertation submitted in partial fulfillment for the
degree of Master of Science

in the

Faculty of Health and Life Sciences

Department of Bioinformatics and Biosciences

2024

Copyright © 2024 by Hafsa Ayub

All rights reserved. No part of this dissertation may be reproduced, distributed, or transmitted in any form or by any means, including photocopying, recording, or other electronic or mechanical methods, by any information storage and retrieval system without the prior written permission of the author.

This dissertation is dedicated to my dear and supportive family and friends who have fully helped me in achieving my life goals.



CERTIFICATE OF APPROVAL

Exploring the Inhibitory Compounds of *Peganum harmala*
against p. Phe508del Mutated CFTR Protein to Treat
Cystic Fibrosis

by

Hafsa Ayub

(MBS221016)

THESIS EXAMINING COMMITTEE

S. No.	Examiner	Name	Organization
(a)	External Examiner	Dr. Saba Mehmood	NUMS, Rawalpindi
(b)	Internal Examiner	Dr. Sania Riaz	CUST, Islamabad
(c)	Supervisor	Dr. Erum Dilshad	CUST, Islamabad

Dr. Erum Dilshad

Research Supervisor

May, 2024

Dr. Syeda Marriam Bakhtiar

Head

Dept. of Bioinformatics and Biosciences

May, 2024

Dr. Sahar Fazal

Dean

Faculty of Health and Life Sciences

May, 2024

Author's Declaration

I, **Hafsa Ayub** hereby state that my MS dissertation titled “**Exploring the Inhibitory Compounds of *Peganum harmala* against p. Phe508del Mutated CFTR Protein to Treat Cystic Fibrosis**” is my own work and has not been submitted previously by me for taking any degree from Capital University of Science and Technology, Islamabad or anywhere else in the country/abroad.

At any time if my statement is found to be incorrect even after my graduation, the University has the right to withdraw my MS Degree.

(Hafsa Ayub)

Registration No: MBS221016

Plagiarism Undertaking

I solemnly declare that research work presented in this dissertation titled “**Exploring the Inhibitory Compounds of *Peganum harmala* against p. Phe508del Mutated CFTR Protein to Treat Cystic Fibrosis**” is solely my research work with no significant contribution from any other person. Small contribution/help wherever taken has been duly acknowledged and that complete dissertation has been written by me.

I understand the zero tolerance policy of the HEC and Capital University of Science and Technology towards plagiarism. Therefore, I as an author of the above titled dissertation declare that no portion of my dissertation has been plagiarized and any material used as reference is properly referred/cited.

I undertake that if I am found guilty of any formal plagiarism in the above titled dissertation even after award of MS Degree, the University reserves the right to withdraw/revoke my MS degree and that HEC and the University have the right to publish my name on the HEC/University website on which names of students are placed who submitted plagiarized work.

(Hafsa Ayub)

Registration No: MBS221016

Acknowledgement

All praise and thanks to the Supreme God to whom we only bow down. I would also like to express my gratitude to my family and friends for their continuous mental and physical support and prayers. I would also wholeheartedly say a big thank you to my supervisor **Dr. Erum Dilshad** (Assistant Professor, Department of Bioinformatics and Biosciences, CUST) for her support with that I would say a special thanks to **Mr. Maaz** (Phd Scholar) for giving his precious time to assist with computational approaches.

Thanks to all.

(Hafsa Ayub)

Registration No: MBS221016

Abstract

Cystic fibrosis is a recessive genetic disease that is caused by the mutation of the CFTR (cystic fibrosis transmembrane conductance regulator) protein. More than 70,000 people are affected globally, and most patients are diagnosed at the age of 2 years. With more than 1900 mutations and a median survival at the age of 40 years, there is a need to develop more effective treatments and therapy methods. For this purpose, many plants were exploited to find natural compounds to work against this disease. The detailed study of the mutated CFTR gene shows that one single mutation, phe508del CFTR, commonly known as F508del- CFTR (categorized in class II), accounts for about 70% of CFTR loss-of-function mutations and is present in approximately 90% of CF patients worldwide. The active compound in *Peganum harmala* was studied to be docked against the phe508del CFTR. 20 ligands from different classes were selected for this purpose. These ligands were then screened out based on Lipinski Rule and through studying the ADMET properties of the ligands. After the docking of the selected ligands with the receptor protein through the CB dock, the lead compound vasicinone was selected against the standard drug ivacaftor. The docking results of both compounds were visualized via PyMol and were analyzed by the use of LigPlot. The result shows that vasicinone can be more effective against phe508del CFTR protein rather than ivacaftor. However further research has to be carried for investigating vasicinone potential medicinal use.

Keywords: F508del CFTR Protein, *Peganum harmala*, CB-dock, ADMET, vasicinone, and ivacaftor.

Contents

Author's Declaration	iv
Plagiarism Undertaking	v
Acknowledgement	vi
Abstract	vii
List of Figures	xi
List of Tables	xiii
Abbreviations	xiv
1 Introduction	1
1.1 Problem Statement	4
1.2 Aim and Objectives	4
1.3 Scope	5
2 Literature Review	6
2.1 Cystic Fibrosis	6
2.2 Causes of Cystic Fibrosis	7
2.3 Diagnosis of Cystic Fibrosis	7
2.4 Role of Modifiers in Cystic Fibrosis	8
2.5 Classification of CF Mutations	8
2.6 Origin	10
2.7 Cystic Fibrosis-Related Innate Immune Cell Mutations: A Signalling Pathway	12
2.8 Symptoms	13
2.9 Treatment for Cystic Fibrosis	14
2.10 CFTR Modulators	15
2.10.1 Ivacaftor	15
2.10.2 Lumacaftor (VX-809)	15
2.10.3 Lumacaftor Plus Ivacaftor	16
2.10.4 VX-661	16
2.10.5 Ataluren (PTC124)	16

2.10.6	Other Potential CFTR Modulators	17
2.10.6.1	4PBA	17
2.10.6.2	VRT-532	17
2.10.6.3	N6022	17
2.11	Medicinal Properties	17
2.12	<i>Peganum harmala</i>	18
2.12.1	Traditional Uses	19
2.12.2	Biological Components of <i>P. harmala</i>	19
2.13	Molecular Docking	20
2.14	Insilico Methods and Molecular Docking	20
2.15	In silico Drug Repositioning on F508del CFTR	21
2.16	F508del CFTR Protein	21
2.17	Natural Compounds as Inhibitors of F508 del CFTR Protein	22
2.18	Potential Inhibitory Compounds in <i>Peganum harmala</i> Used as Antiseptic	23
3	Materials and Methods	25
3.1	Selection of Disease	25
3.2	Selection of Protein	25
3.3	Determination of Physiochemical Properties of Proteins	26
3.4	Cleaning of the Downloaded Protein	26
3.5	Determination of Functional Domains of Target Proteins	26
3.6	Selection of Active Metabolic Ligands	27
3.7	Ligand Preparation	27
3.8	Molecular Docking	27
3.9	Visualization of Docking Result via PyMol	28
3.10	Analysis of Docked Complex via LigPlot	28
3.11	Ligand ADME Properties:	29
3.12	Lead Compound Identification	29
3.13	Comparison with the Standard Drug	29
3.14	Drug-Proposed against Cystic Fibrosis	29
3.15	Overview of Methodology	30
4	Results and Discussion	31
4.1	Structure Modelling	31
4.1.1	3D Structure of the Protein	31
4.1.2	Physical Properties of Protein	33
4.1.3	Identification of Functional Domains of the Protein	34
4.1.4	Structure of Protein refined for Docking	36
4.2	Ligand Selection	37
4.3	Virtual Screening and Toxicity Prediction through Lipinski Rule of Five	39
4.3.1	Toxicity Prediction	40
4.4	Molecular Docking	43
4.5	Interaction of Ligands and the Targeted Protein	47
4.6	ADME Properties of Ligand	65

4.6.1	Pharmacodynamics	65
4.6.2	Pharmacokinetics	65
4.6.3	Absorption	65
4.6.4	Distribution	68
4.6.5	Metabolism	71
4.6.6	Excretion	74
4.7	Lead Compound Identification	76
4.8	Drug Identification against Cystic Fibrosis	76
4.8.1	Ivacaftor	77
4.9	Drug ADMET Properties	77
4.9.1	Toxicity Prediction of Reference Drug	77
4.9.2	Absorption Properties	78
4.9.3	Distribution Properties	78
4.9.4	Metabolic Properties	79
4.9.5	Excretion Properties	79
4.10	Ivacaftor Mechanism of Action	80
4.11	Ivacaftor Effects on the Body	81
4.12	Ivacaftor Docking	82
4.13	Ivacaftor Comparison with Lead Compound	83
4.14	ADMET Properties Comparison	83
4.14.1	Toxicity Comparison	83
4.14.2	Absorption Properties Comparison	85
4.14.3	Metabolic Properties Comparison	85
4.14.4	Distribution Properties Comparison	86
4.14.5	Excretion Properties Comparison	87
4.15	Physiochemical Properties Comparison	87
4.16	Docking Score Comparison	88
4.17	Docking Analysis Comparison	88
5	Conclusion and Future Prospects	93
5.1	Recommendations	93
	Bibliography	95

List of Figures

2.1	(A) A 3D representation of the CFTR gene's so-called topologically associated domain in airway cells is shown. This image highlights the promoter, borders (I and II), and structural proteins CTCF and cohesin. (B) Ribbon depiction of the human CFTR 3D structure in association with VX-770 (ATP-bound, phosphorylated version) [20].	9
2.2	Traditional classification of CF mutations based on their cellular phenotype [24].	10
2.3	Maximum-likelihood tree showing the frequency of alleles at five loci (IVS6aGATT, IVS8CA, T854, IVS17bTA, and TUB20) in normal chromosomes from all populations as well as in CF chromosomes (F508, G542X, N1303K, G551D, and W1282X chromosomes) [27].	11
2.4	A phylogenetic tree constructed based on 38 complete chloroplast genome sequences [28].	12
2.5	CF airway and altered Airway Epithelial Cells mechanisms [32].	13
2.6	Multifactorial causes of abdominal symptoms in CF [33].	14
2.7	<i>P. harmala</i> (A) plant; (B) flower; (C) ripe fruits; (D) seeds [52].	20
3.1	Methodology opted for this study.	30
4.1	Crystal structure of human F508del-CFTR human NBD1 domain with ATP	32
4.2	Functional domains of targeted protein.	35
4.3	1XMJ cleaned protein	36
4.4	Interaction of harmaline with the receptor protein	47
4.5	Interaction of harmalol with receptor protein	48
4.6	Interaction of harmol with receptor protein	48
4.7	Interaction of tetrahydroharmine with receptor protein	49
4.8	Interaction of vasicinone with receptor protein	49
4.9	Interaction of vasicine with receptor protein	50
4.10	Interaction of harmine with receptor protein	50
4.11	Interaction of acetic acid with receptor protein	51
4.12	Interaction of betaine with receptor protein	51
4.13	Interaction of choline with receptor protein	52
4.14	Interaction of succinic acid with receptor protein	52
4.15	Interaction of serotonin with receptor protein	53
4.16	Interaction of lysine with receptor protein	53
4.17	Interaction of sucrose with receptor protein	54

4.18	Interaction of asparagine with receptor protein	54
4.19	Interaction of valine with receptor protein	55
4.20	Interaction of beta carboline with receptor protein	55
4.21	Interaction of proline with receptor protein	56
4.22	Interaction of hydroxyisoleucine with receptor protein	56
4.23	Interaction of linoleic acid with receptor protein	57
4.24	Stylized cells depicting metabolism and mechanism of action of ivacaftor [104]	81
4.25	Interaction of Ivacaftor with the receptor	89
4.26	Interaction of Vasicinone with the receptor	89

List of Tables

4.1	Physical Properties of phe508del CFTR Protein	33
4.2	Structural Information of Selected Ligands	37
4.2	Structural Information of Selected Ligands	38
4.2	Structural Information of Selected Ligands	39
4.3	Applicability of Lipinski Rule on the Ligands	39
4.3	Applicability of Lipinski Rule on the Ligands	40
4.4	Toxicity Values of Ligands	42
4.5	Docking Result of Ligands	46
4.6	Active Ligand Showing Hydrogen and Hydrophobic Interactions . .	58
4.6	Active Ligand Showing Hydrogen and Hydrophobic Interactions . .	59
4.6	Active Ligand Showing Hydrogen and Hydrophobic Interactions . .	60
4.6	Active Ligand Showing Hydrogen and Hydrophobic Interactions . .	61
4.6	Active Ligand Showing Hydrogen and Hydrophobic Interactions . .	62
4.6	Active Ligand Showing Hydrogen and Hydrophobic Interactions . .	63
4.6	Active Ligand Showing Hydrogen and Hydrophobic Interactions . .	64
4.7	Absorption Properties of Ligands	67
4.8	Distribution Properties of Ligands	69
4.8	Distribution Properties of Ligands	70
4.9	Metabolic Properties of Ligands	73
4.10	Excretory Properties of Ligands	75
4.11	Toxicity Properties of Ivacaftor	77
4.11	Toxicity Properties of Ivacaftor	78
4.12	Absorption Properties of Ivacaftor	78
4.13	Distribution Properties of Ivacaftor	79
4.14	Metabolic Properties of Ivacaftor	79
4.15	Excretion Properties of Ivacaftor	80
4.16	Docking Result of Ivacaftor	82
4.17	Comparison of Reference Drug and Lead Compound	83
4.18	Toxicity Properties Comparison	84
4.19	Absorption Properties Comparison	85
4.20	Metabolic Properties Comparison	86
4.21	Distribution Properties Comparison	87
4.22	Excretion Properties Comparison	87
4.23	Physiochemical Properties Comparison	88
4.24	Docking Score Comparison	88
4.25	Docking Analysis Comparison	91

Abbreviations

ADME	Absorption, Digestion, Metabolism, Excretion
BBB	Blood Brain Barrier
CFTR	Cystic Fibrosis Transmembrane Conductance Regulator
CNS	Central Nervous System
CYP2C19	Cytochrome P450 2C19 Enzyme
FDA	Food Drug Authority
MRTD	Maximum Rate Tolerated Dose
PKA	Protein Kinase A
PKC	Protein Kinase C
<i>P. harmala</i>	<i>Peganum harmala</i>
<i>T. pyriformis</i>	<i>Tetrahymena pyriformis</i>
VD_{ss}	Volume Distribution

Chapter 1

Introduction

The CFTR gene, located on chromosome 7q31, has approximately 250 kb in size, is mutated to cause the multisystem hereditary disease known as cystic fibrosis. The mutant gene produces a faulty protein that results in an excessive amount of thick mucus that is difficult to remove.

An 18th-century poetry, "The child whose brow tastes salty when kissed," already made reference to CF. Through the middle of the 20th century, the high sweat salt concentration was the primary marker for the identification of cystic fibrosis. In 1938, the illness was dubbed "cystic fibrosis of the pancreas" due to the clinical characteristics of the condition centered on aberrant pancreatic function. However, it was later discovered that the lung, the gallbladder, the intestinal epithelium, and the intrahepatic bile ducts were among the other mucus-secreting glands that contributed to the illness phenotype [1].

Studying the cystic fibrosis transmembrane conductance regulator (CFTR) is very recommended due to its distinctive functional characteristics and significance in biomedicine. A mutation in the CFTR gene causes cystic fibrosis. Certain mutations result in impaired CFTR biosynthesis, which reduces or eliminates the generation of proteins. Other mutations are missenses, which result in malfunctioning or misfolded proteins. The lung, intestine, pancreas, and kidney's salt balance is disturbed when functional CFTR is absent from epithelial tissues. The most

dangerous outcome is decreased mucus clearance of the airways, which causes persistent inflammation, recurrent infections, and finally respiratory failure [2].

Epithelial cells with cystic fibrosis have reduced chloride conductance as a result of abnormalities in the activation of chloride flux by protein kinase C (PKC) and cyclic AMP-dependent protein kinase (PKA). PKA activation opens chloride channels in normal human epithelia, but it is unable to increase chloride conductance in cells with cystic fibrosis. In human epithelial cells, PKC can also enhance the flow of chloride when there is insufficient calcium available. This type of control is abnormal in CF patients. In contrast, PKC activation shuts chloride channels at high calcium concentrations [3]. Patients with cystic fibrosis do not exhibit this action, which could be due to blockage of an alternative chloride channel. Cystic fibrosis transmembrane conductance regulator defects are the cause of cystic fibrosis. CFTR has been demonstrated to be a substrate for PKA, and it is believed that CFTR is a chloride channel. Thus, it seems likely that direct phosphorylation of CFTR mediates PKA's control of chloride transport [4].

At the time of the disease's beginning, the airways of people having cystic fibrosis show two host defence abnormalities. On the left of Figure 1.1, Antimicrobial action is inhibited by CFTR channel loss, which lowers the pH of the liquid that makes up the airway surface. This liquid is composed of chloride (Cl) and bicarbonate (HCO₃). On the right of Figure 1.1, CFTR channel failure in submucosal glands results in abnormal mucus qualities that prevent it from evaporating after emerging and keep it attached to the gland ducts [5]. Although PKC's effects on chloride channels are more complicated, it is most likely that, similarly to PKA, PKC controls CFTR function by directly phosphorylating it. Examining the molecular underpinnings of CFTR's phosphorylation regulation is crucial. The bulky, hydrophobic protein known as CFTR has not been refined. As a result, it has not yet been feasible to directly analyse the protein biochemically [6]. It has been proposed that phosphorylation of this so-called R-domain, a core region of CFTR, may be the cause of CFTR activation. Since there are many consensus sites for phosphorylation, it is important to determine the phosphorylation kinetics for these sites to identify potential sites that regulate CFTR function [7].

Approximately 70% of all CF alleles are caused by a single missense mutation called phe508del CFTR, sometimes referred to as F508del-CFTR. In certain communities, this mutation is present in up to 90% of CF patients [8]. It causes a phenylalanine deletion at position 508 in the CFTR protein. Around seventy percent of CFTR loss-of-function mutations are present in 90% of CF patients globally. The F508del-CFTR protein misfolds, preventing it from reaching the plasma membrane (PM) and causing it to break down too soon. F508del CFTR is unstable at the cell surface and quickly takes from endosomal recycling towards lysosomal transport and cause destruction, even if CFTR correctors can rescue it at the PM [9].

Antibiotics help in maintaining healthy lungs by preventing or treating lung infections. Antibiotics can be inhaled, taken orally, or intravenously. Inflammation is lessened by anti-inflammatory drugs like ibuprofen or corticosteroids. Lung disease is one of the several cystic fibrosis abnormalities brought on by inflammation. Ibuprofen is particularly helpful for kids, despite its unfavourable side effects, like stomach and kidney issues [10].

The dysfunctional CFTR protein functions better when it is regulated by CFTR modulators. They support the prevention of lung issues as well as other issues and enhance lung function. Luminacaftor, ivacaftor, and a triple combination drug (elexacaftor-tezacaftor-ivacaftor) are a few examples. Up to 90% of cystic fibrosis patients may benefit from this combo medication, making it the first approved treatment. It can currently be used by adults and kids over the age of twelve. Mucus thinners facilitate mucus clearance from the airways. To take these drugs, one must inhale them [11].

Infected CF patients are increasingly using both traditional medications for respiratory symptoms and so-called integrative medications, according to a growing body of research. Among many other things, herbs could provide helpful supportive therapy. To evaluate their appropriate use, nevertheless, further comprehension is necessary [12]. Our study's primary objective is to give proof that cystic fibrosis patients can use paramedical goods that contain *Peganum harmala* extract. The study's novelties include the use of a fractionated and thoroughly characterized extract from *Peganum harmala*, as well as an attempt to confirm its suitability for

treating a particular medical condition in silico under circumstances that partially modeled the respiratory system's microenvironment [13].

1.1 Problem Statement

The CFTR protein is mutated in cystic fibrosis, a recessive genetic disorder. Over 70,000 individuals worldwide are impacted, with the majority receiving a diagnosis by the time they are 2 years old. There is a need to create more potent therapies and treatment approaches because there are over 1900 mutations and a median survival at age 40. In order to undertake in-depth computational investigations using molecular docking, we will use the active chemicals in *Peganum harmala* that have antiseptic qualities to target the mutant CFTR protein of cystic fibrosis.

1.2 Aim and Objectives

The main aim of this study is to predict potential inhibitors against cystic fibrosis by the use of molecular docking of active compounds of *Peganum harmala* showing antiseptic properties against phe508del CFTR protein to control cystic fibrosis.

The following are some of the study's objectives:

- To identify the probable inhibitory compounds present in *Peganum harmala* against phe508del CFTR protein of cystic fibrosis.
- To analyze the interaction between ligand and protein complex by performing molecular docking.
- To explore the best inhibitor compound that shows antiseptic property against phe508del CFTR protein.

1.3 Scope

The clinical problems associated with current cystic fibrosis treatments and medications are unknown, as is the possibility of interactions between these substances and FDA-approved medications.

In fact, a substance like *Peganum harmala* might not cause any medical issues. It is unclear exactly how bioactive substances affect mutant CFTR to improve its trafficking and/or functionalities. This information may influence the sensible development of synthetic CFTR medications, leading to the eventual availability of a safe, efficient, and reasonably priced medication to treat CF patients.

According to recent research, there are active substances that can function as cystic fibrosis inhibitors. Therefore, it is necessary to identify other natural chemicals that may have inhibitory characteristics against cystic fibrosis. The goal of in silico molecular docking would be to find inhibitory chemicals against phe508del CFTR protein, which could aid in the development of drugs to treat cystic fibrosis.

Chapter 2

Literature Review

2.1 Cystic Fibrosis

Pancreatic exocrine insufficiency, fatty liver disease, and progressive lung disease with inflammation are the marks of cystic fibrosis. Of sick youngsters, two thirds have liver problems. True, one of the main characteristics of cystic fibrosis is inflammation, which is brought on by infection of bacteria, neutrophil infiltration in the lung, and elevated cytokine levels. Although the response of inflammation is excessive and dysregulated, it is unknown if aberrant CFTR is the cause or a result. The most widely accepted theory states that a malfunctioning CFTR causes a decrease in airway surface liquid, which prevents contaminated secretions from leaving the lung and sets off an overactive inflammatory response. Therefore, it is still up for debate whether the chronic infection alone is the cause of this hyper-inflammation or if CFTR abnormalities are the primary cause [14]. In terms of the liver, cirrhosis, biliary fibrosis, and steatosis are the three forms of liver disease that are seen in CF patients. The most frequent hepatic change identified in CF patients is fatty infiltration of the liver, which is discovered in 30% of cases during biopsy and in 60% of cases during autopsy. More than 50% of people with CF have CF Related Diabetes (CFRD), and the PI phenotype is a characteristic in patients with two severe alleles, such as F508del. Despite being a distinct condition, CFRD shares characteristics with type 1 and type 2 diabetes [15].

2.2 Causes of Cystic Fibrosis

A mutation in the gene that produces the CFTR protein is the cause of cystic fibrosis; these mutations fall into five distinct types. In patients with the CFTR mutation G551D, ivacaftor is a novel CFTR potentiator that aids in appropriate CFTR channel opening. In one study, sweat chloride concentrations significantly decreased although pulmonary function tests showed increases in patients. The Food and Drug Administration (FDA) approved oral administration of 150 mg twice daily of ivacaftor for G551D CF patients who were older than 6 years [16].

2.3 Diagnosis of Cystic Fibrosis

The most effective method of diagnosing cystic fibrosis is sweat electrolyte testing. The test has to be given by a qualified and experienced person. Because of this, even though prime care physicians show a critical role in finding patients who need additional evaluation, secondary and tertiary care facilities are usually where the diagnosis is made. In the very unusual circumstances when the diagnosis is still unclear, additional diagnostic procedures are available, as measuring a nasal possible variation to determine whether salt transport has changed. Currently, in the UK, a Guthrie blood spot test is used to screen all newborns for cystic fibrosis. The first test checks for elevated amounts of immunoreactive trypsinogen. After ruling out frequent CFTR gene mutations in positive samples, a second screening for immunoreactive trypsinogen will be carried out if needed [17]. Infants who test positive will undergo sweat testing. Improved nutrition, quicker access to specialised treatment, a shorter period of diagnostic ambiguity, and the ability to advise parents on prenatal testing are just a few benefits of early diagnosis. However, there can be certain drawbacks to screening programmes. Programmes will designate as possible patients a subset of healthy heterozygote carriers. Until the diagnosis is ruled out, this could be upsetting and have an impact on the family's mental health. Additional family members may be offered screening after

a diagnosis is made. The disorder should be checked for in all siblings as it may not show any symptoms at all or be presymptomatic. Asymptomatic adult relatives may choose to undergo a carrier status test for the purpose to make an educated choice regarding prenatal screening. The most practical way to screen and counsel additional family members is through primary care physicians; however, genetic laboratories must collaborate to provide quick and affordable testing [18].

2.4 Role of Modifiers in Cystic Fibrosis

Modifiers are crucial even if CFTR's sequence variation still has an impact on lung function. In fact, it is evident that variations in the genotype of cystic fibrosis are not the only cause of the disease's diversity, and extensive genome-wide association studies (GWAS) have been conducted to identify the genetic factors influencing phenotypic variance. A system biology method was used to achieve this goal, including database mining, pathway enrichment analysis, literature mining, network analysis, gene expression research, and protein-protein interactions. Potential moderators of the decreased lung function associated with cystic fibrosis include IFI16, IGFBP2 and CCNE2. Potential modifiers in the pancreas and liver include HLA-DQA1, EPHX1, DSP, HLA-DQB1, and SLC33A1, GPNMB, NCF2, RASGRP1, LGALS3, and PTPN13, in that order. Associated pathways, which connect cystic fibrosis to pancreatic and liver diseases, suggest that the immune system is most likely engaged and that ubiquitin C is most likely a critical node. Additionally, new modifier genes that may have an impact on cystic fibrosis are discovered [19]. Figure 2.1 shows the entire three-dimensional representation of the CFTR gene [20]. However, our *in silico* evaluation requires functional analysis in order to provide results with a physiological meaning.

2.5 Classification of CF Mutations

Numerous different CFTR gene mutations result in varying degrees of sickness severity, which are further influenced by modifying genes, the environment in which

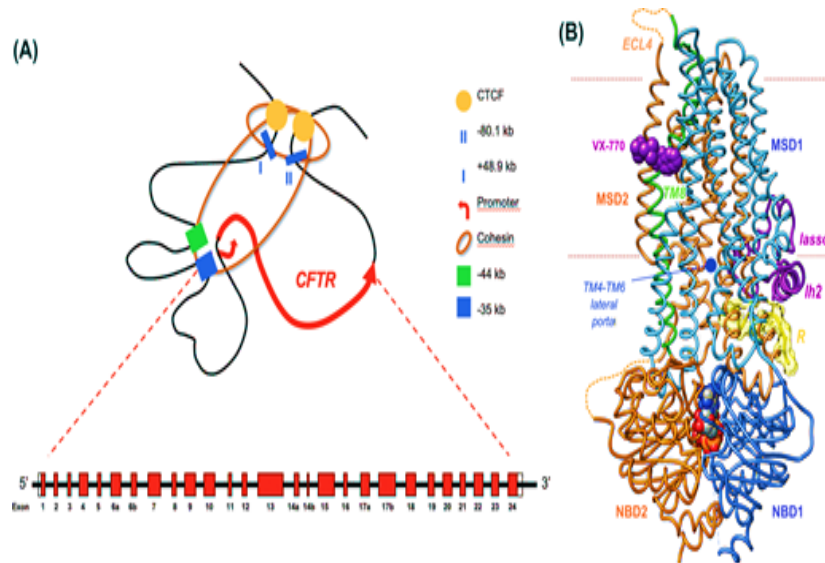


FIGURE 2.1: (A) A 3D representation of the CFTR gene's so-called topologically associated domain in airway cells is shown. This image highlights the promoter, borders (I and II), and structural proteins CTCF and cohesin. (B) Ribbon depiction of the human CFTR 3D structure in association with VX-770 (ATP-bound, phosphorylated version) [20].

the patient lives, and their socioeconomic status. Welsh Smith first classified CF mutations into four categories based on the main physiologic abnormality associated with each type of mutation. As of right now, six major classes are acknowledged [21].

CF mutation based on their cellular phenotype is shown in Figure 2.2. Class I mutations include frame shift, splicing, and nonsense mutations that produce prematurely ending codons (PTC) and significantly reduced or absent CFTR expression. Class II mutations promote misfolding, premature breakdown by the endoplasmic reticulum (ER) quality-control system, and faulty protein synthesis, which significantly reduces the number of CFTR molecules that reach the cell surface. Class III mutations cause abnormal gating with a decreased open probability by interfering with the CFTR channel's ability to regulate itself. Class IV mutations block the ion conduction pore, lowering the channel's unitary conductance [22]. Class V mutations result in abnormal promoter or splicing patterns, which impact protein amount rather than protein structure.

Class VI mutations make the channel unstable in post-ER cells and/or at the surface of the plasma membrane (PM) by reducing the channel's conformational

stability and/or generating additional internalisation signals. While many of the identified variants have unclear disease liability, attempts are being conducted to assess their operational impact and clinical severity [23].

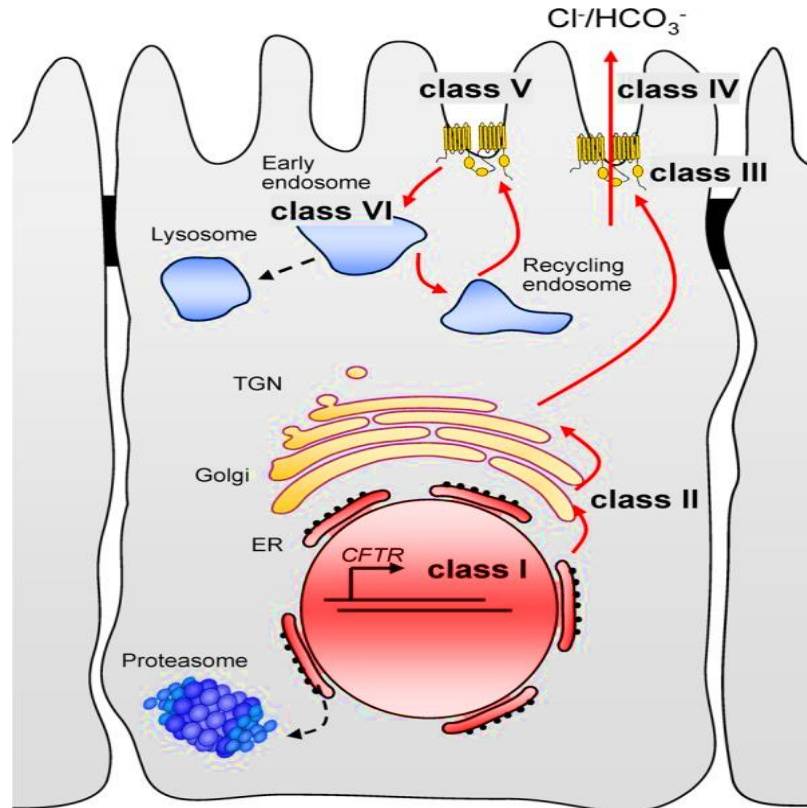


FIGURE 2.2: Traditional classification of CF mutations based on their cellular phenotype [24].

2.6 Origin

Cystic fibrosis is the most common chronic autosomal recessive disease, affecting 1 in 2,500 individuals in communities of European heritage (Figure 2.3). It is caused by mutations that were identified and cloned in 1989 (CF transmembrane conductance regulator) [26]. Since then, there have been reported to be 1,000 mutations. Although there are five mutations, their distribution in Europe exhibits distinct regional patterns [25]. For example, DF508 exhibits a gradient from the northwest to the southeast, exhibits the greatest prevalence in Denmark (87.2% of all CF chromosomes) and exhibits the lowest prevalence in Turkey (21.3%) (European Working Group on CF Genetics 1990). Most frequently (16.7%) found

in the Balearic Islands, G542X is found in most of Europe and is widespread in Mediterranean nations. The Mediterranean region is home to N1303K, which is most prevalent (17.2%) in Tunisia. While it is rare in other regions of Europe, the mutation G551D is frequent in northwest and central Europe. Finally, the mutation W1282X is widespread throughout the Mediterranean region, with Israel having the highest frequency (36.2%) [26].

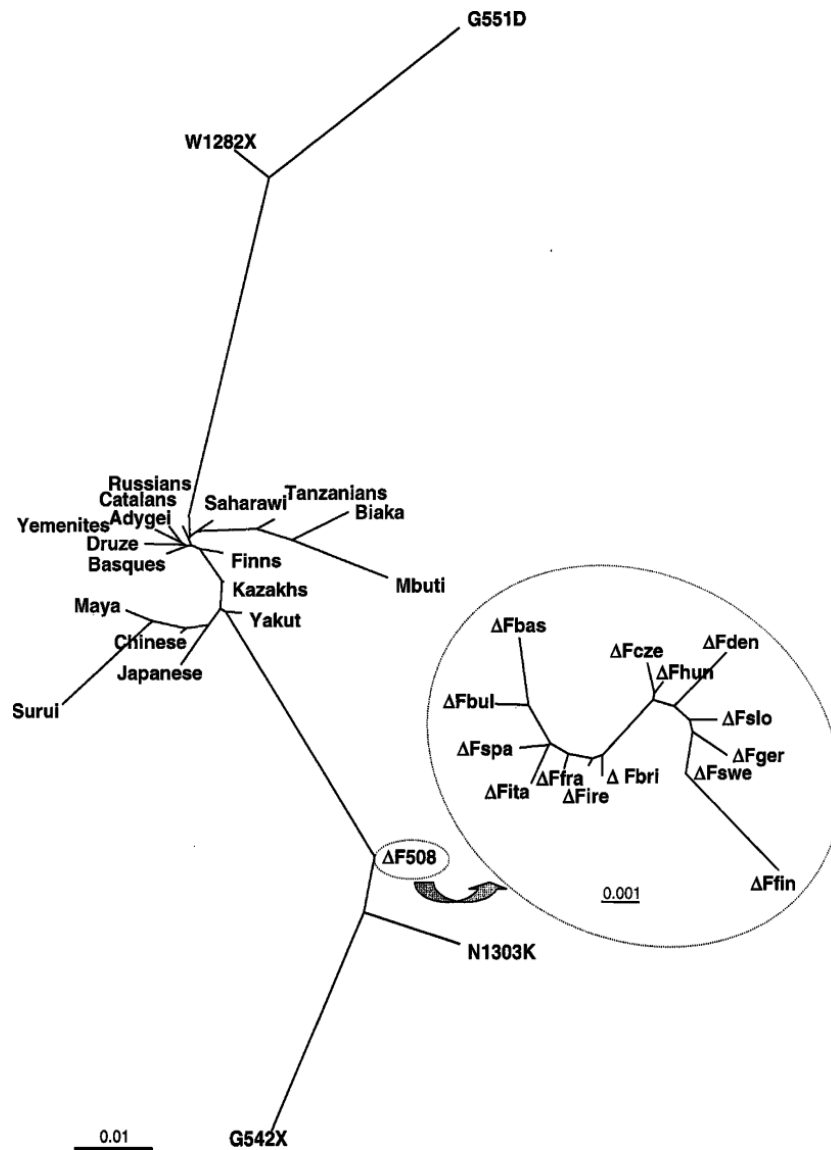


FIGURE 2.3: Maximum-likelihood tree showing the frequency of alleles at five loci (IVS6aGATT, IVS8CA, T854, IVS17bTA, and TUB20) in normal chromosomes from all populations as well as in CF chromosomes (F508, G542X, N1303K, G551D, and W1282X chromosomes) [27].

In the phylogenetic tree (Figure 2.4), *P. harmala* and *Nitrariatangutorum*, a different Nitrariaceae species, formed a single blade. According to the Nitrariaceae

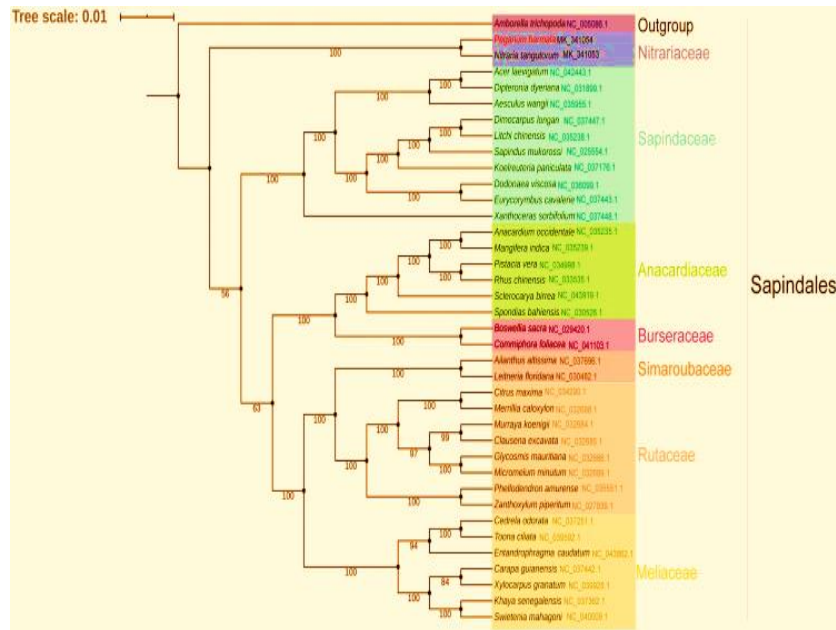


FIGURE 2.4: A phylogenetic tree constructed based on 38 complete chloroplast genome sequences [28].

blade, which is the lowest branch among Nitrariaceae species, Nitrariaceae was once distinct from other Sapindales plants. In a nutshell, this study offers crucial information for comprehending the evolutionary position of plant species in the Nitrariaceae family [28].

2.7 Cystic Fibrosis-Related Innate Immune Cell Mutations: A Signalling Pathway

In CF, CFTR function loss results in increased Na^+ inflow by ENaC, water absorption that dehydrates the periciliary layer (PCL), the buildup of a thick, solid coating of mucus on the apical surface, and chronic opportunistic pathogen colonization. The chronically inflammatory lung milieu promotes neutrophil infiltration, which, upon activation, causes the release of an excessive number of neutrophil extracellular traps (NETs) [29]. The CFTR dysfunction in CF AECs (as shown in Figure 2.5) disrupts the intracellular ionic equilibrium, which causes ENaC to become overactive and increase Na^+ influx and K^+ efflux. Activating the NLRP3 inflammasome leads to an increase in IL-1 and IL-18 secretion as a result of the

exacerbated K^+ efflux, increased ER stress, and reactive oxygen species (ROS) generation [31].

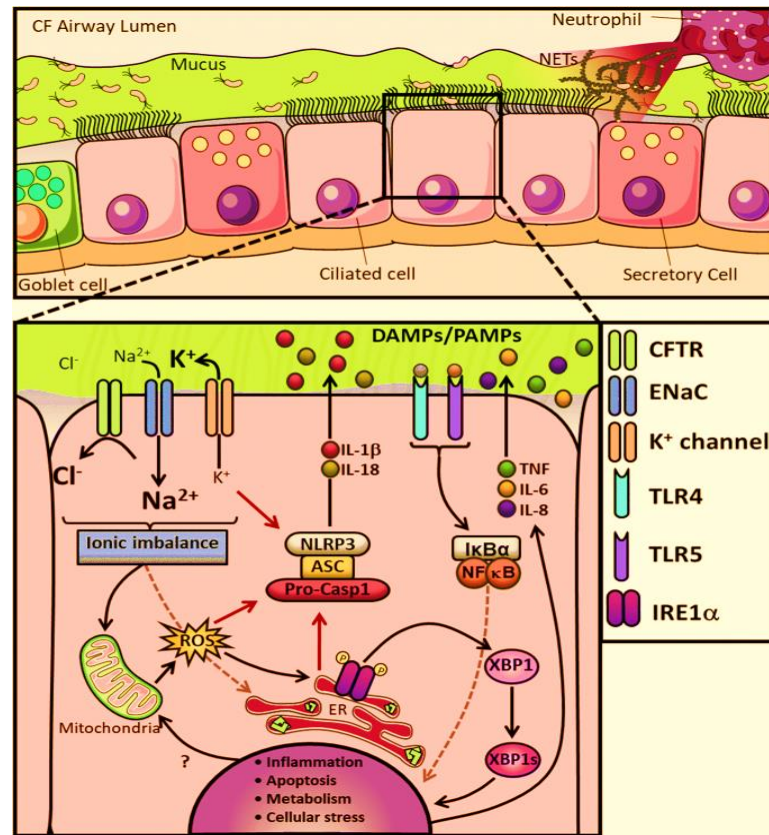


FIGURE 2.5: CF airway and altered Airway Epithelial Cells mechanisms [32].

Additionally linked to the ionic imbalance are elevated levels of ER stress, ROS, and metabolic turnover. A variety of UPR-related genes are activated by the misfolded CFTR, which leads to the activation of IRE1 and the production of the spliced form of XBP1 (XBP1s), which in turn promotes inflammation. In addition to all the other defective signalling pathways, overactivation of surface and intracellular receptors via DMAPs and PAMPs results in an aggravated inflammation associated with increased TNF, IL-6, and IL-8 production [32].

2.8 Symptoms

Three items in the abdominal pain domain measure the frequency, severity, and duration of stomach pain. There are eight non-pain symptoms (in Figure 2.6),

including flatulence, abdominal bloating, constipation, vomiting, nausea, heartburn, greasy stools, and stomach acid reflux [33].

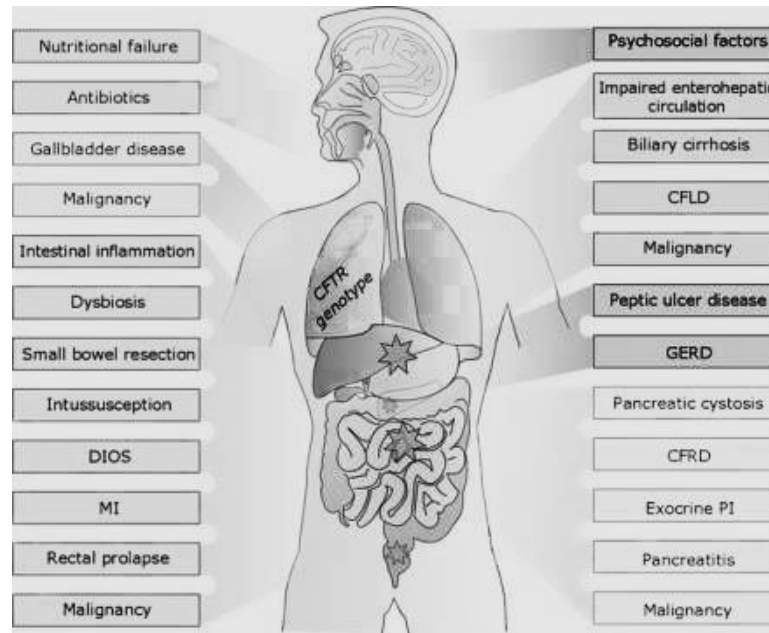


FIGURE 2.6: Multifactorial causes of abdominal symptoms in CF [33].

Lack of hunger, loss of taste, and the necessity for forced feeding are examples of eating and hunger disorders [33]. When a patient received parenteral antibiotic treatment for any 4 of the 12 signs or symptoms listed below, as clinically defined in the research, a serious worsening of respiratory symptoms was stated to have happened. Malaise, weariness, or drowsiness; fever over 38 °C; anorexia or weight loss; changes in sputum; increase in hemoptysis; cough; difficulty in breathing; change in sinus discharge; abnormalities in the physical checkup of the chest; a 10 percent or more decline from a previous measurement in pulmonary function; radiographic abnormalities diagnostic of pulmonary infection [34].

2.9 Treatment for Cystic Fibrosis

Small molecules known as CFTR modulators, which target the underlying cause of the disease, have been developed as a result of the CFTR sequencing gene. Vertex Pharmaceuticals now has four such medications registered and on the market. In comparison to earlier generation medicines, the most recent of these, the triple combination

of ivacaftor, elexacaftor and tezacaftor is suitable for a greater proportion of mutation profiles [35]. It is necessary to meet a crucial prerequisite in order to develop novel therapeutic approaches. Gene therapy is one such tactic that goes after the disease's root cause as opposed to its secondary symptoms.

This approach may significantly alter the course of the disease when paired with small medicines that target the function of the CFTR protein. The main target, the airways, can be accessed easily via current routes; the lungs are normal at birth, indicating a potential therapeutic window; and since CF is a single-gene disorder, heterozygotes exhibit normal phenotypes, indicating that levels are not required to reach those of wild-type.

Although liposome formulations, Adeno-associated virus (AAV) - and adenovirus-mediated transmission of CFTR in clinical studies for CF gene therapy remain promising, they have not yet shown the anticipated clinical advances that this strategy promises. Gene therapy, which involves transferring copies of the normal CFTR gene to the essential cells, should theoretically be well-suited to CF [36].

2.10 CFTR Modulators

2.10.1 Ivacaftor

As the CFTR potentiator, ivacaftor lengthens the time that the CFTR channel opens, enabling chloride ions to cross the CFTR proteins on the epithelial cells that make up its outermost layer [19]. Ivacaftor is the first FDA-approved treatment to target the underlying defect in CF. The study found that in homozygous F508del patients, ivacaftor alone is unsuccessful [37].

2.10.2 Lumacaftor (VX-809)

CFTR proteins in epithelial cells' endoplasmic reticulum are misfolded as a result of the class II mutation F508del, preventing the proteins from entering the

cell surface. The first in vitro research suggested that lumacaftor could speed up the "trafficking" of CFTR proteins, enabling those proteins to penetrate the membrane and transport chloride. The combined effect of lumacaftor and ivacaftor is being studied for F508del mutation patients because of the less-than-significant effects observed with either drug alone in patients homozygous for the mutation [38].

2.10.3 Lumacaftor Plus Ivacaftor

Lumacaftor and ivacaftor are combined because Lumacaftor facilitates the movement of the CFTR protein to the epithelium surface, whereas ivacaftor helps the CFTR protein open and transport chloride [39].

2.10.4 VX-661

Another oral CFTR corrector, VX-661, was created by Vertex Pharmaceuticals in order to treat CF and is similar to lumacaftor. In comparison to VX-661 alone, ivacaftor and VX-661 together increased CFTR activity in vitro. VX-661 is a prospective corrector, according to preliminary findings, and further research may show its potential benefits for CF sufferers [40].

2.10.5 Ataluren (PTC124)

PTC Therapeutics has created Ataluren, a first-of-its-kind PTC suppressor that treats class I CFTR gene mutations. In terms of its structural makeup, ataluren is functionally comparable to the aminoglycoside antibacterial gentamicin.

However, the two substances are structurally different, and ataluren lacks the toxicities or antibacterial properties of an aminoglycoside [41].

2.10.6 Other Potential CFTR Modulators

Preclinical testing has been done on more than 30 substances to see if they are suitable for CFTR modulation. The next three examples are:

2.10.6.1 4PBA

In CF epithelial cells with the F508del mutation, chloride transport was restored in vitro by the short-chain fatty acid sodium 4-phenylbutyrate (4PBA), but its exact mode of action was unknown [42].

2.10.6.2 VRT-532

In proteins with the F508del mutation, the pyrazole VRT-532 was discovered to be a CFTR corrector in human CF airway cells. The surface gene expression of proteins impacted by the F508del and G551D mutations was restored by VRT-532, according to further preclinical experiments, proving that the drug also acts as a CFTR corrector [43].

2.10.6.3 N6022

N6022 is a novel injectable drug that has been demonstrated to raise CFTR levels at the epithelial surface and lower lung inflammation [44].

2.11 Medicinal Properties

Damage to the alveolar-capillary basement membrane and epithelial cells is a hallmark of pulmonary fibrosis. Transforming growth factor β (TGF- β) and TGF- β -receptor-1 overexpression caused lung fibroblasts to differentiate into myofibroblasts, which is a concerning indication and is thought to be the primary event in the development of pulmonary fibrosis [45]. *Peganum harmala*, also referred to as

Syrian rue or Harmal, is a glabrous perennial that grows in semi-arid sandy soils. The shrub has white blossoms and spherical seed capsules with around 50 seeds. Its length ranges from 0.3 to 0.8 metres. This plant is commonly grown for medical purposes throughout the Middle East. It can be found in Jordan's marginal and desert regions, where its seeds have long been boiled or burned to make an antiseptic and disinfectant. Many human illnesses, including as lumbago, asthma, colic, jaundice, and as a stimulating emmenagogue, have been treated with the herb. Additionally, antiviral, antifungal, and antibacterial qualities have been asserted for it [46].

2.12 *Peganum harmala*

Peganum harmala L. is a glabrous perennial plant native to the eastern Mediterranean, grows haphazardly in semi-arid environments, steppe regions, and sandy soils. It is a shrub growing to a height of 0.3–0.8 m that features white blossoms, thin creeping roots, and oval seed capsules with over 50 seeds. The plant is well-known in Iran in addition to being widely accessible and used as a therapeutic herb throughout the Middle East, North Africa, and Central Asia. Australia and America have both adopted it [47]. Iranians burn dried capsules along with other chemicals as a protection against "the evil eye". The name "Espand" for this plant is used in Iran, "Harmel" in North Africa, and "African rue," "Mexican rue," or "Turkish rue" in the United States. For a very long time, Iran and other nations have employed *P. harmala*'s seeds, fruits, root, and bark as traditional medicines. Local herbalists in Pakistan, particularly in Lakki Marwat and Bajaur Agency (a tribal region of Pakistan), have employed the fruit and seeds of *P. harmala* to treat a variety of illnesses. Similar to how fruits can be used as a vermifuge to alleviate heart pain, seeds can be used to cure fever and colic pain by combining them with honey. A decoction of *P. harmala* seeds was used by indigenous communities in Wana, a district in South Waziristan Agency, Pakistan, to heal jaundice, prevent disease, prevent pregnancy, encourage milk flow, and serve as a stimulant. Moreover, galactagogic, antiparasitic, antiperiodic, antispasmodic, and narcotic qualities have been discovered in *P. harmala* seeds [48].

2.12.1 Traditional Uses

Different cultures and ethnic groups have employed *P. harmala* for medicinal, superstitious, and even ritual purposes. In Morocco, where the plant is burned to keep off ghosts and ghouls, *peganum* is used in a superstitious manner [49]. It is employed to protect a person or condition from the evil eye in Iran, Turkey, China, and other Arab nations in Africa and Asia. *Peganum* is burned in two different rituals around the world: one is a special Zoroastrian ceremony where a prayer is recited and the *peganum* is lit on fire; the other is an Indian wedding ritual where *peganum* is burned so that the bride and groom can avoid a life of darkness. However, *Peganum*'s medicinal properties are more well-known because they've been in use for a while in treating diabetes, asthma, arthritis, hypertension, and many other disorders in various cultures [50].

2.12.2 Biological Components of *P. harmala*

Its broad-spectrum antibacterial activity is based on a wide range of compounds. Alkaloids, flavonoids, triterpenoids, anthraquinones, phenylpropanes, carbohydrates, amino acids, volatile oils, sterols, vitamins, proteins, carotene, and trace elements are among the at least 308 distinct chemical components of *P. harmala* that have been isolated and identified. The antimicrobial activity of alkaloids is the strongest. More than 308 substances have been identified from *P. harmala*, including 97 alkaloids, 24 flavonoids, 10 triterpenoids, 3 anthraquinones, 2 phenylpropanoids, 18 carbohydrates, 17 amino acids, 99 volatile oils, 26 fatty acids, 3 sterols, 1 vitamin, 1 protein, 1 carotene, and 6 other trace elements. In terms of concentration, carboline alkaloids (Cs) are the most prevalent substance. Seeds contain up to 10% of alkaloids, with roots and leaves having a lower amount (Figure 2.7). Recently, some new compounds have been discovered; the main ones are harmine, harmaline, harmalol, harmene, and harmol [51].



FIGURE 2.7: *P. harmala* (A) plant; (B) flower; (C) ripe fruits; (D) seeds [52].

2.13 Molecular Docking

For the past three decades, molecular docking has been used to find various molecular structures and to build drugs with the aid of computers. One of the main roles played by docking is to give the analysis of how the ligand interacted with the protein, locking it for optimising the lead compounds for drug development [54]. Docking is preferred when performing virtual screening on the compounds present in databases or libraries for analysis of their functions. To predict the potential outcomes of the receptor-ligand complex, several docking programmes use one or more search techniques. This is the main factor that has made molecular docking so important for applications in molecular modeling and drug discovery. The docking outcome provides an interaction score, and the precision of the scoring system makes docking more reliable for predicting the ligand posture and, consequently, the ligand binding location. This allows it to forecast the binding affiliation, which in turn identifies a potential lead medication in connection with the target protein [55].

2.14 Insilico Methods and Molecular Docking

The phenotypic manifestation of cystic fibrosis, a genetic disorder primarily affecting the digestive, urogenital, and respiratory systems, is lung inflammation. Synthetic compound-based anti-inflammatory medications work well, however they have unfavourable side

effects. This study uses a cutting-edge method to identify the most potent natural ingredient (s) from marine and plant sources to treat cystic fibrosis-related conditions with the least amount of side effects. The development of computational methodologies and insilico methods is linked to drug discovery with cheap investment and good outcomes that offer a focused approach to identifying the lead chemical [56].

2.15 In silico Drug Repositioning on F508del CFTR

Academic institutions and business sectors are becoming more interested in computational drug repositioning due to its capacity to quickly screen a large number of compounds insilico (by utilising extensive drug datasets) and save development costs and time. For cystic fibrosis, a disease mostly brought on by the deletion of Phe 508 (F508del) from the cystic fibrosis transmembrane conductance regulator protein, the possibility of medication repositioning has not yet been thoroughly assessed. As a result, F508del-CFTR is retained in the endoplasmic reticulum and swiftly broken down by the ubiquitin/proteasome pathway. Even now, CF is a deadly illness. Certain CFTR-rescuing medications can already treat it, however new generation medications with greater therapeutic value and fewer adverse reactions are currently being developed. One method that has been effectively used to reposition some medications for the therapy of different ailments is drug repurposing. Drug repurposing has only been considered in relation to CF in order to improve mucociliary clearance and deliver inhaled antibiotics into the lungs; it has not yet been proposed to be used to get around CFTR malfunction [57].

2.16 F508del CFTR Protein

The most prevalent lethal mutant in Caucasian populations, F508del CFTR, is caused by a 3-bp in-frame deletion of codon 508, which is present in 70% of CF chromosomes

worldwide out of over 800 documented CFTR variants. By analyzing $\Delta F508$ CFTR in several heterologous systems, it was discovered that faulty protein maturation causes CFTR expression to be abrogated [58]. In order to leave the endoplasmic reticulum and process in the Golgi compartment, mutant CFTR cannot adopt a protease-resistant mature conformation, which is why it was discovered to be arrested in an early wild type intermediate. Immature F508del CFTR had a prolonged contact with the chaperones calnexin and hsp70, suggesting that the cell's quality control recognized the aberrant protein. This interaction led to the premature destruction of the protein by the ubiquitin-proteasome pathway in a pre-Golgi compartment [59]. Targeting the underlying genetic deficiency in CFTR produced by the F508del CFTR mutation which affects 90% of patients with CF will probably be required in order to repair or improve CFTR function in the majority of CF patients. Because the F508del CFTR mutation prevents the protein from folding correctly, it inhibits CFTR processing in the endoplasmic reticulum (ER). Reduced F508del-CFTR transport to the cell surface results from misfolded F508del-CFTR being retained and broken down by the ER [60]. Furthermore, there is increased turnover and incorrect channel gating in the limited amount of F508del-CFTR that reaches the cell surface. Drug that increases the delivery of functional F508delCFTR to the cell surface may be necessary to improve chloride transport via F508del-CFTR.

2.17 Natural Compounds as Inhibitors of F508del CFTR Protein

The FDA has approved medicine cysteamine, which is cystamine in a reduced form. Here, we report that oral administration of cysteamine to newborn mice with the F508del CFTR mutation significantly lowers mortality and enhances phenotypic. In nasal epithelial cells from F508del homozygous CF patients, cysteamine was likewise able to improve the plasma membrane expression of the F508del-CFTR protein, and these effects remained for 24 hours after cysteamine withdrawal [61]. Genistein was one of the first substances discovered to affect mutant CFTR. The molecule genistein (5,7-dihydroxy-3- (4-hydroxyphenyl) 4H-1-benzopyran-4-one) belongs to the isoflavone family of heterocyclic polyphenols that are naturally present in many legumes. Soya is perhaps one of the richest sources of genistein,

even though it contains the glycoside genistin instead of genistein. [62]. One of the major causes of airway infection in CF patients is *Staphylococcus aureus*. The nutritional supplement curcumin is now readily available and is said to have antioxidant, anti-tumor, and anti-inflammatory properties. Curcumin has been demonstrated to prevent several enzymes in vitro, most notably the sarcoplasmic - endoplasmic reticulum calcium ATPase (SERCA), which is crucial for the F508 CFTR. Curcumin's inhibition of SERCA is thought to prevent calcium from being taken up by the endoplasmic reticulum in an ATP dependent manner, interfering with a variety of calcium-dependent chaperones as well as other calcium-dependent activities) [63].

The administration of medications that combine genistein and curcumin to treat G551D CFTR are also recorded, with genistein causing a peak rise in G551D CFTR currents of nearly 25 times at an 80 microgram concentration, compared to curcumin's peak increase of times at a 40 microgram concentration. Despite the fact that both curcumin and genistein are CFTR potentiators, the finding that they exhibited additive effects shows that they operate via separate processes. A.naturally.occuring.polyphenolic.substance.called.resveratrol. (3, 4', 5 = trihydroxystilbene) is present in many grains and nuts, as well as in many vegetables and fruits. The antimutagenic, anti-inflammatory, anti-oxidant, and chemo-protective qualities of resveratrol, like those of curcumin, are believed to make it beneficial. It is frequently available in health food stores. Resveratrol has been shown to boost cellular cAMP levels by directly activating adenylate cyclase and by blocking cAMP phosphodiesterases, albeit the exact mechanism(s) by which it does so is yet unknown. Resveratrol has been shown in numerous studies to improve the F508 CFTR's capacity to depart the ER, move to the cell surface, and function in cell lines, primary animal tissues, and in vivo mice NPD [64].

2.18 Potential Inhibitory Compounds in *Peganum harmala* Used as Antiseptic

Peganum harmala L., a versatile medicinal plant (analogue of ayahuasca), is increasingly employed for hallucinogenic recreational activities. The primary -carboline

alkaloids in *P. harmala* extracts were discovered and quantified as harmaline, harmine, harmalol, harmol, and tetrahydroharmine. With low concentrations in stems and leaves and absence in flowers, the largest concentrations of alkaloids were found in seeds and roots [65].

Carbolines bind to benzodiazepine, imidazoline, serotonin, and opiate receptors as well as inhibiting MAO, carbolines are naturally occurring alkaloids that have a variety of psychopharmacological effects. *Banisteriopsis caapi* (Malpighiaceae) and *Peganum harmala* L. (Zygophyllaceae), two plants whose extracts demonstrate psychedelic effects mediated and/or amplified by these substances, are found to contain -carboline alkaloids in nature. Ayahuasca, a hallucinogenic beverage consumed in rituals by Amazonian tribes, contains *B. caapi* as one of its ingredients [66].

Chapter 3

Materials and Methods

3.1 Selection of Disease

The autosomal recessive disease known as cystic fibrosis is most common in Caucasian groups. The cystic fibrosis transmembrane regulator protein gene, responsible for encoding the CFTR channel, is mutated in many ways. Therefore, defective CFTR has serious effects on the organism as a whole. Its main symptoms are pancreatic insufficiency and recurrent lung infections [67].

3.2 Selection of Protein

The most frequent deletion associated with CFTR is phenylalanine 508 (F508del-CFTR), which causes incorrect protein folding. Proteins are broken down by this process prior to their entry into the plasma membrane of epithelial cells. NBD1's F508 residue is surface-located and plays a crucial role in directing inter-domain assembly between NBD2 and MSD2 and trafficking the protein to the plasma membrane. Consequently, the endoplasmic reticulum is the intended site of degradation for the majority of F508del-CFTRs. On the other hand, some mutations might cause a protein to translocate to the membrane but lose some of its functionality or quantity [68]

The structure of PHE508 was downloaded from the available resource of protein data bank (PDB). With the DOI <https://doi.org/10.2210/pdb1CKW/pdb> and the PDB ID 1CKW the cystic fibrosis transmembrane conductance regulator: solution structures of peptides based on the phe508 region, the most common site of disease-causing F508del-CFTR mutation was downloaded.

3.3 Determination of Physiochemical Properties of Proteins

Determining the function of a protein requires a thorough examination and assessment of its chemical and physical features. For this, an ExPASy tool called ProtParam was utilized. We examined a variety of physiochemical parameters, including the molecular weight, isoelectric point, number of amino acids present, grand average of hydropathicity, instability index, and quantity of positively and negatively charged residues (Arg+Lys and Asp+Glu).

3.4 Cleaning of the Downloaded Protein

The protein structure was downloaded and the extra constituents attached to the protein was removed which is done by the use of an open source system Pymol.

The linear chain of consisting of range 1-306 amino acids kept for referring as the A chain and remaining all the constituents of the protein was eliminated so that further process is done effectively [69].

3.5 Determination of Functional Domains of Target Proteins

For determining the domains of the target protein InterPro a database that can analyze a protein was used with that it also provides information regarding the

families, functional sites and the domains of the protein under study [70]. By inserting the FASTA sequence of the main protease we got the polypeptide binding sites and homodimer interfaces.

3.6 Selection of Active Metabolic Ligands

Those ligands were selected that have previously shown some antiviral and antimalarial properties. These include the terpenes, monoterpenes, sesquiterpenes, phenolic compounds, flavonoids, coumarins and sterols.

3.7 Ligand Preparation

By using the database PubChem was downloaded for the 3-dimensional structure of the above selected ligands. PubChem is under the National Center of Biotechnology Information (ncbi) and is a database that contains the information regarding the chemical molecules. The information stored is related to the chemical names, molecular formulas, 3 dimensional or simple structures, their isomers, canonical similies and information regarding the activities of the molecules against the biological assays [70]. The structure of the ligands which were obtained from PubChem was downloaded and then the ligands MM2 energy was minimized by using Chem3D ultra. At the end sdf format was selected to save the energy minimized structure of the ligand.

3.8 Molecular Docking

For performing the molecular docking between the protein and the ligand, CBDock (Cavity detection guided blind docking) was used. CB dock finds the sites of docking automatically. CB-Dock is a method of protein and ligand docking which indicates about the sites of bonding, the size and the center is calculated. The box size is adjusted according to the ligand and then docking was performed. The

docking was performed through AutoDock Vina. As it is docking, focused on cavity binding so ratio of accuracy may be higher. For performing the docking we uploaded the 3D structure of protein in pdb format and the 3D structure of ligand in the sdf format. After this, docking was performed. The end result was 5 different poses of interaction. To select the best pose we looked upon the minimum vina score which was given in KJ/m-1 CB-Dock provided an interactive 3D visualization of results in 5 different poses. Best pose was selected on basis of minimum vina score given in (kJ/m-1).

3.9 Visualization of Docking Result via PyMol

Over the past few years the PyMol has emerged as an efficient molecular tool of visualization. The graphics and its ability to view 3D structures had been extraordinary [71]. PyMol provides a plugin which can access the results and make their visualization clearer so that the docking results can be easily studied. The pictures of the docking result can be captured also [72].

For all the process the docking result was saved in the pdb format and after visualization in the PyMol was also be saved in the pdb file format.

3.10 Analysis of Docked Complex via LigPlot

Once we get the docked complex with the lowest vina score, the next step was the analysis of the complex. The complex was in the pdb format. This analysis was done by using the software LigPlot. For the given pdb file format the schematic diagrams of the protein and ligand interactions was generated automatically. These interactions were changed by hydrogen bonds and through hydrophobic contacts.

LigPlot provides the analysis of the hydrophobic and hydrogen bonding interactions. With this LigPlot generated the 2D representation of the protein-ligand complex [73].

3.11 Ligand ADME Properties:

After the analysis the next step was the study of pharmacokinetic and toxicity properties. The weak candidates of the drug was eliminated during preclinical ADME. The remaining candidates were selected as potential drugs against the disease. By using the PkCSM optimization of the ADME (Absorption, Distribution, Metabolism and Excretion) related to human body was done.

3.12 Lead Compound Identification

After all the work was performed the next step was to find the lead compound. The lead compound was identified after applying the rule of 5 which includes:

1. The log value of the drug-like compound must be limited to 5.
2. The molecular weight should also be lesser than 500.
3. Hydrogen bond acceptors maximum number should be 10.
4. Hydrogen bond donors' maximum number should be 5.

The compound that fulfilled these rules, was selected as our lead compound [74].

3.13 Comparison with the Standard Drug

Ivacaftor and the lumacaftor- ivacaftor combination therapy have both been linked to a rate of gradually decrease in respiratory function that is less than the rate seen in untreated patients in the control registry, indicating that potent CFTR modulators may alter the course of disease [75].

3.14 Drug-Proposed against Cystic Fibrosis

Though much work has been done in making use of vaccine and drugs against cystic fibrosis but still the gap occurs in the treatment and cure of this disease. The active compounds derived from *P. harmala* which was selected as the lead

compound and when compared with the existing drug showed more positive result can be the future of medicinal drug against cystic fibrosis [76].

3.15 Overview of Methodology

Overview of methodology opted for this study is shown in Figure 3.1.

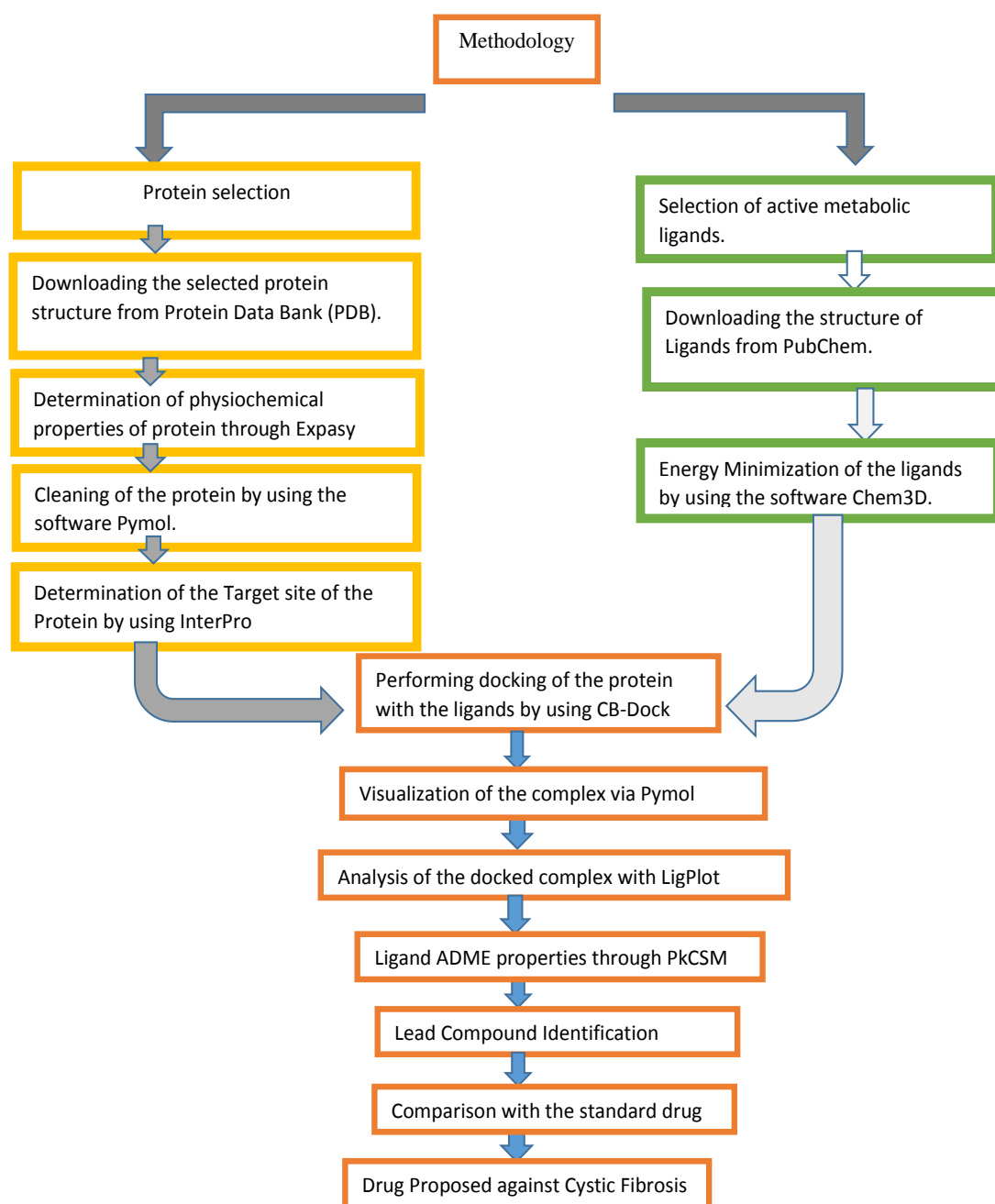


FIGURE 3.1: Methodology opted for this study.

Chapter 4

Results and Discussion

4.1 Structure Modelling

The target protein chosen to fight the necessary elements found in *Peganum harmala* is phe508del CFTR. Protein misfolding, early protein degradation by the endoplasmic reticulum quality-control mechanism, and faulty protein synthesis are all mostly caused by the phe508del CFTR of cystic fibrosis [22].

4.1.1 3D Structure of the Protein

The protein selected which is phe508 del CFTR causes cystic fibrosis, commonly due to deletion of Phe508 in NBD1 (first nucleotide binding domain) results in reduction of functional channels at epithelial cell surface. The F508del-CFTR mutation leads in a decrease in beta-stranded structure and a change in random coil structure, indicating that the structural equilibrium is moved towards a more disordered form or that the altered peptide has a different natural structure. Furthermore, there is an increased sensitivity of the mutant peptide to denaturation, indicating that F508del-CFTR is a mutation related to stability, or folding of proteins. The surface-located F508 residue of NBD1 is essential for controlling the inter-domain assembly process between NBD2 and MSD2 as well as the transportation of the

protein to the plasma membrane. Thus, the majority of F508del is supposed to be degraded at the endoplasmic reticulum [68].

For this reason it is considered as an important mutated type of cystic fibrosis to be targeted. The structure of phe508 was downloaded from the available resource of protein data bank. With the DOI <https://doi.org/10.2210/pdb1XMJ/pdb> and the PDB ID 1XMJ the cystic fibrosis transmembrane conductance regulator: solution structures of peptides based on the phe508 region, the most common site of disease-causing F508del-CFTR mutation is downloaded.

Phe508 del CFTR is a 32.89 kDa protein at almost 14 conserved sites making it an efficient drug target. There is a lot of information about protein-ligand complexes in Protein Data Bank. As seen in Figure 4.1, the resulting protein is coupled with NBD1, which was removed in order to proceed with additional processing.

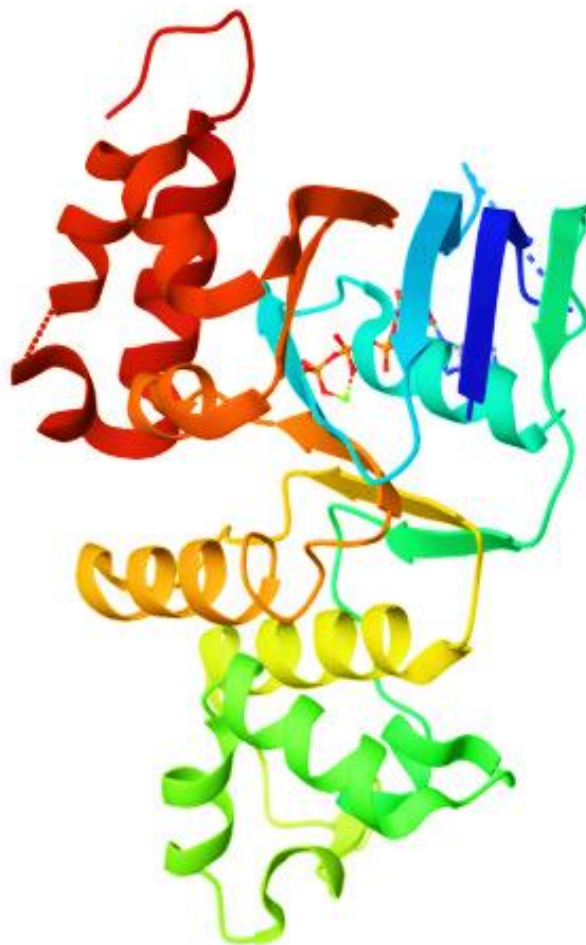


FIGURE 4.1: Crystal structure of human F508del-CFTR human NBD1 domain with ATP

4.1.2 Physical Properties of Protein

For studying the properties of phe508del CFTR protein a tool of ExPASy named as Prot Param is used. It is an online tool that is used for computing the physical and chemical properties of proteins that are entered in the Swiss prot or TrEMBL or for the proteins entered by the users. The parameters which were studied include the molecular weight, protein's amino acid composition, atomic composition, theoretical pI (isoelectric point), estimated half-life, extinction co-efficient, instability index, aliphatic index, and the last is the grand average of hydropathicity (GRAVY) [77].

Accordingly, a protein with a pI value greater than 7 indicates that it is basic, and a protein with a pI value less than 7 suggests that it is acidic. The light absorption is shown by the extinction coefficient, while the protein stability level is indicated by the instability index. If the protein stability index is less than 40, it is considered stable. Any number higher than 40 indicates the instability of the protein [78].

The thermal stability of a protein is indicated by the aliphatic index. Positive and negative amino acid residues are both visible in the protein's molecular weight (MW). Asp+Glu are the negative residues denoted by NR, while Arg+Lys are the positive charge residues denoted by PR. The interaction with the water molecules is indicated by the low GRAVY value. Every one of the aforementioned factors was taken into account [78].

The physical properties of the selected phe508del CFTR protein are discussed in Table 4.1

TABLE 4.1: Physical Properties of phe508del CFTR Protein

Sr No.	Physical Properties	Values
1.	Molecular Weight	168141.57
2.	soelectric Point	8.91
3.	Aliphatic Index	102.82
4.	Extinction Coefficient 1	187225
5.	Positive.Amino Acids Residues	170
6.	Instability Index	43.80
7.	Extinction Coefficient 2	18100
8.	Negative.Amino Acids Residues	151
9.	GRAVY	0.024

The Table 4.1 shows the molecular weight of phe508del CFTR protein as 168141.57 which is a collective weight of negative and positive amino acids residues. The pI is 8.91 which indicates that the selected protein is basic in nature. The values of light absorption in terms of extinction coefficient is 18225 and 18100. The instability index value of 43.80 shows that selected protein phe508del CFTR is quite an unstable protein. Aliphatic index also shows that selected protein is thermostable. Positive value of GRAVY indicates hydrophobicity.

4.1.3 Identification of Functional Domains of the Protein

For identifying the functional domains InterPro consortium was used. InterPro helps in finding the functional analysis of proteins and classifies them into families which is done by finding functional domains and other important sites. Functional domains are the active part of the protein that is used by the protein for interacting with other proteins or other substances. The job ID for finding the functional domain of 1XMJ is:

<https://www.ebi.ac.uk:443/interpro//result/InterProScan/iprscan5-R20231218-143-727-0706-74780309-p1m/>

Figure 4.2 shows the functional domains of the protein to be targeted. Two parts of CFTR possessed: Six membrane-spanning alpha-helices (TM1-6 or TM7-12) make up the Trans-Membrane Domain (TMD), which is joined by extra- and intracellular loops. A Nucleotide-Binding Domain (NBD) located in the cytoplasm. The sequence between residues 423 and 646 is known as NBD1, and the sequence between residues 1210 and 1443 is known as NBD2. Walker A and Walker B, ATP-binding sequences, are present in the two NBDs [79].

The extra regulatory (R) region that connects the two protein halves and the lengthy N- and C-terminal extensions that are roughly 80 and 30 residues long, respectively, are what give CFTR its specificity. Around 200 residues in the R domain seem to be rather unorganized [80]. The sequence and structure of ABC proteins' nucleotide-binding regions are remarkably conserved. A typical F1ATPase core subdomain, consisting of an alpha-helix encircled by antiparallel beta-sheets,

is present in NBDs. The conserved Walker A and B motifs, which are important in ATP binding, are present in this area. The ABC-signature motif, which is crucial for the hydrolysis of ATP, is present in the alpha-helical subdomain. It is also known that the alpha-helical subdomain mediates interaction with the transmembrane domains based on X-ray structures of bacterial transporters [81].

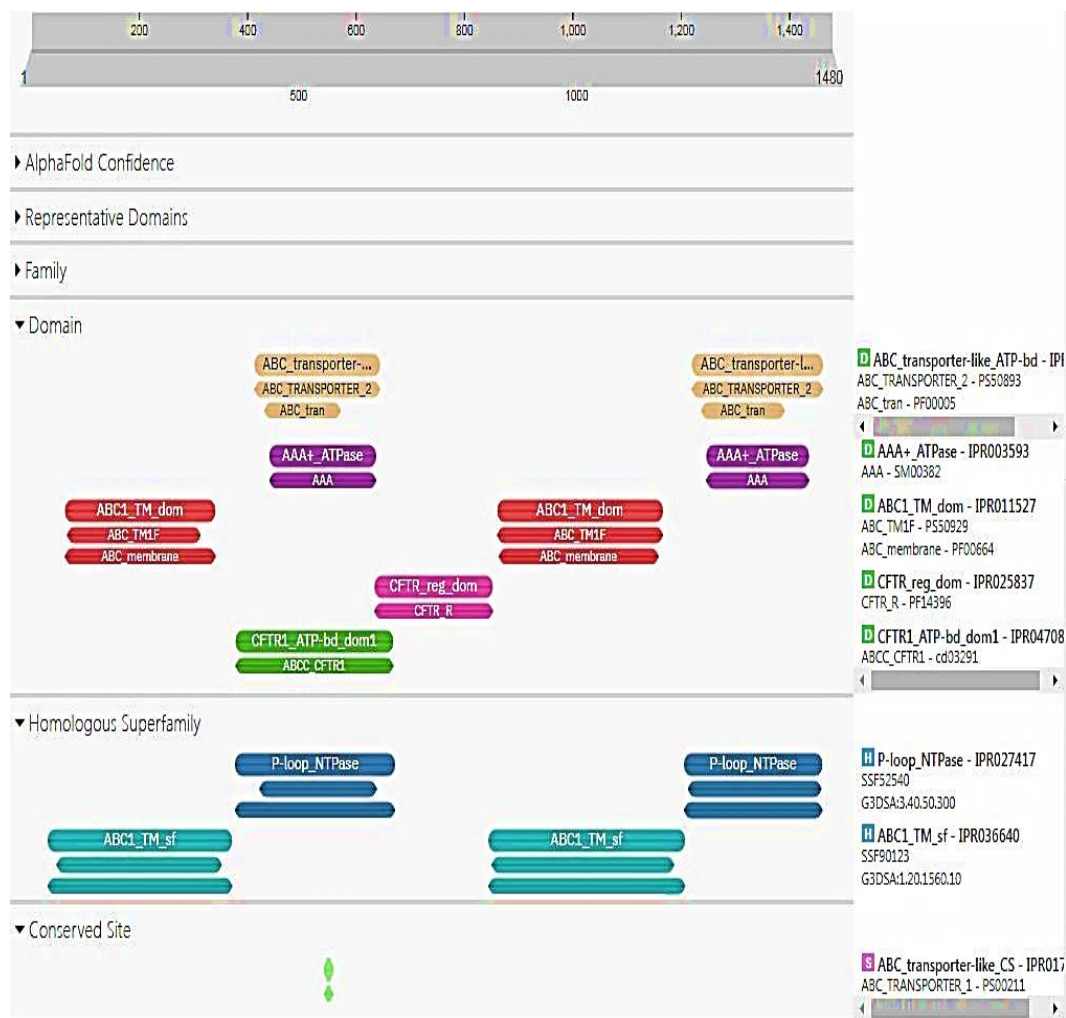


FIGURE 4.2: Functional domains of targeted protein.

The folding of NBD1 and the mechanism(s) through which $\Delta F508$ disrupts folding have been the subject of much research. The three subdomains that make up NBD1 are the ATP binding site-containing N-terminal subdomain, the Phe508-containing α -helical subdomain, and the central α/β core, which is similar to the F1-type ATPase and has a six-stranded, mainly parallel β -sheet. Additionally, NBD1 has a distinct unstructured regulatory insertion (residues 404–436), a structurally varied

area (residues 526–547), a C-terminal regulatory extension, and the typical LSGGQ signature motif (residues 548–552) [82].

4.1.4 Structure of Protein refined for Docking

PyMol is used to enhance the protein's structure. The water molecules must be removed from the protein structure. As seen in Figure 4.3, the protein is now ready for docking. NBD1 is composed of three subdomains: the N-terminal subdomain, which contains the ATP binding site; the α -helical subdomain, which contains Phe508; and the central α/β core, which resembles the F1-type ATPase and features a six-stranded, mostly parallel β -sheet. Moreover, NBD1 features a characteristic LSGGQ signature motif (residues 548–552), a structurally variable region (residues 526–547), a distinct unstructured regulatory insertion (residues 404–436), and a C-terminal regulatory extension [82].



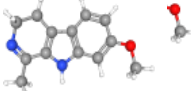
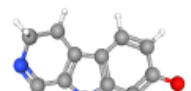
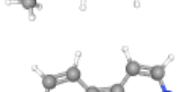
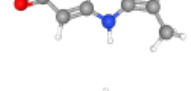
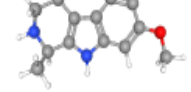
FIGURE 4.3: 1XMJ cleaned protein

4.2 Ligand Selection

Because of this, the best resolving structure based on the chemical family of the crystal bonded to the protein and subsequent binding affinities are used to pick the ligand. In this case, the ligand's conformational selection is crucial. A ligand selectively binds to one of those who conform in this selection process, strengthening it and increasing its population relative to the protein's total population. The ligands which are the active constituents of the selected plant were searched from the world's largest chemical databank- PubChem. The 3D structures of these ligands were downloaded from PubChem in the SDF format. Table 4.2 shows all the selected ligands with the information regarding their structure protein [83] - [87].

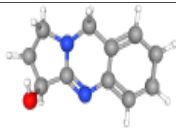
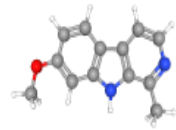
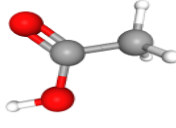

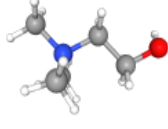
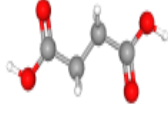
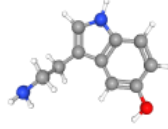
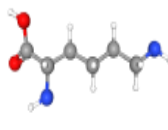
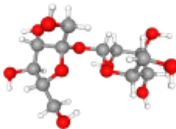
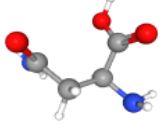
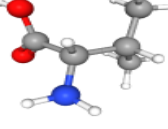
After downloading the structures of the ligands that were selected the next step that was performed was minimizing the energy of these ligands. This step is an important one as we can't use simply the downloaded structure as the ligands are unstable and it can directly affect the docking vina scores.

TABLE 4.2: Structural Information of Selected Ligands

Sr No.	Ligand Name	Molecular Formula	Molecular Weight	Structure
1.	harmaline	C ₁₃ H ₁₄ N ₂ O	214.26 g/mol	
2.	harmalol	C ₁₂ H ₁₂ N ₂ O	200.24g/mol	
3.	harmol	C ₁₂ H ₁₀ N ₂ O	198.22g/mol	
4.	tetrahydroharmine	C ₁₃ H ₁₆ N ₂ O	216.28g/mol	
5.	vasicinone	C ₁₁ H ₁₀ N ₂ O ₂	202.21g/mol	

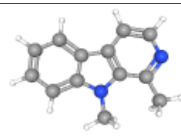
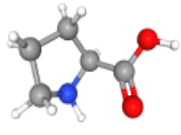
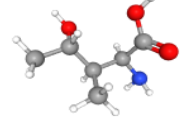
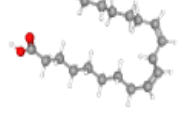
Continued on next page

TABLE 4.2: Structural Information of Selected Ligands

Sr No.	Ligand Name	Molecular Formula	Molecular Weight	Structure
6.	vasicine	$C_{11}H_{12}N_2O$	188.23g/mol	
7.	harmine	$C_{13}H_{12}N_2O$	212.25g/mol	
8.	acetic acid	$C_2H_4O_2$	60.05g/mol	
9.	betaine	$C_5H_{11}NO_2$	117.15g/mol	
10.	choline	$C_5H_{14}NO^+$	104.17g/mol	
11.	succinic acid	$C_4H_6O_4$	118.09g/mol	
12.	serotonin	$C_{10}H_{12}N_2O$	176.21g/mol	
13.	lysine	$C_6H_{14}N_2O_2$	146.19g/mol	
14.	sucrose	$C_{12}H_{22}O_{11}$	342.3g/mol	
15.	asparagine	$C_4H_8N_2O_3$	132.12g/mol	
16.	valine	$C_5H_{11}NO_2$	117.15g/mol	

Continued on next page

TABLE 4.2: Structural Information of Selected Ligands

Sr No.	Ligand Name	Molecular Formula	Molecular Weight	Structure
17.	betacarboline	C ₁₃ H ₁₂ N ₂	196.25g/mol	
18.	proline	C ₅ H ₉ NO ₂	115.13g/mol	
19.	hydroxyisoleucine	C ₆ H ₁₃ NO ₃	147.17g/mol	
20.	linoleic acid	C ₁₈ H ₃₂ O ₂	280.4g/mol	

Concluded

4.3 Virtual Screening and Toxicity Prediction through Lipinski Rule of Five

For compounds to be separated as drug-like and non-drug-like Lipinski rule of five and ADME properties are followed [89], [90]. The Lipinski rule deals with certain parameters like Molecular weight which should be ≤ 500 , $\log P \leq 5$, H-bond donors ≤ 5 , H-bond acceptors ≤ 10 . These rules are to be followed by orally active compounds. The drug-like is dependent on the mode of administration [90]. A compound is considered a drug when it follows 3 or more rules and if a compound violates two or more rules it is considered poorly absorbed [90]. Table 4.3 gives the value of Lipinski Rule for the selected Ligands.

TABLE 4.3: Applicability of Lipinski Rule on the Ligands

Sr No.	Ligand	Log P value	Molecular Weight	H-bond Acceptor	H-bond donor
1.	harmaline	2.5416	214.26 g/mol	2	1
2.	harmalol	2.2386	200.24g/mol	2	2

Continued on next page

TABLE 4.3: Applicability of Lipinski Rule on the Ligands

Sr No.	Ligand	Log P value	Molecular Weight	H-bond Acceptor	H-bond donor
3.	harmol	2.31782	198.22g/mol	3	2
4.	tetrahydroharmine	2.3832	216.28g/mol	2	2
5.	vasicinone	0.8336	202.21g/mol	3	1
6.	vasicine	1.2968	188.23g/mol	2	1
7.	harmine	3.03312	212.25g/mol	2	1
8.	acetic acid	0.0909	60.05g/mol	2	1
9.	betaine	-1.5575	117.15g/mol	2	0
10.	choline	-0.3151	104.17g/mol	1	1
11.	Succinic acid	-0.0642	118.09g/mol	4	2
12.	serotonin	1.3747	176.21g/mol	2	3
13.	lysine	-0.4727	146.19g/mol	4	3
14.	sucrose	-5.3956	342.3g/mol	11	8
15.	asparagine	-1.7263	132.12g/mol	4	3
16.	valine	0.0543	117.15g/mol	3	2
17.	betacarboline	3.03492	196.25g/mol	1	0
18.	proline	-0.177	115.13g/mol	3	2
19.	hydroxyisoleucine	-0.5848	147.17g/mol	4	3
20.	linoleic acid	5.8845	280.4g/mol	2	1

Concluded

The above table shows that out of 20 ligands, sucrose disobeys two Lipinski rule that are of hydrogen bond donor and acceptor.

4.3.1 Toxicity Prediction

The web application PkCSM can be used to forecast the values of ADMET for compounds that are bioactive and drugs. This tool will allow us to assess the toxicity of the ligands that have been chosen; several techniques are used to determine the toxicity of a particular ligand. AMES toxicity test is used to test the mutagenic potential of the compound by using bacteria. If it shows a positive response, then the ligand is mutagenic which can also act as a carcinogen [90]. *T. Pyriformis* toxicity method uses *T. Pyriformis* (protozoa bacteria) toxicity as a toxic endpoint. Any value >-0.5 log ug/L is considered toxic. The values predicted

in the Minnow toxicity test are used to represent the concentration at which the compound could cause the death of 50% of the minnows. The value below 0.5 mM is regarded as acute toxic. The values for MRTD (maximum recommended tolerated dose) gives a picture of the starting dose of a certain pharmaceutical at clinical phase I. Value $\leq 0.477 \log \text{ mg/kg/day}$ is low and a value greater than this value is considered as high [91]. For the oral rat chronic test of toxicity, the predicted log value of the lowest observed adverse effect in $\log \text{ mg/kg bw/day}$ is given which relates to the concentration of the compound given that requires the treatment time. A hepatotoxicity test predicts that if a compound could affect the liver functioning or not. A skin test predicts whether the compound could give any skin reactions or not. The hERG I and II inhibitor test determine the potential of any compound to cause the inhibition of the potassium channels associated with hERG. An inhibitor of these channels could lead to QT syndrome and on a long-term basis the person could develop ventricular arrhythmia [92]. The toxicity predicted values of the selected ligands are shown in the Table 4.4.

TABLE 4.4: Toxicity Values of Ligands

Sr. No.	Name of Ligands	AMES Toxicity	Max. tolerated dose (human)	hERG I inhibitor	hERG II inhibitor	Oral rat acute toxicity	Oral rat chronic toxicity	Hepatotoxicity	Skin sensitization	<i>T.pyriformis</i> toxicity	Minnow toxicity
1.	harmaline	No	-0.179	No	No	2.452	1.699	No	No	1.34	0.529
2.	harmalol	Yes	-0.616	No	No	2.42	1.7786	No	No	0.854	0.921
3.	harmol	Yes	-0.196	No	No	2.623	0.904	No	No	0.475	0.91
4.	tetrahydroharmine	No	-0.192	No	No	2.811	2.085	No	No	0.735	1.12
5.	vasicinone	No	0.332	No	No	1.91	1.708	No	No	0.619	1.236
6.	vasicine	Yes	0.204	No	No	2.697	1.427	No	No	0.736	1.86
7.	harmine	Yes	0.062	No	No	2.477	1.499	No	No	0.672	-0.137
8.	acetic acid	No	1.372	No	No	1.774	2.555	No	No	-0.954	2.77
9.	betaine	No	0.838	No	No	1.654	0.254	No	Yes	-0.057	2.97
10.	choline	No	0.952	No	No	1.939	0.885	No	Yes	-0.449	2.842
11.	Succinic acid	No	0.641	No	No	1.618	3.052	No	No	-0.065	2.829
12.	serotonin	No	-0.243	No	No	2.932	1.466	No	No	0.19	1.816
13.	lysine	No	1.227	No	No	2.046	3.083	No	No	0.274	2.542
14.	sucrose	No	1.574	No	No	1.677	4.527	No	No	0.285	9.287
15.	asparagine	No	1.145	No	No	1.965	2.332	No	No	0.192	3.633
16.	valine	No	1.137	No	No	2.019	2.901	No	No	0.184	2.422
17.	betacarboline	Yes	-0.021	No	No	3.327	1.034	No	No	0.543	-0.023
18.	proline	No	1.546	No	No	1.574	2.522	No	No	0.284	3.009
19.	hydroxyisoleucine	No	1.277	No	No	2.061	2.936	No	No	0.283	3.272
20.	linoleic acid	No	-0.827	No	No	1.429	3.187	Yes	Yes	0.701	-1.31

The toxicity values of all ligands are given in Table 4.4. The toxicity values of harmaline and harmalol shows that both have a low MRTD value. All other test values are in the safe range that shows harmaline are not the cause for AMES toxicity. They both are the hERG I and II inhibitors. They both have a safe toxic rate with respect to test on rat and on *T. pyriformis* with that they are not toxic to liver and does not provide any sensitivity to skin. The toxicity values of harmol and tetrahydroharmine indicates that both have a low MRTD value and it does not provide any sensitivity to skin. All other parameters of toxicity and Hepatotoxicity and that of hERG I and II inhibitors are all in the safe range. The toxicity values of vasicinone, vasicine and harmine indicates that all these three ligands have low MRTD values. All the toxicity parameters, Hepatotoxicity, hERG I and II inhibitors, skin sensitivity and *T. pyriformis* are in the positive range. Acetic Acid, betaine and choline have high MRTD values. Among all three, betaine and choline shows sensitivity to skin and indicates Hepatotoxicity, hERG I and II inhibitors, and *T. pyriformis* of all three ligands toxicity are in safe range. Succinic acid and serotonin have high MRTD values. Among all three, serotonin and lysine indicates *T. pyriformis* toxicity are in safe range. AMES toxicity, hERG I and II inhibitor, hepatotoxicity and skin sensitization of succinic acid, serotonin and lysine are in safe range. Sucrose, asparagine and valine all have the value in the safe range of AMES Toxicity, hERG I and II inhibitor, hepatotoxicity, skin sensitization and *T. pyriformis*. Betacarboline, proline, hydroxyisoleucine and linoleic Acid all values are in positive range of hERG I and II inhibitors and *T. pyriformis*. Among all these, betacarboline shows AMES Toxicity and betacarboline, proline and hydroxyisoleucine are in safe range of hepatotoxicity and skin sensitization.

4.4 Molecular Docking

Molecular docking is a technique that determines the proper structure of the ligand that binds to the binding site and estimates the strength between a ligand attached to a receptor protein through the vina score function. Docking is carried out using

the three-dimensional structures of the protein and ligands. CB dock, an online blind auto docking tool, is used for this [90], [92].

CB Dock predicts the binding sites of the protein and calculates the cavity sizes. After docking, CB Dock gives us the five best poses and receptor models. Among these five the best pose was selected depending on the vina score and the size of the cavity [91], [92].

Molecular docking is performed by using phe508del CFTR as the receptor protein and the 20 ligands selected above. The protein is in the PDB format and the ligands are in the SDF format. CB dock then checks the input files and then converts them into pdbqt format files by using OpenBabel and MGL Tools. Then CB dock predicts the cavities of the receptor and also calculates the centers and sizes of the top five cavities. Among the five best conformations the best one is selected based on a high-affinity score of the interaction between the protein and the ligand [92]. Ligands showing the best binding score between the selected ligands and the protein phe508del CFTR are shown in Tables 4.5.

Table 4.5 shows the docking result of five selected ligands that is of harmaline, harmalol, harmol, tetrahydroharmine and vasicinone. It shows that harmaline has a binding score of -6.7, with accepting two and donating one hydrogen. The logP value of this docked result is 2.5416. Harmalol shows the docking score of -6.6 with accepting or donating two hydrogen, and gives a logP value of 2.2386. Harmol, tetrahydroharmine and vasicinone shows a binding score of -6.5, -6.7 which is same as harmaline and -7.8 respectively which is less than other ligands. Among five ligands: vasicine, harmine, acetic acid, betaine and choline, vasicine is the one showing the highest binding score of -6.9. Other than vasicine, harmine shows quite a good binding score of -6.7. After these acetic acid and betaine shows a score of -3.4 and -3.9 respectively. Out of these five, choline has shown a lowest binding score of -3.3. The docking result of ligands that are succinic acid, serotonin, lysine, sucrose and asparagine shows that out of all these five ligands, sucrose shows the highest binding score. Serotonin shows a score of -5.7, lysine shows a binding score of -5.0 and succinic acid and asparagine shows a binding score of -4.9 and -4.8 respectively. Beta carboline shows highest binding affinity among 5

ligands (valine, beta carboline, proline, hydroxyisoleucine, linoleic acid). Proline and linoleic acid shows the binding affinity of -5.1 and -5.4 respectively. Whereas valine and hydroxyisoleucine shows the score of -4.4 and -4.7 respectively.

Some of the parameters of excretory properties of harmaline and harmalol has already been studied by T Akabli, F Lamchouri, S Senhaji and H Taufi in 2019 [92]. Some of the parameters of excretory properties of tetrahydroharmine, vasicine, harmol, harmine, vasicinone have been reported by Pratama, Mohammad Rizki Fadhil, et al in 2023 [93]. Pkcs_m excretion properties of beta carboline has already been reported by Y. Oloruntyiun et al in 2021 [94]. Pkcs_m excretion properties of hydroxyisoleucine and leucine have already been reported by I. Ahmad et al in 2023 [95].

TABLE 4.5: Docking Result of Ligands

Sr. No.	Name of Ligands	Binding Score	Cavity Size	HBD	HBA	LogP	Molecular Weight g/mol	Rotatable Bonds	Grid Map
1.	harmaline	-6.7	1228	1	2	2.5416	214.26g/mol	1	61
2.	harmalol	-6.6	1228	2	2	2.2386	200.24 g/mol	0	61
3.	harmol	-6.5	1228	2	3	2.31782	198.22 g/mol	0	61
4.	tetrahydroharmine	-6.7	1228	2	2	2.3832	216.28 g/mol	1	61
5.	vasicinone	-7.8	1228	1	3	0.8336	202.21 g/mol	0	61
6.	vasicine	-6.9	1228	1	2	1.2968	188.23g/mol	0	61
7.	harmine	-6.7	1228	1	2	3.03312	212.25 g/mol	1	61
8.	acetic acid	-3.4	1228	1	2	0.0909	60.05 g/mol	0	61
9.	betaine	-3.9	1228	0	2	-1.5575	117.15 g/mol	2	61
10.	choline	-3.3	1228	1	1	-0.3151	104.17 g/mol	2	61
11.	succinic acid	-4.9	1228	2	4	-0.0642	118.09g/mol	3	61
12.	serotonin	-5.7	1228	3	2	1.3747	176.21 g/mol	2	61
13.	lysine	-5.0	1228	3	4	-0.4727	146.19 g/mol	5	61
14.	sucrose	-6.4	1228	8	11	-5.3956	342.3 g/mol	0	61
15.	asparagine	-4.8	1228	3	4	-1.7263	132.12 g/mol	3	61
16.	valine	-4.4	1228	2	3	0.0543	117.15g/mol	2	61
17.	betacarboline	-6.1	1228	0	1	3.03492	196.25 g/mol	0	61
18.	proline	-5.1	1228	2	3	-0.177	115.13 g/mol	1	61
19.	hydroxyisoleucine	-4.7	1228	3	4	-0.5848	147.17 g/mol	3	61
20.	linoleic acid	-5.4	375	1	2	5.8845	280.4 g/mol	14	57

4.5 Interaction of Ligands and the Targeted Protein

The result deduced from docking is analyzed through LigPlot and PyMol. The interaction between the Ligands and the receptor protein is predicted through LigPlot+. LigPlot's graphical system uses the 3D coordinates to automatically create 2D images of interactions. The two-dimensional images show the hydrophobic contacts and hydrogen bond interactions between the ligand and side chain or main chain components of the receptor protein [92]. Table 4.6 displays the hydrogen and hydrophobic interactions, while Figures 4.4–4.23 shows the 2D schematics of the ligand–protein interaction.

Figure 4.4 shows the interaction of harmaline with receptor phe508del CFTR protein. It shows that harmaline has formed eleven hydrophobic interactions.

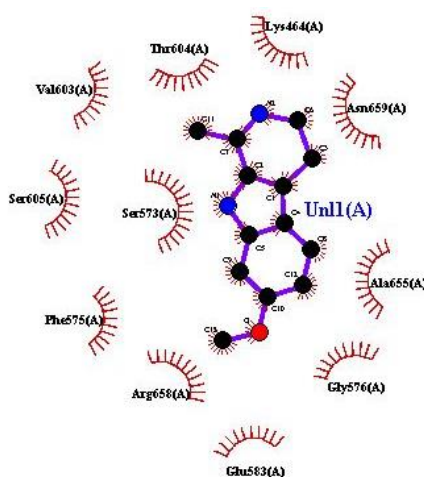


FIGURE 4.4: Interaction of harmaline with the receptor protein

Figure 4.5 shows the interaction of harmalol with receptor phe508del CFTR protein. It shows that harmalol has formed ten hydrophobic interactions and one hydrogen bond.

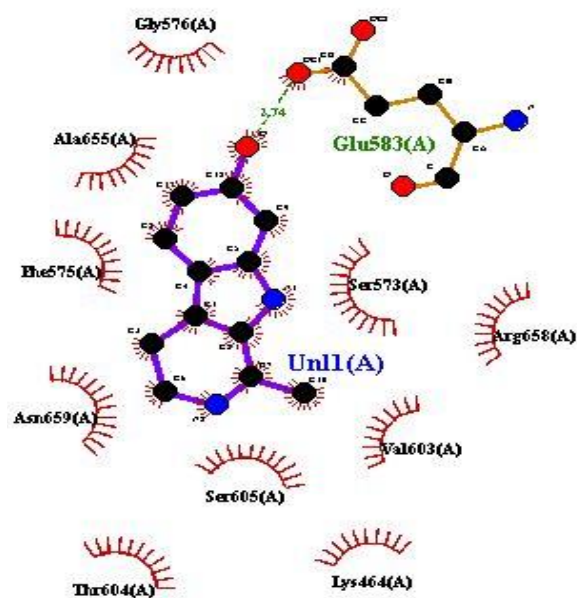


FIGURE 4.5: Interaction of harmolol with receptor protein

Figure 4.6 shows the interaction of harmolol with receptor phe508del CFTR protein. It shows that harmolol has formed nine hydrophobic interaction.

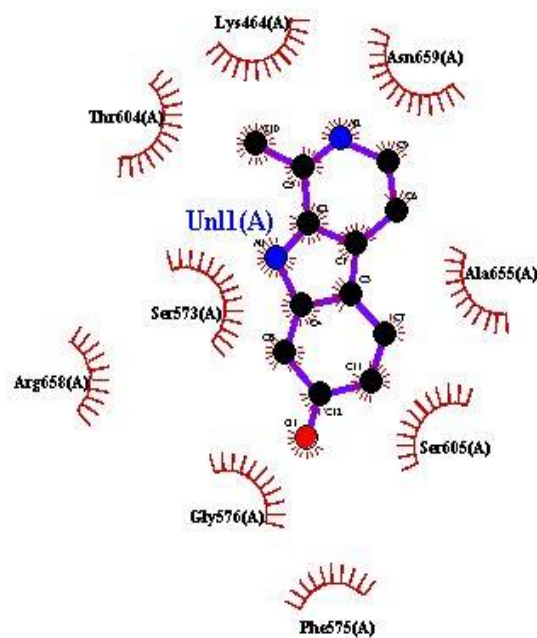


FIGURE 4.6: Interaction of harmolol with receptor protein

Figure 4.7 shows the interaction of tetrahydroharmine with receptor phe508del CFTR protein. It shows that tetrahydroharmine has formed eight hydrophobic interactions and two hydrogen bonds.

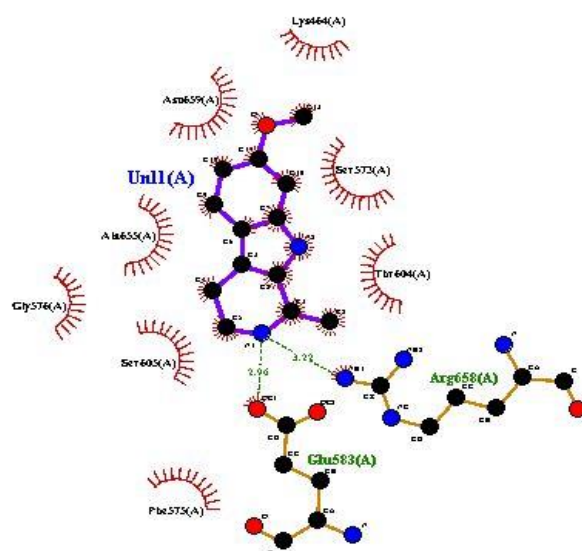


FIGURE 4.7: Interaction of tetrahydroharmine with receptor protein

Figure 4.8 shows the interaction of vasicinone with receptor phe508del CFTR protein. It shows that vasicinone has formed six hydrophobic interactions and five hydrogen bonds.

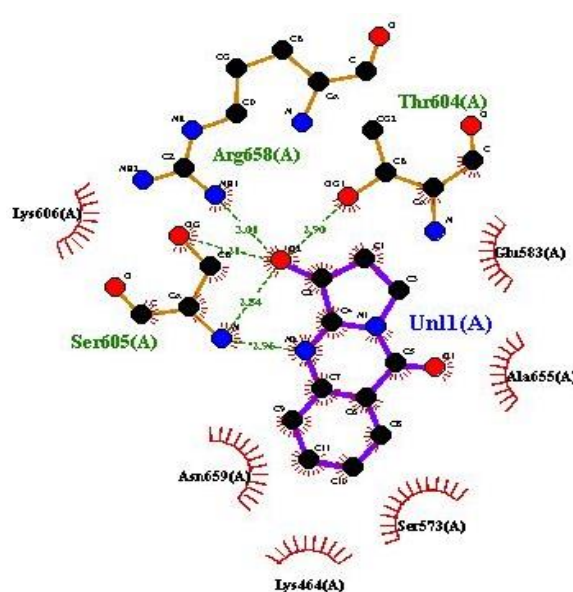


FIGURE 4.8: Interaction of vasicinone with receptor protein

Figure 4.9 shows the interaction of vasicine with receptor phe508del CFTR protein. It shows that vasicine has formed eight hydrophobic interactions and three hydrogen bonds.

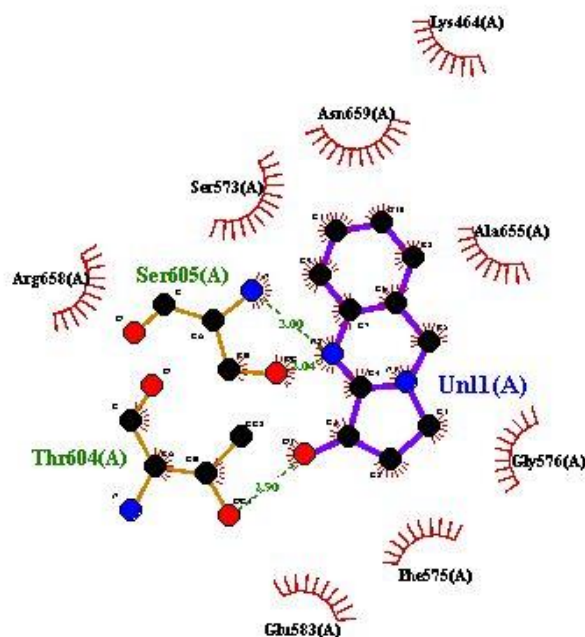


FIGURE 4.9: Interaction of vasicine with receptor protein

Figure 4.10 shows the interaction of harmine with receptor phe508del CFTR protein. It shows that harmine has formed eleven hydrophobic interactions.

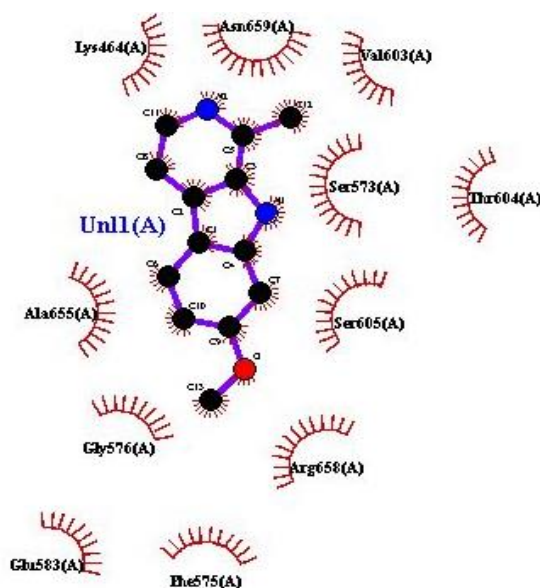


FIGURE 4.10: Interaction of harmine with receptor protein

Figure 4.11 shows the interaction of acetic acid with receptor phe508del CFTR protein. It shows that acetic acid has formed three hydrophobic interactions and four hydrogen bonds.

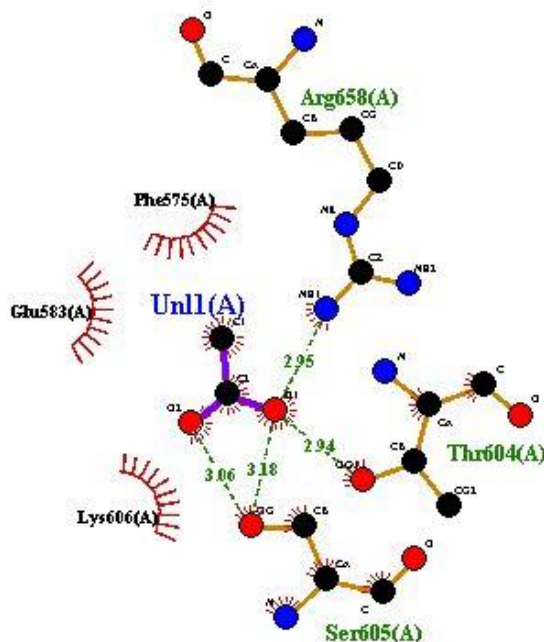


FIGURE 4.11: Interaction of acetic acid with receptor protein

Figure 4.12 shows the interaction of betaine with receptor phe508del CFTR protein. It shows that betaine has formed two hydrophobic interactions and six hydrogen bonds.

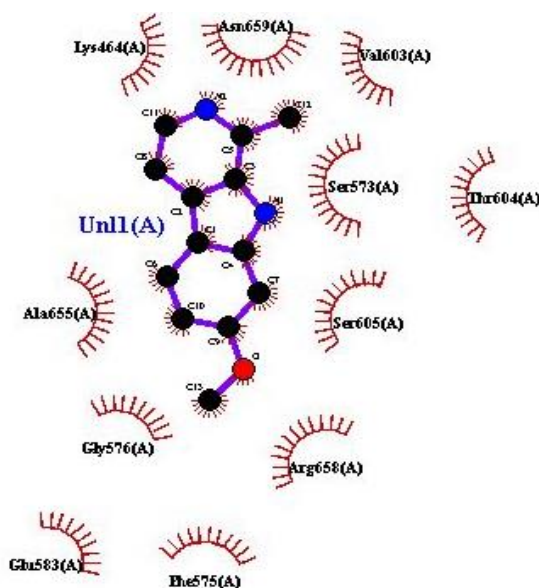


FIGURE 4.12: Interaction of betaine with receptor protein

Figure 4.13 shows the interaction of choline with receptor phe508del CFTR protein. It shows that choline has formed three hydrophobic interactions and four hydrogen bonds.

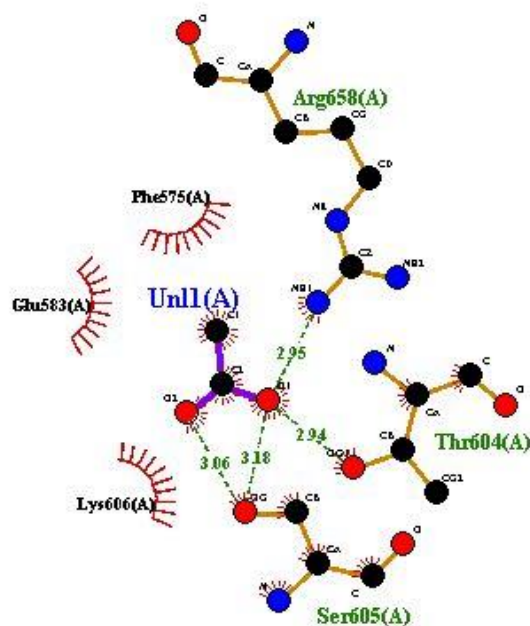


FIGURE 4.13: Interaction of choline with receptor protein

Figure 4.14 shows the interaction of succinic acid with receptor phe508del CFTR protein. It shows that succinic acid has formed three hydrophobic interactions and five hydrogen bonds.

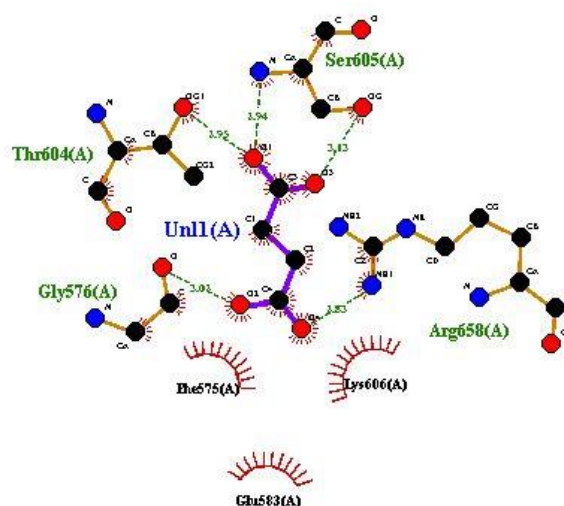


FIGURE 4.14: Interaction of succinic acid with receptor protein

Figure 4.15 shows the interaction of serotonin with receptor phe508del CFTR protein. It shows that serotonin has formed eight hydrophobic interactions and three hydrogen bonds.

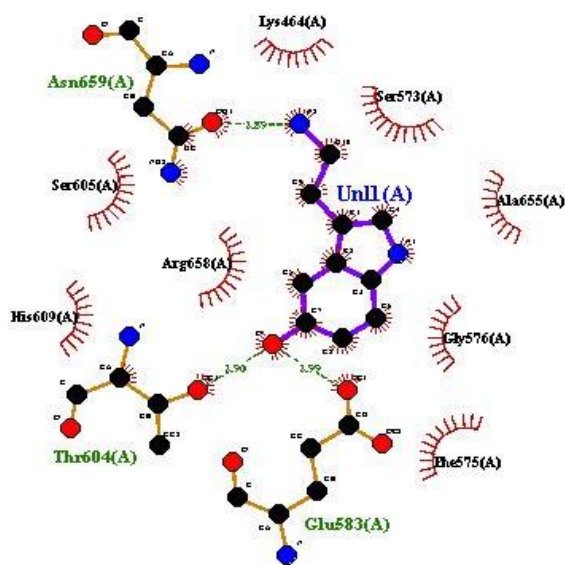


FIGURE 4.15: Interaction of serotonin with receptor protein

Figure 4.16 shows the interaction of lysine with receptor phe508del CFTR protein. It shows that lysine has formed six hydrophobic interactions and six hydrogen bonds.

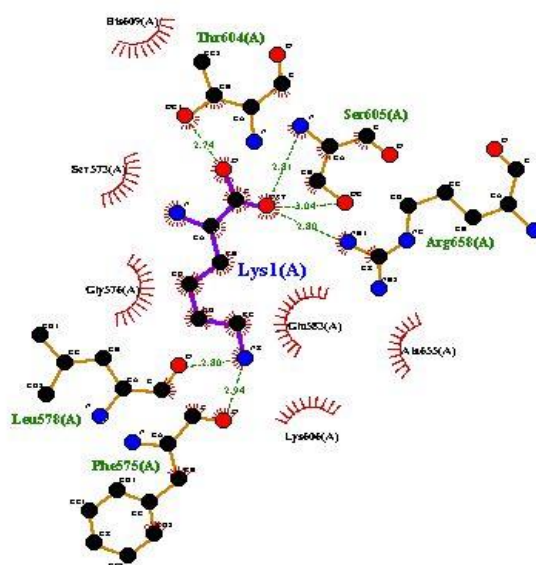


FIGURE 4.16: Interaction of lysine with receptor protein

Figure 4.17 shows the interaction of sucrose with receptor phe508del CFTR protein. It shows that sucrose has formed six hydrophobic interactions and ten hydrogen bonds.

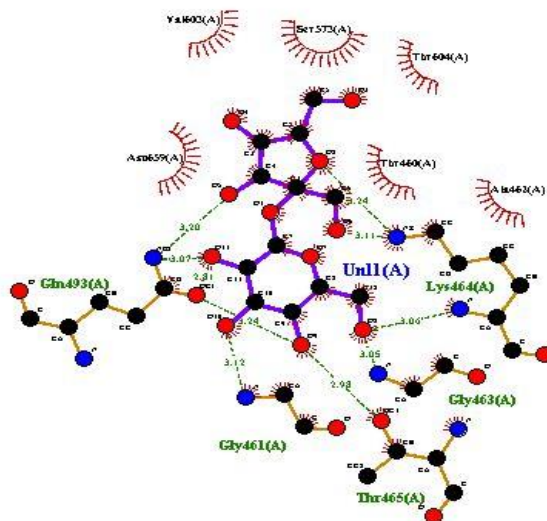


FIGURE 4.17: Interaction of sucrose with receptor protein

Figure 4.18 shows the interaction of asparagine with receptor phe508del CFTR protein. It shows that asparagine has formed three hydrophobic interactions and five hydrogen bonds.

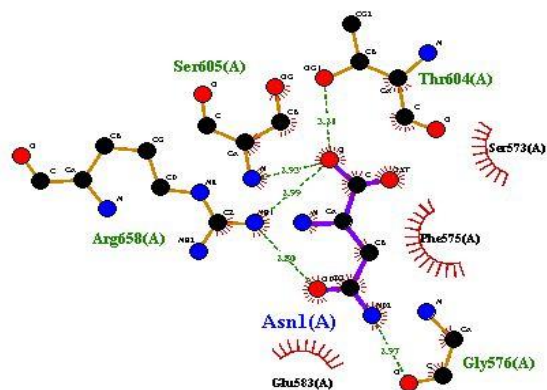


FIGURE 4.18: Interaction of asparagine with receptor protein

Figure 4.19 shows the interaction of valine with receptor phe508del CFTR protein. It shows that valine has formed five hydrophobic interactions and three hydrogen bonds.

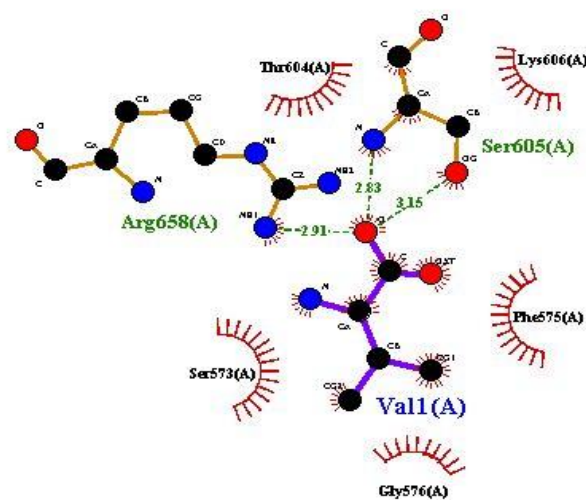


FIGURE 4.19: Interaction of valine with receptor protein

Figure 4.20 shows the interaction of beta carboline with receptor phe508del CFTR protein. It shows that beta carboline has formed nine hydrophobic interactions.

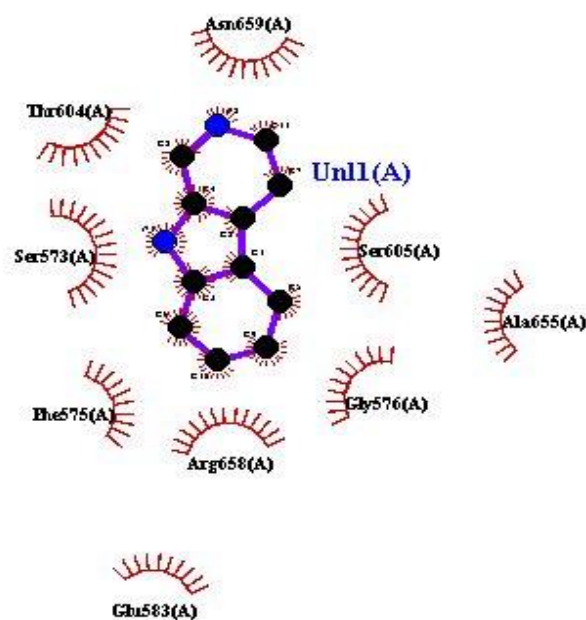


FIGURE 4.20: Interaction of beta carboline with receptor protein

Figure 4.21 shows the interaction of proline with receptor phe508del CFTR protein. It shows that proline has formed five hydrophobic interactions and four hydrogen bonds.

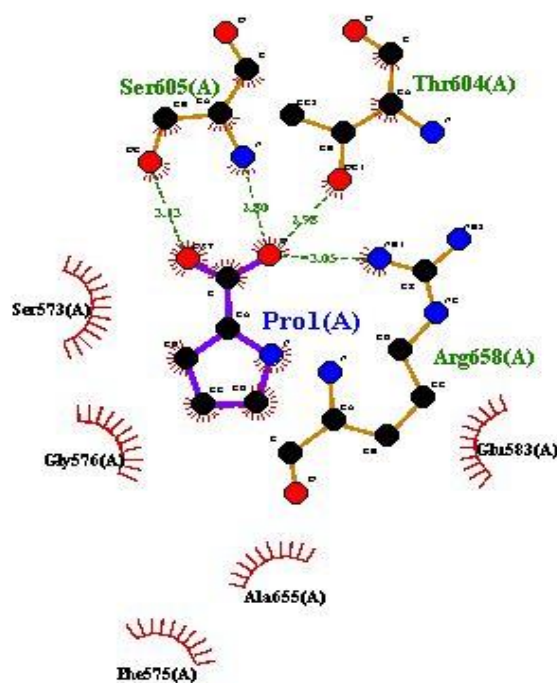


FIGURE 4.21: Interaction of proline with receptor protein

Figure 4.22 shows the interaction of hydroxyisoleucine with receptor phe508del CFTR protein. It shows that hydroxyisoleucine has formed seven hydrophobic interactions and two hydrogen bonds.

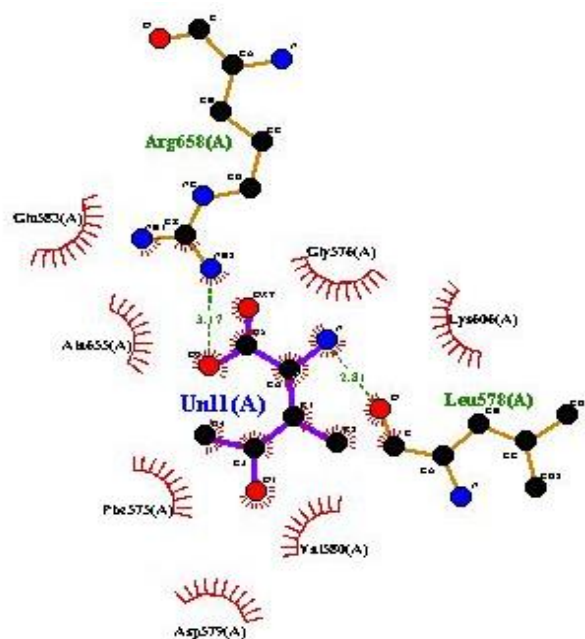


FIGURE 4.22: Interaction of hydroxyisoleucine with receptor protein

Figure 4.23 shows the interaction of linoleic acid with receptor phe508del CFTR protein. It shows that linoleic acid has formed twelve hydrophobic interactions and three hydrogen bonds.

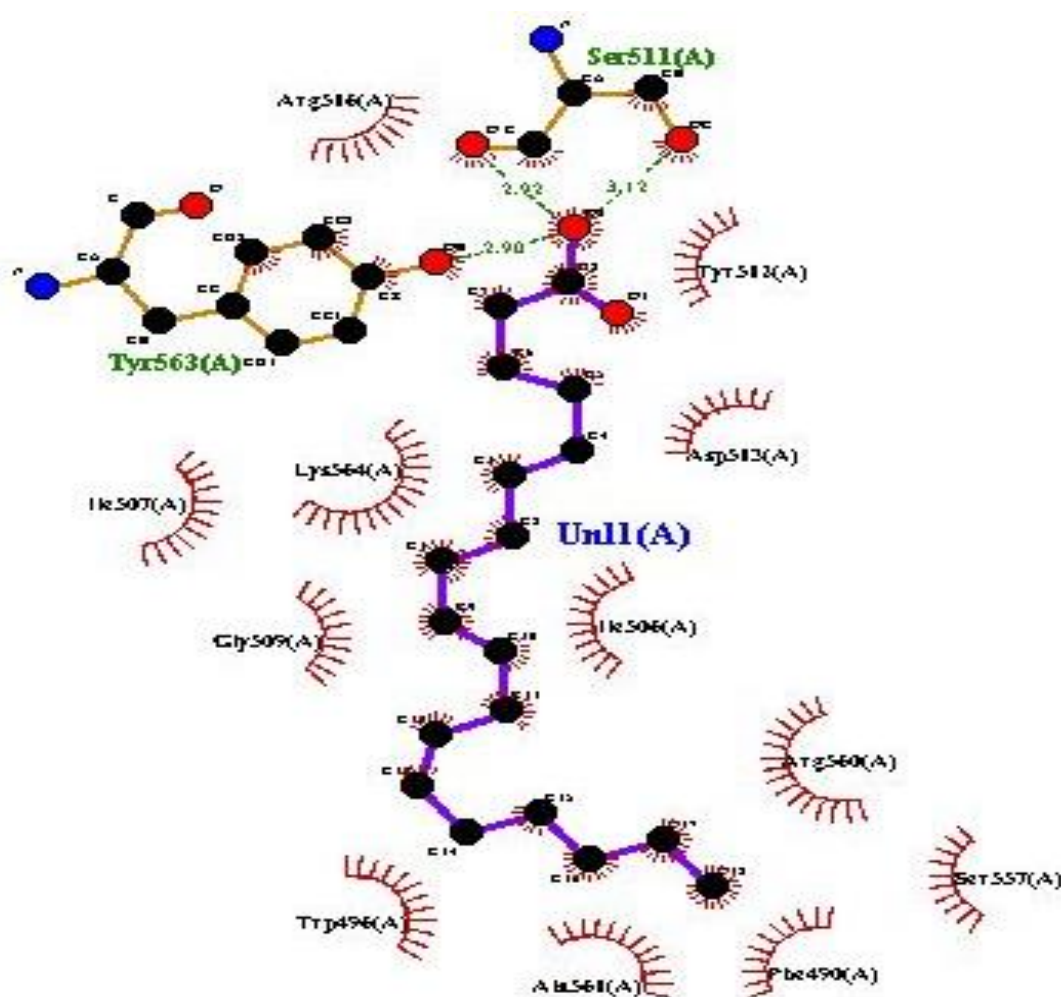


FIGURE 4.23: Interaction of linoleic acid with receptor protein

The Table 4.6 below shows the details of hydrogen and hydrophobic interactions of the selected ligands with the receptor protein. The values show that linoleic acid forms the highest hydrophobic interactions in number which is twelve, next is harmaline and harmine with eleven hydrophobic bonds, ten hydrophobic bonds are made by harmalol, nine hydrophobic interactions are made by harmol and beta carboline. The hydrogen bonds formed by sucrose are ten which is the highest in number out of all the selected ligands whereas betaine forms six hydrogen bonds. Vasicinone, succinic acid and asparagine forms five hydrogen bonds.

TABLE 4.6: Active Ligand Showing Hydrogen and Hydrophobic Interactions

Sr No.	Ligand Name	Binding Energy	No. of HBs	Bonding		Hydrophobic Bonding
				Amino Acids	Distance	
1	harmaline	-6.7	0	-	-	Val03 Ser605 Phe575 Thr604 Ser573 Arg658 Glu583 Lys464 Asn659 Ala655 Gly576
2	harmalol	-6.6	1	OE1-Glu583-O	2.74	Gly576 Ala655 Phe575 Asn659 Thr604 Ser605 Ser573 Val603 Lys464 Arg658

Continued on next page

TABLE 4.6: Active Ligand Showing Hydrogen and Hydrophobic Interactions

Sr No.	Ligand Name	Binding Energy	No. of HBs	Bonding		Hydrophobic Bonding
				Amino Acids	Distance	
3	harmol	-6.5	0	-	-	Thr604 Ser573 Arg658 Gly576 Phe575 Lys464 Asn659 Ala655 Ser605
4	tetrahydroharmine	-6.7	2	NH1-Arg658-N1 OE1-Glu583_N1	3.22 2.96	Lys644 Ser573 Thr604 Asn659 Ala655 Gly576 Ser605 Phe575
5	vasicinone	-7.8	5	NH1-Arg658-O1 OG-Ser605-O1 N-Ser605-O1 OG1-Thr604-O1 N-Ser605-N2	3.01 3.21 2.84 2.9 2.96	Glu583 Ala655 Ser573 Lys464 Asn659

Continued on next page

TABLE 4.6: Active Ligand Showing Hydrogen and Hydrophobic Interactions

Sr No.	Ligand Name	Binding Energy	No. of HBs	Bonding		Hydrophobic Bonding
				Amino Acids	Distance	
6	vasicine	-6.9	3	OG1-Thr604-O1	2.9	Lys606
				N-Ser605-N2	3	Lys464
				OG-Ser605-N2	3.04	Asn659
						Ser573
7	harmine	-6.7	0	-	-	Ala655
						Arg658
						Gly576
						Phe575
						Glu583
						Lys464
						Thr604
						Val603
						Asn659
						Ser605
						Ser573
						Ala655
8	acetic acid	-3.4	4	NH1-Arg658-O1	2.95	Phe575
				OG1-Thr604-O1	2.94	Glu583

Continued on next page

TABLE 4.6: Active Ligand Showing Hydrogen and Hydrophobic Interactions

Sr No.	Ligand Name	Binding Energy	No. of HBs	Bonding		Hydrophobic Bonding
				Amino Acids	Distance	
9	betaine	-3.9	6	OG-Ser605-O1	3.18	Lys606
				OG-Ser605-O2	3.06	
				N-Ala462-O2	3.13	Ser466
				N-Gly463-O2	3.18	Gly461
				N-Lys464-O2	2.96	
				N2-Lys464-O2	3.24	
10	choline	-3.3	4	N-Thr465-O1	3.05	
				OG1-Thr465-O1	3.11	
				N-Ala462-O1	2.86	Gly461
				NZ-Lys464-O1	3.08	Thr465
11	succinic acid	-4.9	5	N-Gly463-O1	3.04	Gln493
				N-Lys464-O1	2.96	
				OG1-Thr604-O1	2.95	Phe575
				N-Ser605-O1	2.94	Glu583
				OG-Ser605-O3	3.13	Lys606
12	serotonin	-5.7	3	O-Gly576-O2	3.02	
				NH1-Arg658-O4	2.83	
				OD1-Asn659-N2	2.89	Lys464
				OG1-Thr604-O	2.9	Ser573
				OE1-Glu583-O	2.99	Ser605
						Arg658
						Ala655

Continued on next page

TABLE 4.6: Active Ligand Showing Hydrogen and Hydrophobic Interactions

Sr No.	Ligand Name	Binding Energy	No. of HBs	Bonding		Hydrophobic Bonding
				Amino Acids	Distance	
13	lysine	-5	6	OG1-Thr604-O	2.74	His609
				N-Ser605-OXT	2.81	Gly576
				OG-Ser605-OXT	3.04	Phe575
				NH1-Arg658-OXT	2.8	His609
				O-Leu578-NZ	2.8	Ser573
				O-Phe575-NZ	2.94	Gly576
14	sucrose	-6.4	10	NE2-Gln493-O5	3.2	Lys606
				NE2-Gln493-O11	3.07	Ala655
				OE1-Gln493-O11	2.81	Glu583
				OE1-Gln493-O9	3.24	Ser573
				NZ-Lys464-O2	3.24	Asn659
				NZ-Lys44-O6	3.11	Val603
				N-Lys464-O8	3.06	Thr604
				N-Gly461-O10	3.12	Thr460
				OG1-Thr465-O9	2.98	Ala462
				N-Gly463-O8	3.05	
15	asparagine	-4.8	5	NH1-Arg658-O	2.99	Glu583
				NH1-Arg658-OG1	2.8	Phe575
				N-Ser605-O	2.93	Ser573

Continued on next page

TABLE 4.6: Active Ligand Showing Hydrogen and Hydrophobic Interactions

Sr No.	Ligand Name	Binding Energy	No. of HBs	Bonding		Hydrophobic Bonding				
				Amino Acids	Distance					
16	valine	-4.4	3	OG1-Thr604-O	3.21	Lys606 Thr604 Phe575 Ser573 Gly576				
				O-Gly576-ND2	2.97					
				NH1-Arg58-O	2.91					
				N-Ger05-O	2.83					
				O-Ger605-O	3.15					
17	betacarboline	-6.1	0	-	-	Asn659 Thr604 Ser573 Ser605 Ala655 Phe575 Arg658 Gly576 Glu583				
				18	proline	-5.1	4	N-Ser605-O	2.8	Ser573
								OG-Ser605-OXT	3.13	Gly576
								OG1-Thr604-O	2.98	Ala655
								NH1-Arg658-O	3.05	Phe575 Glu583

Continued on next page

TABLE 4.6: Active Ligand Showing Hydrogen and Hydrophobic Interactions

Sr No.	Ligand Name	Binding Energy	No. of HBs	Bonding		Hydrophobic Bonding
				Amino Acids	Distance	
19	hydroxyisoleucine	-4.7	2	NH2-ARG658-O2	3.17	Glu583
				O-Leu578-N	2.81	Ala655 Phe575 Asp579 Val580 Gly576 Lys606
20	linoleic acid	-5.4	3	O-Ser511-O2	2.92	Arg516
				OG-Ser511-O2	3.12	Gly509
				OH-Tyr563-O2	2.9	Lys56 Ile507 Ser557 Phe490 Ala561 Trp496 Tyr512 Asp513 Ile506 Arg560
						Concluded

4.6 ADME Properties of Ligand

Lipinski's five drug law is used as a first step for the assessment of availability either verbal or artificial [88]. pkCSM is the second tool that is used for the assessment of ADME properties [89].

4.6.1 Pharmacodynamics

One of the broader terms used in pharmacology is pharmacodynamics which deals with the study of drug effects on the body [91].

4.6.2 Pharmacokinetics

The other term used in pharmacology is pharmacokinetics which deals with the study of the effect of the body on the drug, that how the body reacts after the drug enters the body. The absorption, distribution, metabolism, and excretion of drugs are also studied [91].

4.6.3 Absorption

The CaCO_2 solubility helps in predicting the absorption of the drugs which are administered orally. Value >0.90 ($\log P_{app}$ in 10^{-6} cm/s) is considered as high CaCO_2 permeability [56]. The water solubility of the ligands is given as $\log \text{mol/L}$. this indicates the compound solubility in water at 25°C . Hence the lipid-soluble drugs will be less soluble than the water-soluble drugs. Intestinal absorption indicates the value or proportion of the compound that will absorb into the intestines. A value less than 30% is considered poorly absorbed. P-glycoprotein is an ABC transporter that functions to extrude toxins or other xenobiotics from the cells by acting as a biological barrier. P-glycoprotein inhibition can be a therapeutic target or it can act in contradiction Skin permeability is important for developing transdermal drugs. Any compound with a value > -2.5 has a low skin permeability [96].

The absorption properties of all ligands are given in Table 4.7.

Table 4.7 shows that harmaline, harmalol, harmol, tetrahydroxyharmine all have low skin permeability with that these four and vasicinone are the glycoprotein substrates. Also harmol has low CaCO₂ solubility. Apart from all these the values of other parameters are in the range.

TABLE 4.7: Absorption Properties of Ligands

Sr. No.	Name of Ligands	Water Solubility	CaCO ₂ Solubility	Intestinal Absorption (Human)	Skin Permeability	P-glycoprotein substrate	P-glycoprotein I inhibitor	P-glycoprotein II inhibitor
1.	harmaline	-3.123	1.621	93.622	-2.513	Yes	No	No
2.	harmalol	-3.221	1.221	92.396	-2.846	Yes	No	No
3.	harmol	-3.425	1.149	94.795	-2.747	Yes	No	No
4.	tetrahydroharmine	-2.926	1.61	92.546	-2.774	Yes	No	No
5.	vasicinone	-2.075	1.172	92.532	-3.045	Yes	No	No
6.	vasicine	-2.433	1.595	86.22	-2.827	No	No	No
7.	harmine	-3.148	1.496	93.499	-2.774	No	No	No
8.	acetic acid	0.702	1.55	95.463	-2.788	No	No	No
9.	betaine	0.723	1.44	100	-2.78	Yes	No	No
10.	choline	0.765	1.473	100	-3.102	Yes	No	No
11.	succinic acid	-0.66	0.603	71.748	-2.735	No	No	No
12.	serotonin	-2.31	0.501	91.394	-2.742	Yes	No	No
13.	lysine	-2.888	0.737	62.673	-2.735	No	No	No
14.	sucrose	-2.892	1.53	81.328	-2.735	No	No	No
15.	asparagine	-2.888	-0.344	36.213	-2.736	No	No	No
16.	valine	-2.888	0.541	76.187	-2.736	No	No	No
17.	betacarboline	-2.938	1.534	97.73	-2.173	Yes	No	No
18.	proline	0.204	1.116	87.223	-2.735	No	No	No
19.	hydroxyisoleucine	-2.888	0.505	57.573	-2.735	No	No	No
20.	linoleic acid	-5.862	1.57	92.329	-2.723	No	No	No

Some of the parameters of excretory properties of harmaline and harmalol has already been studied by T Akabli, F Lamchouri, S Senhaji and H Taufi in 2019 [92]. Some of the parameters of excretory properties of tetrahydroharmine, vasicine, harmol, harmine, vasicinone have been reported by Pratama, Mohammad Rizki Fadhil, et al in 2023 [93]. PkcsM excretion properties of beta carboline has already been reported by Y. Oloruntyun et al in 2021 [94]. PkcsM excretion properties of hydroxyisoleucine and leucine have already been reported by I. Ahmad et al in 2023 [95].

Table 4.7 shows the absorption properties of ligands like vasicine, harmine, acetic acid, betaine and choline. Harmine, betaine and choline have low CaCO₂ solubility. With that vasicine has low intestinal absorption. Whereas betaine is a glycoprotein substrate and all five ligands are not P-glycoprotein I and II inhibitor. All five ligands are not P-glycoprotein I and II inhibitors, with that serotonin is a P-glycoprotein substrate. Other than that water solubility, CaCO₂ solubility, intestinal absorption values are all in the pkcsM range. Hydroxyisoleucine has low CaCO₂ solubility with that beta carboline is a P-glycoprotein substrate. Whereas all five ligands are an inhibitor of P-glycoprotein I and II. The remaining ligands in Table 4.7 are valine, proline and linoleic acid gives the values of absorption parameters which are water solubility, CaCO₂ solubility, intestinal absorption, skin permeability, P-glycoprotein substrate and its inhibitors, all have indicated the values in pkcsM range.

Based on the information, we get through pkcsM absorption running we can screen several ligands which could be a step behind other ligands. Based on low CaCO₂ solubility succinic acid, serotonin, lysine, asparagine, valine and hydroxyisoleucine stays aback in the selection of lead compound whereas harmaline, harmalol, harmol, tetrahydroharmine, vasicinone, betaine, choline, serotonin and beta carboline are all P-glycoprotein substrates whereas asparagine has low intestinal absorption.

4.6.4 Distribution

The theoretical volume, or VD_{ss}, indicates the entire dosage of the medication that must be dispersed evenly to provide the same concentration as that found in blood plasma. The drug is more widely disseminated in the tissues than in the plasma

if the VD_{ss} value is more than 2.81 L/kg. If the number is less than 0.71 L/kg, the VD_{ss} will be low. Many drugs in the plasma exist in an equilibrium between a bounded and an unbounded state to the serum proteins. As a drug binds more to the serum proteins it will have less efficiency of diffusion to cellular membranes. The blood- brain barrier protects the brain and reduces the exogenous compounds to enter directly into the brain. If a compound has a value of logBB >0.3 then it will easily cross the BBB barrier hence been effective and if it is logBB <-1 then it is poorly distributed [58]. Compounds with a value of logPS >-2 penetrate the CNS whereas value logPS <-3 does not penetrate the CNS [91].

The values of the distribution of ligands harmaline, harmalol, harmol, tetrahydroharmine, vasicinone are given below in Table 4.8. The parameters through which the distribution properties are determined includes VD_{ss} in which harmaline, harmalol and vasicinone has low VD_{ss} whereas vasicinone is poorly distributed to blood brain. All these ligands mentioned in Table 4.8 can cross the blood brain barriers.

TABLE 4.8: Distribution Properties of Ligands

Sr. No.	Name of Ligands	VD _{ss} (human)	Fraction unbound (human)	BBB Permeability	CNS Permeability
1.	harmaline	0.264	0.267	0.39	-2.017
2.	harmalol	0.337	0.341	0.312	-2.102
3.	harmol	0.836	0.337	0.471	-2.175
4.	tetrahydroharmine	0.828	0.509	0.352	-1.901
5.	vasicinone	0.142	0.394	-0.206	-2.323
6.	vasicine	0.08	0.4	-0.127	-2.159
7.	harmine	0.358	0.218	0.417	-1.466
8.	acetic acid	-0.619	0.767	-0.321	-2.69
9.	betaine	-0.304	0.875	-0.214	-2.804

Continued on next page

TABLE 4.8: Distribution Properties of Ligands

Sr. No.	Name of Ligands	VDss (human)	Fraction unbound (human)	BBB Permeability	CNS Permeability
10.	choline	0.224	0.865	0.087	-2.901
11.	succinic acid	-1.013	0.638	-0.163	-3.06
12.	serotonin	1.392	0.656	-0.331	-2.355
13.	lysine	-0.511	0.47	-0.518	-3.497
14.	sucrose	-0.386	0.405	0.023	-4.667
15.	asparagine	-0.485	0.486	-0.515	-3.568
16.	valine	-0.572	0.462	-0.354	-3.353
17.	betacarboline	0.421	0.268	0.209	-1.613
18.	proline	-0.356	0.811	-0.31	-3.398
19.	hydroxyisoleucine	-0.539	0.474	-0.564	-3.489
20.	linoleic acid	-0.587	0.054	-0.142	-1.6

Concluded

Some of the parameters of excretory properties of harmaline and harmalol has already been studied by T Akabli, F Lamchouri, S Senhaji and H Taufi in 2019 [92]. Some of the parameters of excretory properties of tetrahydroharmine, vasicine, harmol, harmine, vasicinone have been reported by Pratama, Mohammad Rizki Fadhil, et al in 2023 [93]. PkcsM excretion properties of beta carboline has already been reported by Y. Oloruntyiun et al in 2021 [94]. PkcsM excretion properties of hydroxyisoleucine and leucine have already been reported by I. Ahmad et al in 2023 [95].

Table 4.8 shows the distribution properties of vasicine, harmine, acetic acid, betaine, choline. The table indicates that all five ligands cross the blood brain barrier and with that also are permeable to central nervous system. Other parameters gives

the distribution of ligands and gives the amount of the unbounded ligand. The distribution properties of succinic acid, serotonin, lysine, sucrose, asparagine indicates that all these ligands, only serotonin is permeable to the central nervous system and that they can easily cross the blood brain barrier. Other ligands distribution and fraction unbounded values are also given. The distribution properties of valine, beta carboline, proline, hydroxyisoleucine and linoleic acid indicates that valine, proline and hydroxyisoleucine all three ligands as drugs cannot pass through the central nervous system.

4.6.5 Metabolism

Cytochrome P450 is an enzyme held responsible for detoxification in the liver. Many drugs get deactivated by this enzyme but certain drugs can be activated. Inhibitors of this enzyme can directly affect the metabolism of drug hence should not be used. Similarly, CYP2D6 and CYP3A4 are responsible for the metabolism of the drugs. Inhibition to these affects the pharmacokinetics of the drug in use [97].

The prediction of the metabolism of the ligands is given below.

Table 4.9 shows the metabolic properties of harmaline, harmalol, harmol, tetrahydroharmine and vasicinone. All the five ligands mentioned are neither CYP3A4 substrate nor CYP2C19, CYP2C9 and CYP3A4 inhibitors. The metabolic properties of vasicine, harmine, acetic acid, betaine and choline indicates that all the five ligands mentioned are not CYP2D6 substrates. Except for vasicine all other ligands are not CYP3A4 substrates. All five ligands are not CYP2C9, CYP2D6 and CYP3A4 inhibitors.

The metabolic properties of succinic acid, serotonin, lysine, sucrose, asparagine are neither CYP2D6, CYP3A4 substrates nor CYP2C19, CYP2C9, CYP2D6 and CYP3A4 inhibitors. Whereas only succinic acid, lysine and asparagine are CYP1A2 inhibitor. Valine, beta carboline, proline, hydroxyisoleucine, linoleic acid indicates that all these ligands are CYP2C19, CYP2C9, CYP2D6, CYP3A4 inhibitors. Or CYP2D6 substrate, only proline is the substrate whereas beta

carboline, hydroxyisoleucine and linoleic acid are CYP1A2 inhibitors with that linoleic acid is also CYP3A4 substrate.

TABLE 4.9: Metabolic Properties of Ligands

Sr. No.	Name of Ligands	CYP2D6 substrate	CYP3A4 substrate	CYP1A2 inhibitor	CYP2C19 inhibitor	CYP2C9 inhibitor	CYP2D6 inhibitor	CYP3A4 inhibitor
1.	harmaline	Yes	No	Yes	No	No	No	No
2.	harmalol	Yes	No	Yes	No	No	No	No
3.	harmol	No	No	Yes	No	No	Yes	No
4.	tetrahydroharmine	Yes	No	Yes	No	No	Yes	No
5.	vasicinone	No	No	Yes	No	No	No	No
6.	vasicine	No	Yes	No	No	No	No	No
7.	harmine	Yes	No	Yes	No	No	No	No
8.	acetic acid	No	No	No	No	No	No	No
9.	betaine	No	No	No	No	No	No	No
10.	choline	No	No	No	No	No	No	No
11.	succinic acid	No	No	No	No	No	No	No
12.	serotonin	No	No	Yes	No	No	No	No
13.	lysine	No	No	No	No	No	No	No
14.	sucrose	No	No	Yes	No	No	No	No
15.	asparagine	No	No	No	No	No	No	No
16.	valine	No	No	No	No	No	No	No
17.	betacarboline	No	No	Yes	No	No	No	No
18.	proline	Yes	No	No	No	No	No	No
19.	hydroxyisoleucine	No	No	Yes	No	No	No	No
20.	linoleic acid	No	Yes	Yes	No	No	No	No

Some of the parameters of excretory properties of harmaline and harmalol has already been studied by T Akabli, F Lamchouri, S Senhaji and H Taufi in 2019 [92]. Some of the parameters of excretory properties of tetrahydroharmine, vasicine, harmol, harmine, vasicinone have been reported by Pratama, Mohammad Rizki Fadhil, et al in 2023 [93].

Pkcs_m excretion properties of beta carboline has already been reported by Y. Oloruntyiun et al in 2021 [94]. Pkcs_m excretion properties of hydroxyisoleucine and leucine have already been reported by I. Ahmad et al in 2023 [95].

4.6.6 Excretion

The Renal OCT2 substrate acts as a transporter that helps in clearing the drugs and other compounds. Total clearance indicates hepatic clearance which means the drug is metabolized and renal clearance indicates the drug is excreted [97]. The excretion values of the ligands are given below.

Table 4.10 shows the excretory properties of harmaline, harmalol, harmol, tetrahydroharmine, vasicinone. The table indicates that harmol is not renal OCT2 substrates which means the ligands would not be cleared out of the body and hence the total clearance values are given accordingly.

Vasicine, harmine, acetic acid, betaine and choline indicates that all these ligands are not renal OCT2 substrates which means the ligands would not be cleared out of the body and hence the total clearance values are given accordingly.

The excretory properties of succinic acid, serotonin, lysine, sucrose and asparagine indicates that all these ligands are not renal OCT2 substrates which means the ligands would not be cleared out of the body and hence the total clearance values are given accordingly.

Valine, beta carboline, proline, hydroxyisoleucine and linoleic acid indicates that all these ligands are not renal OCT2 substrates which means the ligands would not be cleared out of the body and hence the total clearance values are given accordingly.

TABLE 4.10: Excretory Properties of Ligands

Sr. No.	Name of Ligands	Total Clearance	Renal OCT2 Substrate
1.	harmaline	0.576	Yes
2.	harmalol	0.522	Yes
3.	harmol	0.621	No
4.	tetrahydroharmine	1.158	Yes
5.	vasicinone	0.568	No
6.	vasicine	0.58	No
7.	harmine	0.65	No
8.	acetic acid	0.595	No
9.	betaine	0.326	No
10.	choline	0.932	No
11.	succinic acid	0.722	No
12.	serotonin	1.004	No
13.	lysine	0.5	No
14.	sucrose	2.535	No
15.	asparagine	0.34	No
16.	valine	0.205	No
17.	betacarboline	0.574	No
18.	proline	0.632	No
19.	hydroxyisoleucine	0.35	No
20.	linoleic acid	1.936	No

Some of the parameters of excretory properties of harmaline and harmalol has already been studied by T Akabli, F Lamchouri, S Senhaji and H Taufi in 2019 [92].

Some of the parameters of excretory properties of tetrahydroharmine, vasicine, harmol, harmine, vasicinone have been reported by Pratama, Mohammad Rizki Fadhil, et al in 2023 [93].

Pkcs_m excretion properties of beta carboline has already been reported by Y. Oloruntyiun et al in 2021 [94]. Pkcs_m excretion properties of hydroxyisoleucine and leucine have already been reported by I. Ahmad et al in 2023 [95].

4.7 Lead Compound Identification

The physiochemical and the pharmacokinetics properties of the ligands determine their fate as for being drug or non-drug compounds. Lipinski's rule is the first filter and pharmacokinetics is the second filter for this identification. Only sucrose does not follow the Lipinski Rule as the H bond acceptors, and hydrogen bond donor values of sucrose exceed the Lipinski rule, but as it falls from two it is acceptable.

So, in the first stage, only sucrose has been evaluated to be knocked out. The next knockout stage is pharmacokinetic screening. In this screening harmalol, harmol, vasicine, harmine and Beta carboline because of being carcinogenic have been knocked out. At the end of this, the compounds left are harmaline, tetrahydro-harmine, vasicinone, acetic acid, betaine, choline, succinic acid, serotonin, lysine, asparagine, valine, proline, hydroxyisoleucine, linoleic acid. Among all these lysine, succinic acid, asparagine and vasicinone are selected as the top four compounds but out of them vasicinone is selected as the lead compound.

4.8 Drug Identification against Cystic Fibrosis

Many drugs approved by the FDA were used for drug repurposing in an effort to determine the most effective treatment for cystic fibrosis after the disease became recognized. Ivacaftor was approved by the U.S. Food and Drug Administration (FDA) in January 2012. Shortly after, the European Medicines Agency (EMA) and Canada also approved it, along with a few other European nations [98].

4.8.1 Ivacaftor

Ivacaftor, a CFTR potentiator, was initially licenced for use in patients over 6 years of age in the US in January 2012. It is the first drug meant to treat CF that targets the gating function of CFTR in order to address an underlying cause of the disease. Less chloride is transported through the CFTR channel as a result of the G551D-CFTR mutation, which affects about 4% of the CF population [99]. Ivacaftor enhances the total chloride transport and channel open probability (gating) of cell surface localised CFTR in vitro. This effect is observed even with mutant versions of the protein, such as G551D-CFTR. Ivacaftor restored up to 50% of normal CFTR chloride transport for G551D-CFTR in vitro; this amount is likely sufficient to reduce the CF phenotype [100].

4.9 Drug ADMET Properties

The same program, pkCSM, as previously mentioned is used to examine the drugs ADMET characteristics.

4.9.1 Toxicity Prediction of Reference Drug

Ivacaftor's toxicity properties are listed in Table 4.11. Ivacaftor's toxicity parameters value indicates that it may be harmful to the liver, but other parameters fall within the range of positive results. This suggests that Ivacaftor is not an inhibitor of hERG I and may cause skin sensitivity. Moreover, the dosage value of 0.313 is acceptable. Therefore, the fact that AMES is not poisonous suggests that it is not carcinogenic.

TABLE 4.11: Toxicity Properties of Ivacaftor

Sr No.	Model Name	Predicted Value of Ivacaftor
1.	AMES Toxicity	No
2.	Max. tolerated dose (human)	0.313

Continued on next page

TABLE 4.11: Toxicity Properties of Ivacaftor

Sr No.	Model Name	Predicted Value of Ivacaftor
3.	hERG I inhibitor	No
4.	hERG II inhibitor	Yes
5.	Oral rat acute toxicity	2.201
6.	Oral rat chronic toxicity	1.897
7.	Hepatotoxicity	Yes
8.	Skin sensitization	No
9.	T.pyriformis toxicity	0.325
10.	Minnow toxicity	-0.086

Concluded

4.9.2 Absorption Properties

Table 4.12 shows the absorption properties of Ivacaftor. The values show that azithromycin shows a very low CaCO_2 solubility and water solubility. Though the intestinal absorption is low but it still is in the safe range. Ivacaftor also has a lower value of skin permeability. Ivacaftor is also a P-glycoprotein substrate and an inhibitor to P-glycoprotein I but not a P-glycoprotein II inhibitor.

TABLE 4.12: Absorption Properties of Ivacaftor

Sr No.	Reference drug	Ivacaftor
1.	Water Solubility	-4.343
2.	CaCO_2 Solubility	0.99
3.	Intestinal Absorption (Human)	92.183
4.	Skin Permeability	-2.736
5.	P-glycoprotein substrate	Yes
6.	P-glycoprotein I inhibitor	Yes
7.	P-glycoprotein II inhibitor	Yes

4.9.3 Distribution Properties

Table 4.13 shows the distribution properties of Ivacaftor. The distribution parameters value shows that the value of VD_{ss} is low which means the drug would not be

distributed properly. Ivacaftor can penetrate in CNS and also can pass the blood brain barrier.

TABLE 4.13: Distribution Properties of Ivacaftor

Sr. No.	Reference drug	Ivacaftor
1.	VDss (human)	-0.47
2.	Fraction unbound (human)	0
3.	BBB Permeability	-0.598
4.	CNS Permeability	-1.419

4.9.4 Metabolic Properties

Table 4.14 shows the metabolic properties of ivacaftor. It indicates that ivacaftor is not a CYP2D6 substrate rather than it is a CYP3A4 substrate and it is a CYP1A2, CYP2C19, CYP2C9 and CYP3A4 inhibitor.

TABLE 4.14: Metabolic Properties of Ivacaftor

Sr. No.	Reference drug	Ivacaftor
1.	CYP2D6 substrate	No
2.	CYP3A4 substrate	Yes
3.	CYP1A2 inhibitor	Yes
4.	CYP2C19 inhibitor	Yes
5.	CYP2C9 inhibitor	Yes
6.	CYP2D6 inhibitor	No
7.	CYP3A4 inhibitor	Yes

The above table shows the metabolic efficiency of ivacaftor.

4.9.5 Excretion Properties

Ivacaftor's excretion properties are reported in Table 4.15. It indicates that ivacaftor is not a renal OCT2 substrate, indicating that it will not aid in the medication's clearance.

TABLE 4.15: Excretion Properties of Ivacaftor

Sr. No.	Reference drug	Ivacaftor
1.	Total Clearance	-0.08
2.	Renal OCT2 Substrate	No

4.10 Ivacaftor Mechanism of Action

An oral medication called ivacaftor improves the ion function of activated cell-surface CFTR. It has been shown through in vitro research employing bronchial epithelial cells from CF patients' lungs that aberrant CFTR-mediated ion transport may be corrected to raise the air-surface fluid level and ciliary beat frequency. Decreased mucus plugging by improved hydration of the airway surface and greater mucus drainage could potentially reduce airway blockage [101].

Among more than 228,000 small-molecule compounds, ivacaftor was found by high throughput screening using a cell-based fluorescence membrane potential assay designed to identify CFTR potentiators. The effects of ivacaftor on CFTR-mediated chloride secretion have been studied in vitro using recombinant cell lines and primary cultures of human bronchial epithelial cells. These studies have demonstrated that ivacaftor increases ciliary beat frequency, apical fluid height, and the probability of the CFTR channel being open, all of which improve chloride transfer. The exact mechanism of action of ivacaftor at the CFTR channel is unclear. Further in vitro studies have elucidated the process and shown that ivacaftor opens the defective channel gate of the mutant CFTR in an ATP-independent but phosphorylation-dependent manner [102].

Compared to patients with Gly551Asp, patients with Phe508del CFTR have had far less success with ivacaftor monotherapy. The efficacy findings of a pioneering clinical study that randomly assigned 140 homozygous individuals with the Phe508del mutation (4:1) to receive 150 mg of ivacaftor every 12 hours in addition to their prescribed CF drugs for 16 weeks were disappointing [103]. Ivacaftor medication did not enhance any of the secondary outcome measures, such as weight gain or an improvement in quality of life, or the key end measure, which is an increase

in predicted FEV1 after 16 weeks. Sweat chloride levels in the ivacaftor group decreased somewhat from baseline (2.9 mmol/L), but these changes were not statistically significant [104].

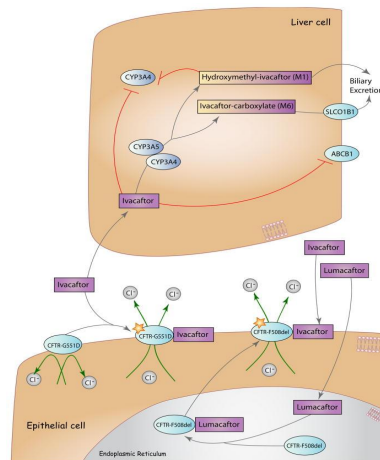


FIGURE 4.24: Stylized cells depicting metabolism and mechanism of action of ivacaftor [104]

To restore chloride gating function in CFTR with class III gating abnormalities, such the G551D variation, ivacaftor potentiates CFTR. As shown in Figure 4.24, both the CFTR-F508del and CFTR-G551D protein icons have star symbols to signify that they are active. It is demonstrated how ivacaftor is metabolised and how the liver gets rid of its byproducts. The method of action of lumacaftor, which chaperones the CFTR-F508del protein folding and restores proper protein localization, is similarly depicted in the picture. Ivacaftor is used to enhance gating function in this context [104].

4.11 Ivacaftor Effects on the Body

Both adolescents and adults who receive treatment with the CFTR potentiator ivacaftor see improvements in their BMI and weight growth because it enhances the CFTR channel's ion transport function.

It has been anecdotally demonstrated that ivacaftor reduces sinus mucus buildup. An enhanced sense of smell may stimulate appetite, which would increase energy

intake [105]. Ivacaftor-treated patients showed increases in mucociliary clearance and ppFEV1, two indicators of lung function. While pulmonary function was the main outcome measure of the ivacaftor investigations, there are potential gastrointestinal variables that could have affected weight gain in these trials. Both bicarbonate and chloride channels make up CFTR. Both adolescents and adults who receive treatment with the CFTR potentiator ivacaftor see improvements in their BMI and weight growth because it enhances the CFTR channel's ion transport function [106].

It has been anecdotally demonstrated that ivacaftor reduces sinus mucus buildup. An enhanced sense of smell may stimulate appetite, which would increase energy intake. Ivacaftor-treated patients showed increases in mucociliary clearance and ppFEV1, two indicators of lung function. While pulmonary function was the main outcome measure of the ivacaftor investigations, there are potential gastrointestinal variables that could have affected weight gain in these trials. Both bicarbonate and chloride channels make up CFTR [107].

4.12 Ivacaftor Docking

Docking result of ivacaftor is shown in Table 4.16. The table indicates that ivacaftor has a binding score of -7.7.

TABLE 4.16: Docking Result of Ivacaftor

S. No.	Compound	Ivacaftor
1	Binding Score	-7.7
2	Cavity Size	375
3	HBD	3
4	HBA	4
5	logP	5.6
6	Molecular Weight g/mol	392.5 g/mol
7	Rotatable Bonds	4
8	Grid Map	61

Ivacaftor's docking studies with the phe508del CFTR protein reveals that it has three hydrogen bond donors and four hydrogen bond acceptors, as well as a rather strong binding score. There are four rotatable bond in ivacaftor.

4.13 Ivacaftor Comparison with Lead Compound

The standard drug ivacaftor is compared with the lead compound vasicinone and their pharmacokinetic and physicochemical properties are compared for the assessment of bioavailability, efficiency, safety, and drug-likeness. The Table 4.17 shows vasicinone follows all rules of LogP, Molecular weight, H-bond acceptor and H-bond donar according to Lipinski.

TABLE 4.17: Comparison of Reference Drug and Lead Compound

Sr. No.	Name of Compound	LogP-value	Molecuar Weight g/mol	H-bond acceptor	H-bond donor
1.	Ivacaftor	5.6	392.5 g/mol	4	3
2.	Vasicinone	0.8336	202.21g/mol	3	1

4.14 ADMET Properties Comparison

In order to identify a better drug candidate, the absorption, distribution, metabolic excretion, and toxicity properties of the drug and the lead chemical are compared using the ADMET properties comparison [108].

4.14.1 Toxicity Comparison

Nine models are used to assess the toxicity of the lead ingredient and the standard medication. According to Model 1 of AMES toxicity, lead and standard chemicals do not cause mutations. According to Model 2 of the Maximum Tolerated Dosage, a number is considered low if it is equal to or less than 0.477 log mg/kg/day, and considered high if it is larger. The table below demonstrates the low tolerable dose

value of ivacaftor. 3rd model is of hERG I inhibitors both these compounds are not inhibitors but of hERG II ivacaftor is only inhibitor. The relative toxicity is evaluated using the fourth model of oral rat acute toxicity. Model 5 of oral rat chronic toxicity provides the lowest dose values that could have an adverse result. Hepatotoxicity Model 6 indicates that a medicine may harm the liver. It is clear from the table that ivacaftor is hepatotoxic. The number seven is used to verify the dermal products model's sensitivity to the skin. The lead chemical and the standard are not skin-sensitive. To test for toxicity, Model 8 employs *T. Pyriformis*, while Model 9 uses minnows. Both drugs pass this toxicity test for *T. Pyriformis*, where a value of >-0.5 is regarded toxic, and both compounds pass for minnows, where a value of less than 0.5mM is considered toxic and ivacaftor is somewhat toxic. Table 4.18 shows the comparative values of toxicity of ivacaftor and vasicinone.

TABLE 4.18: Toxicity Properties Comparison

Sr. No.	Model Name	Ivacaftor	Vasicinone
1.	AMES Toxicity	No	No
2.	Max. tolerated dose (human)	0.313	0.332
3.	hERG I inhibitor	No	No
4.	hERG II inhibitor	Yes	No
5.	Oral rat acute toxicity	2.201	1.91
6.	Oral rat chronic toxicity	1.897	1.708
7.	Hepatotoxicity	Yes	No
8.	Skin sensitization	No	No
9.	<i>T. pyriformis</i> toxicity	0.325	0.619
10.	Minnow toxicity	-0.086	1.236

4.14.2 Absorption Properties Comparison

Six models serve as the basis for the absorption parameter. The compound's solubility in water at 25 is indicated by the water solubility model. When a drug is administered orally, its absorption is predicted using the CaCO₂ solubility model. Vasicinone is absorbed more than ivacaftor when the value is more than 0.90, which is indication of significant intestine absorption. Less than 30% on the intestinal absorption model is regarded as poor absorption. The standard and lead compound values indicate that vasicinone has a high intestine absorption rate. Both compounds pass the skin permeability test for transdermal drugs, as indicated by the skin permeability model, which considers values less than $\log K_p > -2.5$ to be low. Because P-glycoprotein functions as a biological barrier and an ABC transporter, the P-glycoprotein substrate model is important. The substrates is ivacaftor. The final P-glycoprotein inhibitor model shows whether a given molecule functions as an inhibitor or not. Vasicinone is not an inhibitor of P-glycoprotein I and II, as Table 4.19 shows. On the other hand, ivacaftor inhibits P-glycoproteins I and II.

TABLE 4.19: Absorption Properties Comparison

Sr. No.	Reference drug	Ivacaftor	Vasicinone
1.	Water Solubility	-4.343	-2.075
2.	CaCO ₂ Solubility	0.99	1.172
3.	Intestinal Absorption (human)	92.183	92.532
4.	Skin Permeability	-2.736	-3.045
5.	P-glycoprotein substrate	Yes	Yes
6.	P-glycoprotein I inhibitor	Yes	No
7.	P-glycoprotein II inhibitor	Yes	No

4.14.3 Metabolic Properties Comparison

Mostly located in the liver, cytochrome P450 is an enzyme involved in detoxification because it oxidizes foreign substances to make them easier for the body to eliminate.

It either deactivates or activates certain drugs. Therefore, determining whether a chemical is a P450 substrate or not, as well as if it is a P450 inhibitor, is crucial. Table 4.20 indicates that vasicinone is not a CYP2D6 substrate, CYP3A4 substrate, or CYP2D6 inhibitor, CYP2C19 inhibitor, or CYP3A4 substrate, while ivacaftor is a CYP3A4 substrate.

TABLE 4.20: Metabolic Properties Comparison

Sr. No.	Reference Drug	Ivacaftor	Vasicinone
1.	CYP2D6 substrate	No	No
2.	CYP3A4 substrate	Yes	No
3.	CYP1A2 inhibitor	Yes	Yes
4.	CYP2C19 inhibitor	Yes	No
5.	CYP2C9 inhibitor	Yes	No
6.	CYP2D6 inhibitor	No	No
7.	CYP3A4 inhibitor	Yes	No

4.14.4 Distribution Properties Comparison

The relative distribution features of vasicinone and ivacaftor are shown in Table 4.21. Four models serve as the basis for the distribution parameter. The drug's uniform distribution in blood plasma is measured by the volume of distribution (VD_{ss}); if this number is higher than 2.81 L/kg, the drug is more evenly distributed in the tissues than in the blood plasma. Vasicinone and ivacaftor both have a high VD_{ss} value. The second model is predicated on the proportion of medicines in plasma that are unbound, since drugs that are bounded have an impact on drug efficiency. The amount of a drug that is still unbounded is indicated by the given value. A drug can readily pass the blood-brain barriers if its BBB permeability value is more than 0.3 log BB; if it is less than -1 log BB, the drug is either not transported to the brain or is distributed poorly. These values show that the brain can readily receive both values. Comparably, the central nervous system (CNS) model is predicated on the idea that drugs with a logPS value more than -2 can readily enter the CNS, whereas drugs with a logPS value less than -3 cannot enter the CNS. Both substances are capable of passing through the central nervous system.

TABLE 4.21: Distribution Properties Comparison

Sr. No.	Reference Drug	Ivacaftor	Vasicinone
1.	VDss (human)	-0.47	0.142
2.	Fraction unbound (human)	0	0.394
3.	BBB Permeability	-0.598	-0.206
4.	CNS Permeability	-1.419	-2.323

4.14.5 Excretion Properties Comparison

The value of total clearance is a combination of hepatic and renal clearance and is important so that the dose rates of the drugs can be assessed. Compared to ivacaftor, vasicinone has a higher overall clearance. The renal OCT2 (organic cation transporter 2) model is the second one, and it aids in the renal clearance of drugs and other substances. In respect to inhibitors, one may experience adverse impacts from being an OCT2 substrate. Thus, vasicinone and ivacaftor are not Renal OCT2 substrates. Table 4.22 shows the values of excretory properties of ivacaftor and vasicinone.

TABLE 4.22: Excretion Properties Comparison

Sr. No.	Reference Drug	Ivacaftor	Vasicinone
1.	Total Clearance	-0.08	0.568
2.	Renal OCT2 Substrate	No	No

4.15 Physiochemical Properties Comparison

Physiochemical properties are studied to determine the fundamental properties of the compound. Through this screening, it shows that ivacaftor has 24 carbon atoms, 28 hydrogen atoms, 2 nitrogen atoms, and 3 oxygen atoms whereas vasicinone has 11 carbon atoms, 10 hydrogen atoms, and 2 nitrogen atoms and 2 oxygen atoms. This shows that vasicinone is a simple bio-compound in relevance to ivacaftor. Ivacaftor can donate 2 hydrogen atoms whereas vasicinone can donate only 1 hydrogen atoms showing the oxidation state. Ivacaftor can accept 4 Hydrogen atoms whereas vasicinone can accept 3 hydrogen atoms. Although the Log P value of vasicinone is less than ivacaftor,

the molecular weight of ivacaftor is far greater than vasicinone. In a comparison of rotatable bonds ivacaftor has 4 whereas vasicinone has only 0 rotatable bonds. Table 4.23 shows the comparison of physiochemical properties of ivacaftor and vasicinone.

TABLE 4.23: Physiochemical Properties Comparison

Sr. No.	Reference drug	Ivacaftor	Vasicinone
1.	Molecular formula	C ₂₄ H ₂₈ N ₂ O ₃	C ₁₁ H ₁₀ N ₂ O ₂
2.	H-bond donor	2	1
3.	H-bond acceptor	4	3
4.	Log P-value	5.6	0.8336
5.	Molecular weight g/mol	392.5 g/mol	202.21g/mol
6.	Rotatable bonds	4	0

4.16 Docking Score Comparison

We docked the lead and standard compounds against the phe508del CFTR protein, and the best binding score was obtained from the docking result. Vasicinone, the main chemical, has a significantly higher vina score than ivacaftor, the standard drugs, as Table 4.24 shows. The binding score of vasicinone is -7.8 and that for ivacaftor is -7.7 which is lesser than that of the lead compound. This result shows that vasicinone can block the phe508del CFTR Protein or bind with it more efficiently than that of ivacaftor.

TABLE 4.24: Docking Score Comparison

Sr. No.	Compound	Binding score
1.	Ivacaftor	-7.7
2.	Vasicinone	-7.8

4.17 Docking Analysis Comparison

The docking results are analyzed by LigPlot based on the number of hydrogen bonds, number of hydrophobic interactions, number of interacting amino acids, and that of steric interactions.

Figure 4.25 and 4.26 shows the docking results of ivacaftor and vasicinone. Table 4.25 shows that ivacaftor has formed two hydrogen bonds and five hydrophobic interactions.

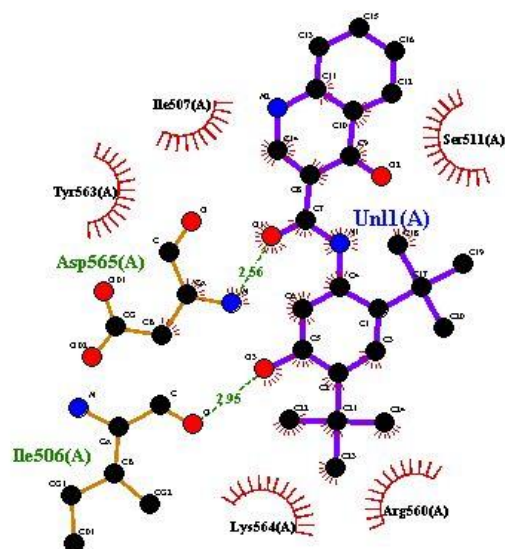


FIGURE 4.25: Interaction of Ivacaftor with the receptor

Whereas vasicinone has formed six hydrophobic interactions and five hydrogen bonds.

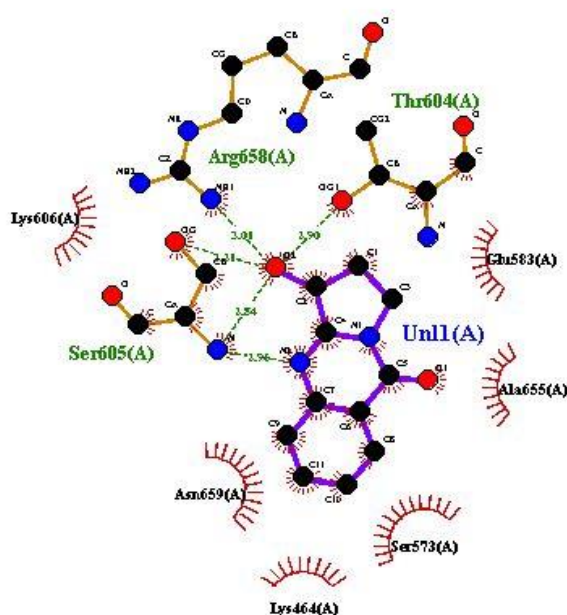


FIGURE 4.26: Interaction of Vasicinone with the receptor

The details of hydrogen and hydrophobic interactions are mentioned in the Table 4.25. Vasicinone forms five hydrogen bonds whereas ivacaftor forms 2 hydrogen bond, this is mainly because vasicinone O1 and N2 has made interactions with the receptor. Ivacaftor makes 5 hydrophobic interactions whereas vasicinone makes 6 of them. With all this information vasicinone succeeds to be much better than ivacaftor.

TABLE 4.25: Docking Analysis Comparison

Sr No.	Ligand Name	Binding Energy	No. of HBs	Bonding Amino Acids	Distance	Hydrophobic Bonding
1	Ivacaftor	-7.7	2	N-Asp565-O1	2.56	Ser511
				O-Ile506-O3	2.95	Ile507 Arg560 Lys564 Tyr563
2	Vasicinone	-7.8	5	NH1-Arg658-O1	3.01	Glu583
				OG-Ser605-O1	3.21	Ala655
				N-Ser605-O1	2.84	Ser573
				OG1-Thr604-O1	2.9	Lys464
				N-Ser605-N2	2.96	Asn659 Lys606

The above Table 4.25 shows that Ser511, Ile507, Arg560, Lys564, Tyr563 participates in forming hydrophobic interaction between the protein and ivacaftor. The nitrogen atom of Asp565 forms a hydrogen bond with the first oxygen of ivacaftor forming an N-Asp565-O1 bond.

Whereas Glu583, Ala655, Ser573, Lys464, Asn659, Lys606 participates in forming hydrophobic interaction between the protein and vasicinone. The oxygen atom of Ser605 termed as OG forms a hydrogen atom with O1 and nitrogen atom of Ser605 forms a hydrogen atom with O1 forming OG-Ser605-O1, N-Ser605-O1 bonds respectively. Whereas nitrogen atom of Ser605 forms a hydrogen atom with N2 forms an N-Ser605-N2 bond. Nitrogen atom of Arg658 forms a hydrogen atom with O1 forms NH1-Arg658-O1 bond and oxygen atom of Thr604 named as OG1 forms a hydrogen atom with O1 forms OG1-Thr604-O1 bond.

Chapter 5

Conclusion and Future Prospects

The study was aimed to determine active constituents in the plant *Peganum harmala* which is also known as serian rue in common language. For this purpose, 20 ligands were selected to be docked against the phe508del CFTR protein. The structure of all the 20 ligands was easily available in PubChem and protein structure was also available in PDB. All the ligands were docked against the receptor protein via CB Dock. The results were visualized using PyMol and were analyzed through LigPlot. Out of those 20 ligands, sucrose was first screened out based on Lipinski's rule, and based on second screening Harmalol, harmol, vasicine, harmine and Beta carboline were knocked out. After these 14 ligands were left and out of those vasicinone and ivacaftor were the two best active ligands. Based on the hydrophobic and hydrogen bonding vasicinone was selected as a lead against the standard drug ivacaftor which is in use for the treatment of cystic fibrosis. With the final results, it was cleared that vasicinone can bind far better to phe508TR protein than that of ivacaftor.

5.1 Recommendations

As per the findings of this research vasicinone should be exploited more against phe508del CFTR protein. With this other active constituent like asparagine, succinic acid, tetrahydroharmine, betaine and lysine have also shown a positive result in response to phe508del CFTR protein. Previously *Peganum harmala* has

been used as asthma, paralysis, gastrointestinal, urinary problems and epilepsy for this reason *Peganum harmala* should be explored more for its effectiveness against cystic fibrosis.

Bibliography

- [1] B. García-Pinel *et al.*, “Lipid-Based Nanoparticles: Application and recent advances in cancer treatment,” *Nanomaterials*, vol. 9, no. 4, p. 638, Apr. 2019, doi: 10.3390/nano9040638.
- [2] Vankeerberghen, H. Cuppens, and J. J. Cassiman, “The cystic fibrosis transmembrane conductance regulator: an intriguing protein with pleiotropic functions,” *Journal of Cystic Fibrosis*, vol. 1, no. 1, pp. 13–29, Mar. 2002, doi: 10.1016/s1569-1993(01)00003-0.
- [3] J. F. Chmiel and P. B. Davis, “State of the Art: Why do the lungs of patients with cystic fibrosis become infected and why can’t they clear the infection?,” *Respiratory Research*, vol. 4, no. 1, Aug. 2003, doi: 10.1186/1465-9921-4-8.
- [4] R. C. Boucher, “Evidence for airway surface dehydration as the initiating event in CF airway disease,” *Journal of Internal Medicine*, vol. 261, no. 1, pp. 5–16, Jan. 2007, doi: 10.1111/j.1365-2796.2006.01744.x.
- [5] D. A. Stoltz, D. K. Meyerholz, and M. J. Welsh, “Origins of cystic fibrosis lung disease,” *The New England Journal of Medicine*, vol. 372, no. 4, pp. 351–362, Jan. 2015, doi: 10.1056/nejmra1300109.
- [6] Z. Zhang and J. Chen, “Atomic structure of the cystic fibrosis transmembrane conductance regulator,” *Cell*, vol. 167, no. 6, pp. 1586–1597.e9, Dec. 2016, doi: 10.1016/j.cell.2016.11.014.
- [7] F. L. Theodoulou and I. D. Kerr, “ABC transporter research: going strong 40 years on,” *Biochemical Society Transactions*, vol. 43, no. 5, pp. 1033–1040, Oct. 2015, doi: 10.1042/bst20150139.

- [8] “Phosphorylation of the cystic fibrosis transmembrane conductance regulator,” *PubMed*, Jun. 25, 1992. <https://pubmed.ncbi.nlm.nih.gov/1377674/>
- [9] M. P. Rogan, D. A. Stoltz, and D. B. Hornick, “Cystic fibrosis transmembrane conductance regulator intracellular processing, trafficking, and Opportunities for Mutation-Specific treatment,” *Chest*, vol. 139, no. 6, pp. 1480–1490, Jun. 2011, doi: 10.1378/chest.10-2077.
- [10] C. Benden and C. Schwarz, “CFTR modulator therapy and its impact on lung transplantation in cystic fibrosis,” *Pulmonary Therapy*, vol. 7, no. 2, pp. 377–393, Aug. 2021, doi: 10.1007/s41030-021-00170-9.
- [11] A. Zaher, J. ElSaygh, D. ElSORI, H. ElSaygh, and A. Sanni, “A review of TriKafTa: Triple Cystic Fibrosis Transmembrane Conductance Regulator (CFTR) Modulator therapy,” *Cureus*, Jul. 2021, doi: 10.7759/cureus.16144.
- [12] M. Ekor, “The growing use of herbal medicines: issues relating to adverse reactions and challenges in monitoring safety,” *Frontiers in Pharmacology*, vol. 4, Jan. 2014, doi: 10.3389/fphar.2013.00177.
- [13] D. Foster, R. S. Phillips, M. B. Hamel, and D. M. Eisenberg, “Alternative medicine use in older Americans,” *Journal of the American Geriatrics Society*, vol. 48, no. 12, pp. 1560–1565, Dec. 2000, doi: 10.1111/j.1532-5415.2000.tb03864.x.
- [14] B. Betapudi, “Cystic fibrosis and liver disease,” *StatPearls - NCBI Bookshelf*, Jan. 09, 2023. <https://www.ncbi.nlm.nih.gov/books/NBK556086/>
- [15] K. Olivier, K. N. Gibson-Corley, and D. K. Meyerholz, “Animal models of gastrointestinal and liver diseases. Animal models of cystic fibrosis: gastrointestinal, pancreatic, and hepatobiliary disease and pathophysiology,” *American Journal of Physiology-gastrointestinal and Liver Physiology*, vol. 308, no. 6, pp. G459–G471, Mar. 2015, doi: 10.1152/ajpgi.00146.2014.
- [16] R. S. Pettit, “Cystic Fibrosis Transmembrane Conductance Regulator–Modifying Medications: The Future of Cystic Fibrosis Treatment,” *Annals of*

- Pharmacotherapy*, vol. 46, no. 7–8, pp. 1065–1075, Jul. 2012, doi: 10.1345/aph.1r076.
- [17] K. E. Tipirneni and B. A. Woodworth, “Medical and surgical advancements in the management of cystic fibrosis chronic rhinosinusitis,” *Current Otorhinolaryngology Reports*, vol. 5, no. 1, pp. 24–34, Feb. 2017, doi: 10.1007/s40136-017-0139-3.
- [18] J. DeCeglie-Germana, L. Bonitz, E. Langfelder-Schwind, C. Kier, B. L. Diener, and M. Berdella, “Diagnostic and communication challenges in cystic fibrosis newborn screening,” *Life*, vol. 13, no. 8, p. 1646, Jul. 2023, doi: 10.3390/life13081646.
- [19] P. Trouvé, E. Génin, and C. Férec, “In silico search for modifier genes associated with pancreatic and liver disease in Cystic Fibrosis,” *PLOS ONE*, vol. 12, no. 3, p. e0173822, Mar. 2017, doi: 10.1371/journal.pone.0173822.
- [20] C. M. Farinha and I. Callebaut, “Molecular mechanisms of cystic fibrosis – how mutations lead to misfunction and guide therapy,” *Bioscience Reports*, vol. 42, no. 7, Jul. 2022, doi: 10.1042/bsr20212006.
- [21] D. N. Sheppard, D. P. Rich, L. S. Ostedgaard, R. J. Gregory, A. E. Smith, and M. J. Welsh, “Mutations in CFTR associated with mild-disease-form CI- channels with altered pore properties,” *Nature*, vol. 362, no. 6416, pp. 160–164, Mar. 1993, doi: 10.1038/362160a0.
- [22] J. DeCeglie-Germana, L. Bonitz, E. Langfelder-Schwind, C. Kier, B. L. Diener, and M. Berdella, “Diagnostic and communication challenges in cystic fibrosis newborn screening,” *Life*, vol. 13, no. 8, p. 1646, Jul. 2023, doi: 10.3390/life13081646.
- [23] D. N. Sheppard, D. P. Rich, L. S. Ostedgaard, R. J. Gregory, A. E. Smith, and M. J. Welsh, “Mutations in CFTR associated with mild-disease-form CI- channels with altered pore properties,” *Nature*, vol. 362, no. 6416, pp. 160–164, Mar. 1993, doi: 10.1038/362160a0.

- [24] G. Veit *et al.*, “From CFTR biology toward combinatorial pharmacotherapy: expanded classification of cystic fibrosis mutations,” *Molecular Biology of the Cell*, vol. 27, no. 3, pp. 424–433, Feb. 2016, doi: 10.1091/mbc.e14-04-0935.
- [25] P. Kumaran, G. Rengasamy, S. Sekaran, K. Sankaran, V. P. Veeraraghavan, and R. Eswaramoorthy, “Molecular docking analysis of Indole based oxadiazoles with the H-binding protein from *Treponema denticola*,” *PubMed*, vol. 19, no. 1, pp. 79–84, Jan. 2023, doi: 10.6026/97320630019079.
- [26] J. Bertranpetit and F. Calafell, “Genetic and geographical variability in cystic fibrosis: Evolutionary considerations,” *Novartis Foundation Symposium*, pp. 97–118, Sep. 2007, doi: 10.1002/9780470514887.ch6.
- [27] E. Mateu, F. Calafell, M. D. Ramos, T. Casals, and J. Bertranpetit, “Can a place of origin of the main cystic fibrosis mutations be identified?,” *American Journal of Human Genetics*, vol. 70, no. 1, pp. 257–264, Jan. 2002, doi: 10.1086/338243.
- [28] X. Zha, P. Zhao, F. Gao, and Y. Zhou, “Complete chloroplast genome sequence of *Peganum harmala*, an important medicinal plant,” *Mitochondrial DNA Part B*, vol. 5, no. 1, pp. 652–653, Jan. 2020, doi: 10.1080/23802359.2019.1711230.
- [29] K. Manthiram, Q. Zhou, I. Aksentijevich, and D. L. Kastner, “The monogenic autoinflammatory diseases define new pathways in human innate immunity and inflammation,” *Nature Immunology*, vol. 18, no. 8, pp. 832–842, Jul. 2017, doi: 10.1038/ni.3777.
- [30] A. Tarique *et al.*, “CFTR-dependent defect in alternatively-activated macrophages in cystic fibrosis,” *Journal of Cystic Fibrosis*, vol. 16, no. 4, pp. 475–482, Jul. 2017, doi: 10.1016/j.jcf.2017.03.011.
- [31] M. P. Ribeiro and R. C. Boucher, “Role of endoplasmic reticulum stress in cystic Fibrosis-Related airway inflammatory responses,” *Annals of the American Thoracic Society*, vol. 7, no. 6, pp. 387–394, Oct. 2010, doi: 10.1513/pats.201001-017aw.

- [32] S. Lara-Reyna, J. Holbrook, H. Jarosz-Griffiths, D. Peckham, and M. F. McDermott, “Dysregulated signalling pathways in innate immune cells with cystic fibrosis mutations,” *Cellular and Molecular Life Sciences*, vol. 77, no. 22, pp. 4485–4503, May 2020, doi: 10.1007/s00018-020-03540-9.
- [33] E. Bosch *et al.*, “Variation in short tandem repeats is deeply structured by genetic background on the human Y chromosome,” *American Journal of Human Genetics*, vol. 65, no. 6, pp. 1623–1638, Dec. 1999, doi: 10.1086/302676.
- [34] H. Tabori *et al.*, “Abdominal symptoms in cystic fibrosis and their relation to genotype, history, clinical and laboratory findings,” *PLOS ONE*, vol. 12, no. 5, p. e0174463, May 2017, doi: 10.1371/journal.pone.0174463.
- [35] H. J. Fuchs *et al.*, “Effect of Aerosolized Recombinant Human DNase on Exacerbations of Respiratory Symptoms and on Pulmonary Function in Patients with Cystic Fibrosis,” *The New England Journal of Medicine*, vol. 331, no. 10, pp. 637–642, Sep. 1994, doi: 10.1056/nejm199409083311003.
- [36] J. Guo, A. Garratt, and A. Hill, “Worldwide rates of diagnosis and effective treatment for cystic fibrosis,” *Journal of Cystic Fibrosis*, vol. 21, no. 3, pp. 456–462, May 2022, doi: 10.1016/j.jcf.2022.01.009.
- [37] M. S. Schechter, A. K. Fink, K. Homa, and C. H. Goss, “The Cystic Fibrosis Foundation Patient Registry as a tool for use in quality improvement,” *BMJ Quality & Safety*, vol. 23, no. Suppl 1, pp. i9–i14, Jan. 2014, doi: 10.1136/bmjqs-2013-002378.
- [38] H. Grasemann and F. Ratjen, “Emerging therapies for cystic fibrosis lung disease,” *Expert Opinion on Emerging Drugs*, vol. 15, no. 4, pp. 653–659, Sep. 2010, doi: 10.1517/14728214.2010.517746.
- [39] F. Van Goor *et al.*, “Correction of the F508del-CFTR protein processing defect in vitro by the investigational drug VX-809,” *Proceedings of the National Academy of Sciences of the United States of America*, vol. 108, no. 46, pp. 18843–18848, Oct. 2011, doi: 10.1073/pnas.1105787108.

- [40] J. Clancy *et al.*, “Results of a phase IIa study of VX-809, an investigational CFTR corrector compound, in subjects with cystic fibrosis homozygous for the *F508del-CFTR* mutation,” *Thorax*, vol. 67, no. 1, pp. 12–18, Aug. 2011, doi: 10.1136/thoraxjnl-2011-200393.
- [41] “Vertex and Cystic Fibrosis Foundation Therapeutics to collaborate on discovery and development of new medicines to treat the underlying cause of cystic fibrosis | Vertex Pharmaceuticals,” *Vertex Pharmaceuticals*.
<https://investors.vrtx.com/news-releases/news-release-details/vertex-and-cystic-fibrosis-foundation-therapeutics-collaborate>
- [42] M. Du, X. Liu, E. Welch, S. Hirawat, S. W. Peltz, and D. M. Bedwell, “PTC124 is an orally bioavailable compound that promotes suppression of the human *CFTR* -G542X nonsense allele in a CF mouse model,” *Proceedings of the National Academy of Sciences of the United States of America*, vol. 105, no. 6, pp. 2064–2069, Feb. 2008, doi: 10.1073/pnas.0711795105.
- [43] R. C. Rubenstein, M. E. Egan, and P. L. Zeitlin, “In vitro pharmacologic restoration of CFTR-mediated chloride transport with sodium 4-phenylbutyrate in cystic fibrosis epithelial cells containing delta F508-CFTR.,” *Journal of Clinical Investigation*, vol. 100, no. 10, pp. 2457–2465, Nov. 1997, doi: 10.1172/jci119788.
- [44] Y. Wang, M. C. Bartlett, T. W. Loo, and D. M. Clarke, “Specific rescue of cystic fibrosis transmembrane conductance regulator processing mutants using pharmacological chaperones,” *Molecular Pharmacology*, vol. 70, no. 1, pp. 297–302, Apr. 2006, doi: 10.1124/mol.106.023994.
- [45] N. Annam, K. A. Peele, M. Doble, S. Krupanidhi, and T. C. Venkateswarulu, “An in silico study on pulmonary fibrosis inhibitors from *Tinospora cordifolia* and *Curcuma longa* targeting TGF- β RI,” *Journal of Biomolecular Structure & Dynamics*, pp. 1–17, Jan. 2022, doi: 10.1080/07391102.2022.2029772.
- [46] H. Al-Momani *et al.*, “The efficacy of biosynthesized silver nanoparticles against *Pseudomonas aeruginosa* isolates from cystic fibrosis patients,” *Scientific Reports*, vol. 13, no. 1, Jun. 2023, doi: 10.1038/s41598-023-35919-6.

- [47] M. Moloudizargari, P. Mikaili, S. Aghajanshakeri, M. H. Asghari, and J. Shayegh, "Pharmacological and therapeutic effects of *Peganum harmala* and its main alkaloids," *Pharmacognosy Reviews*, vol. 7, no. 14, p. 199, Jan. 2013, doi: 10.4103/0973-7847.120524.
- [48] J. Sharifi-Rad *et al.*, "Peganum spp.: A Comprehensive Review on Bioactivities and Health-Enhancing Effects and Their Potential for the Formulation of Functional Foods and Pharmaceutical Drugs," *Oxidative Medicine and Cellular Longevity*, vol. 2021, pp. 1–20, Jun. 2021, doi: 10.1155/2021/5900422.
- [49] M. C. Niroumand, M. H. Farzaei, and G. Amin, "Medicinal properties of *Peganum harmala* L. in traditional Iranian medicine and modern phytotherapy: a review," *Journal of Traditional Chinese Medicine*, vol. 35, no. 1, pp. 104–109, Feb. 2015, doi: 10.1016/s0254-6272(15)30016-9.
- [50] M. W. Abbas *et al.*, "Antioxidant and Anti-Inflammatory Effects of *Peganum harmala* Extracts: An In Vitro and In Vivo Study," *Molecules*, vol. 26, no. 19, p. 6084, Oct. 2021, doi: 10.3390/molecules26196084.
- [51] Herraiz T, Gonzalez D, Ancin-Azpilicueta C, Aran VJ, Guillen H. beta-Carboline alkaloids in *Peganum harmala* and inhibition of human monoamine oxidase (MAO) *Food Chem Toxicol.* 2010;48: 839–845.
- [52] Z. Zhu, S. Zhao, and C. Wang, "Antibacterial, Antifungal, Antiviral, and Antiparasitic Activities of *Peganum harmala* and Its Ingredients: A Review," *Molecules*, vol. 27, no. 13, p. 4161, Jun. 2022, doi: 10.3390/molecules27134161.
- [53] Orro *et al.*, "In silico drug repositioning on F508del-CFTR: A proof-of-concept study on the AIFA library," *European Journal of Medicinal Chemistry*, vol. 213, p. 113186, Mar. 2021, doi: 10.1016/j.ejmech.2021.113186.
- [54] Y. Wang, M. C. Bartlett, T. W. Loo, and D. M. Clarke, "Specific rescue of cystic fibrosis transmembrane conductance regulator processing mutants using pharmacological chaperones," *Molecular Pharmacology*, vol. 70, no. 1, pp. 297–302, Apr. 2006, doi: 10.1124/mol.106.023994.

- [55] G. Righetti *et al.*, “Molecular docking and QSAR studies as computational tools exploring the rescue ability of F508DEL CFTR correctors,” *International Journal of Molecular Sciences*, vol. 21, no. 21, p. 8084, Oct. 2020, doi: 10.3390/ijms21218084.
- [56] M. W. Abbas *et al.*, “Antioxidant and Anti-Inflammatory Effects of *Peganum harmala* Extracts: An In Vitro and In Vivo Study,” *Molecules*, vol. 26, no. 19, p. 6084, Oct. 2021, doi: 10.3390/molecules26196084.
- [57] Orro, A., Uggeri, M., Rusnati, M., Urbinati, C., Pedemonte, N., Pesce, E., ... & D’Ursi, P. (2021). In silico drug repositioning on F508del-CFTR: A proof-of-concept study on the AIFA library. *European Journal of Medicinal Chemistry*, 213, 113186.
- [58] N. Kälin, A. Claaß, M. Sommer, É. Puchelle, and B. Tümmler, “ Δ F508 CFTR protein expression in tissues from patients with cystic fibrosis,” *Journal of Clinical Investigation*, vol. 103, no. 10, pp. 1379–1389, May 1999, doi: 10.1172/jci5731.
- [59] M. L. Drumm *et al.*, “Chloride Conductance Expressed by Δ F508 and Other Mutant CFTRs In *Xenopus* Oocytes,” *Science*, vol. 254, no. 5039, pp. 1797–1799, Dec. 1991, doi: 10.1126/science.1722350.
- [60] T. V. Strong *et al.*, “Cystic Fibrosis Gene Mutation in Two Sisters with Mild Disease and Normal Sweat Electrolyte Levels,” *The New England Journal of Medicine*, vol. 325, no. 23, pp. 1630–1634, Dec. 1991, doi: 10.1056/nejm199112053252307.
- [61] D. De Stefano *et al.*, “Restoration of CFTR function in patients with cystic fibrosis carrying the F508del-CFTR mutation,” *Autophagy*, vol. 10, no. 11, pp. 2053–2074, Nov. 2014, doi: 10.4161/15548627.2014.973737.
- [62] L. Maiuri *et al.*, “Tissue transglutaminase activation modulates inflammation in cystic fibrosis via PPAR γ Down-Regulation,” *Journal of Immunology*, vol. 180, no. 11, pp. 7697–7705, Jun. 2008, doi: 10.4049/jimmunol.180.11.7697.

- [63] N. Bouazza *et al.*, “Population pharmacokinetics and pharmacodynamics of cysteamine in nephropathic cystinosis patients,” *Orphanet Journal of Rare Diseases*, vol. 6, no. 1, p. 86, Jan. 2011, doi: 10.1186/1750-1172-6-86.
- [64] R. Paine *et al.*, “A randomized trial of recombinant human granulocyte-macrophage colony stimulating factor for patients with acute lung injury*,” *Critical Care Medicine*, vol. 40, no. 1, pp. 90–97, Jan. 2012, doi: 10.1097/ccm.0b013e31822d7bf0.
- [65] H. Sodaiezadeh, M. Rafieiohossaini, J. Havlík, and P. Van Damme, “Allelopathic activity of different plant parts of *Peganum harmala* L. and identification of their growth inhibitors substances,” *Plant Growth Regulation*, vol. 59, no. 3, pp. 227–236, Sep. 2009, doi: 10.1007/s10725-009-9408-6.
- [66] T. Herraiz, D. González, C. Ancín-Azpilicueta, V. J. Arán, and H. Guillén, “ β -Carboline alkaloids in *Peganum harmala* and inhibition of human monoamine oxidase (MAO),” *Food and Chemical Toxicology*, vol. 48, no. 3, pp. 839–845, Mar. 2010, doi: 10.1016/j.fct.2009.12.019.
- [67] L. Vinhoven, F. Stanke, S. Hafkemeyer, and M. Nietert, “Complementary Dual Approach for In Silico Target Identification of Potential Pharmaceutical Compounds in Cystic Fibrosis,” *International Journal of Molecular Sciences*, vol. 23, no. 20, p. 12351, Oct. 2022, doi: 10.3390/ijms232012351.
- [68] G. Righetti *et al.*, “Molecular docking and QSAR studies as computational tools exploring the rescue ability of F508DEL CFTR correctors,” *International Journal of Molecular Sciences*, vol. 21, no. 21, p. 8084, Oct. 2020, doi: 10.3390/ijms21218084.
- [69] “Pagadala, N.S., Syed, K. and Tuszynski, J. (2017) Software for Molecular Docking A Review. *Biophysical Reviews*, 9, 91-102. - References - Scientific Research Publishing.”
[https://www.scirp.org/\(S\(lz5mqp453ed%20snp55rrgjt55\)\)/reference/referencpapers.aspx?referenceid=2295121](https://www.scirp.org/(S(lz5mqp453ed%20snp55rrgjt55))/reference/referencpapers.aspx?referenceid=2295121)

- [70] Mitchell *et al.*, “The InterPro protein families database: the classification resource after 15 years,” *Nucleic Acids Research*, vol. 43, no. D1, pp. D213–D221, Nov. 2014, doi: 10.1093/nar/gku1243.
- [71] “DeLano, W.L. (2002) The PyMOL Molecular Graphics System. Delano Scientific, San Carlos.References.Scientific.Research.Publishing.”
[https://www.scirp.org/\(S\(vtj3fa45qm1ean45vvffcz55\)\)/reference/ReferencesPapers.aspx?ReferenceID=1958992](https://www.scirp.org/(S(vtj3fa45qm1ean45vvffcz55))/reference/ReferencesPapers.aspx?ReferenceID=1958992)
- [72] S. Yuan, H. C. Chan, and Z. Hu, “Using PyMOL as a platform for computational drug design,” *Wiley Interdisciplinary Reviews: Computational Molecular Science*, vol. 7, no. 2, Jan. 2017, doi: 10.1002/wcms.1298.
- [73] S. I. Mostafa, “Mixed ligand complexes with 2-piperidine-carboxylic acid as primary ligand and ethylene diamine, 2,2′-bipyridyl, 1,10-phenanthroline and 2(2′-pyridyl) quinoxaline as secondary ligands: preparation, characterization and biological activity,” *Transition Metal Chemistry*, vol. 32, no. 6, pp. 769–775, Jul. 2007, doi: 10.1007/s11243-007-0247-x.
- [74] B. Russell *et al.*, “Associations between immune-suppressive and stimulating drugs and novel COVID-19—a systematic review of current evidence,” *Ecancer medical science*, vol. 14, Mar. 2020, doi: 10.3332/ecancer.2020.1022.
- [75] M. W. Konstan *et al.*, “Assessment of safety and efficacy of long-term treatment with combination lumacaftor and ivacaftor therapy in patients with cystic fibrosis homozygous for the F508del-CFTR mutation (PROGRESS): a phase 3, extension study,” *The Lancet Respiratory Medicine*, vol. 5, no. 2, pp. 107–118, Feb. 2017, doi: 10.1016/s2213-2600(16)30427-1.
- [76] L. Vinhoven, F. Stanke, S. Hafkemeyer, and M. Nietert, “Complementary Dual Approach for In Silico Target Identification of Potential Pharmaceutical Compounds in Cystic Fibrosis,” *International Journal of Molecular Sciences*, vol. 23, no. 20, p. 12351, Oct. 2022, doi: 10.3390/ijms232012351.
- [77] Garg, V. K., Avashthi, H., Tiwari, A., Jain, P. A., Ramkete, P. W., Kayastha, A. M., & Singh, V. K. (2016). MFPPPI—multi FASTA ProtParam interface. *Bioinformatics*, 12(2), 74.

- [78] Morya, V. K., Yadav, S., Kim, E. K., & Yadav, D. (2012). In silico characterization of alkaline proteases from different species of *Aspergillus*. *Applied biochemistry and biotechnology*, 166(1), 243-257.
- [79] Structure and function of the CFTR chloride channel. Sheppard DN, Welsh MJ. *Physiol. Rev.* 79, S23-45, (1999).
- [80] The major cystic fibrosis causing mutation exhibits defective propensity for phosphorylation. Pasyk S, Molinski S, Ahmadi S, Ramjeesingh M, Huan LJ, Chin S, Du K, Yeger H, Taylor P, Moran MF, Bear CE. *Proteomics* 15, 447-61, (2015).
- [81] Serohijos, Adrian WR, et al. "Diminished self-chaperoning activity of the $\Delta F508$ mutant of CFTR results in protein misfolding." *PLoS Computational Biology* 4.2 (2008): e1000008.
- [82] Kim, Soo Jung, and William R. Skach. "Mechanisms of CFTR folding at the endoplasmic reticulum." *Frontiers in pharmacology* 3 (2012): 201.
- [83] Valles, J., Garcia, S., Hidalgo, O., Martin, J., Pellicer, J., Sanz, M., & Garnatje, T. (2011). Biology, genome evolution, biotechnological issues, and research including applied perspectives in *Artemisia* (Asteraceae). *Advances in botanical research*, 60, 349-419.
- [84] Willcox, M. (2009). *Artemisia* species: from traditional medicines to modern antimalarials—and back again. *The Journal of Alternative and Complementary Medicine*, 15(2), 101-109.
- [85] C'avar, S., Maksimovi'c, M., Vidic, D., & Pari'c, A. (2012). Chemical composition and antioxidant and antimicrobial activity of essential oil of *Artemisia annua* L. from Bosnia. *Industrial Crops and Products*, 37(1), 479-485.
- [86] Li, K. M., Dong, X., Ma, Y. N., Wu, Z. H., Yan, Y. M., & Cheng, Y. X. (2019). Antifungal coumarins and lignans from *Artemisia annua*. *Fitoterapia*, 134, 323-328

- [87] Septembre-Malaterre, A., Lalarizo Rakoto, M., Marodon, C., Bedoui, Y., Nakab, J., Simon, E., & Gasque, P. (2020). *Artemisia annua*, a Traditional Plant Brought to Light. *International Journal of Molecular Sciences*, 21(14), 4986.
- [88] Ntie-Kang, F. (2013). An in silico evaluation of the ADMET profile of the StreptomeDB database. *Springerplus*, 2(1), 1-11.
- [89] Lipinski, C. A. (2004). Lead-and drug-like compounds: the rule-of-five revolution. *Drug Discovery Today: Technologies*, 1(4), 337-341.
- [90] Bhattacharya, P., & Patel, T. N. (2021). Deregulation of MMR-Related Pathways and Anticancer Potential of Curcuma Derivatives—A Computational Approach.
- [91] Istifli, E. S., S,ihog? lu Tepe, A., SarikU rkcU , C., & Tepe, B. (2020). Interaction of certain monoterpenoid hydrocarbons with the receptor binding domain of 2019 novel coronavirus (2019-nCoV), transmembrane serine protease 2 (TM- PRSS2), cathepsin B, and cathepsin L (CatB/L) and their pharmacokinetic properties. *Turkish journal of biology = Turk biyoloji dergisi*, 44(3), 242–264.
- [92] Akabli, Taoufik, et al. “Molecular docking, ADME/Tox prediction, and in vitro study of the cell growth inhibitory activity of five β -carboline alkaloids.” *Structural Chemistry* 30 (2019): 1495-1504.
- [93] Pratama, Mohammad Rizki Fadhil, et al. ”Peganum harmala and its alkaloids as dopamine receptor antagonists: in silico study.” *Biointerface Res Appl Chem* 11.3 (2021): 10301-16.
- [94] Ayipo, Yusuf Oloruntoyin, et al. ” β -Carboline alkaloids induce structural plasticity and inhibition of SARS-CoV-2 nsp3 macrodomain more potently than remdesivir metabolite GS-441524: Computational approach.” *Turkish Journal of Biology* 45.7 (2021): 503-517.
- [95] Ahmad, Imad et al. “Computational pharmacology and computational chemistry of 4-hydroxyisoleucine: Physicochemical, pharmacokinetic, and

- DFT-based approaches.” *Frontiers in chemistry* vol. 11 1145974. 13 Apr. 2023, doi:10.3389/fchem.2023.1145974
- [96] Sankar, M., Ramachandran, B., Pandi, B., Mutharasappan, N., Ramasamy, V., Prabu, P. G., Shanmugaraj, G., Wang, Y., Muniyandai, B., Rathinasamy, S., Chandrasekaran, B., Bayan, M. F., Jeyaraman, J., Halliah, G. P., & Ebenezer, S. K. (2021). In silico Screening of Natural Phytocompounds Towards Identification of Potential Lead Compounds to Treat COVID-19. *Frontiers in molecular biosciences*, 8, 637122.
- [97] Yabrir, B., Belhassan, A., Lakhli, T., Salgado M, G., Bouachrine, M., Munoz C, P., ... & Ramirez T, R. (2021). Minor composition compounds of Algerian herbal medicines as inhibitors of SARS-CoV-2 main protease: Molecular Docking and ADMET properties prediction. *Journal of the Chilean Chemical Society*, 66(1), 5067-5074
- [98] ("Kalydeco 50mg granules sachets - Summary of Product Characteristics (SmPC)". (*emc*). 30 August 2019. Archived from the original on 21 November 2019. Retrieved 20 November 2019.
- [99] F. Van Goor, S. Hadida, P.D. Grootenhuis, B. Burton, D. Cao, T. Neuberger, et al. Rescue of CF airway epithelial cell function in vitro by a CFTR potentiator, VX-770 *Proc Natl Acad Sci U S A*, 106 (2009), pp. 18825-18830
- [100] Taylor-Cousar, Jennifer, et al. "Effect of ivacaftor in patients with advanced cystic fibrosis and a G551D-CFTR mutation: safety and efficacy in an expanded access program in the United States." *Journal of Cystic Fibrosis* 15.1 (2016): 116-122.
- [101] Condren, Michelle E., and Marquita D. Bradshaw. "Ivacaftor: a novel gene-based therapeutic approach for cystic fibrosis." *The Journal of Pediatric Pharmacology and Therapeutics* 18.1 (2013): 8-13.
- [102] Eckford PD Li C Ramjeesingh M Bear CE Cystic fibrosis transmembrane conductance regulator (CFTR) potentiator VX-770 (ivacaftor) opens the defective channel gate of mutant CFTR in a phosphorylation-dependent but ATP-independent manner *J Biol Chem* 2012 287 36639 36649 22942289

- [103] Ramsey BW, Davies J, McElvaney NG. A CFTR potentiator in patients with cystic fibrosis and the G551D mutation. *N Engl J Med* 2011; 365: 1663–1672. doi:10.1056/NEJMoa1011979
- [104] Ruth O'Reilly & Heather E Elphick (2013) Development, clinical utility, and place of ivacaftor in the treatment of cystic fibrosis, *Drug Design, Development and Therapy*, 7:, 929-937, DOI: 10.2147/DDDT.S30345
- [105] Hayes D Jr, McCoy KS, Sheikh SI. Improvement of sinus disease in cystic fibrosis with ivacaftor therapy. *Am J Respir Crit Care Med*. 2014;190:468.
- [106] Rowe SM, Heltshe SL, Gonska T, et al. Clinical mechanism of the cystic fibrosis transmembrane conductance regulator potentiator ivacaftor in *G551D*-mediated cystic fibrosis. *Am J Respir Crit Care Med*. 2014;190:175–184.
- [107] Borowitz, D., Lubarsky, B., Wilschanski, M. *et al.* Nutritional Status Improved in Cystic Fibrosis Patients with the *G551D* Mutation After Treatment with Ivacaftor. *Dig Dis Sci* **61**, 198–207 (2016). <https://doi.org/10.1007/s10620-015-3834-2>
- [108] Daina, A., Michielin, O., & Zoete, V. (2017). SwissADME: a free web tool to evaluate pharmacokinetics, drug-likeness and medicinal chemistry friendliness of small molecules. *Scientific reports*, 7(1), 1-13.
- [109] Khurshid, Z. (2021). Determination of Potential Antioxidants of *Artemisia annua* by Computational Approaches (Doctoral dissertation, CAPITAL UNIVERSITY).